COMPRESSIVE BEHAVIOUR OF CFRP LAMINATES EXPOSED IN HOT-WET ENVIRONMENTS

Thesis submitted for the degree of
Doctor of Philosophy
at the University of Leicester

by
Durmuş Türkmen
Department of Engineering
University of Leicester

January 1996

ProQuest LLC
789 East Eisenhower Parkway
P.O. Box 1346
Ann Arbor, MI 48106-1346


LEICESTER UNIVERSITY LIBRARY

PREFACE

This dissertation presents the results of research studies carried out in the Engineering Department of the University of Leicester. The content is original, except where specific reference is made to the work of others, and includes nothing which is the outcome of work done in collaboration.

No part of this dissertation has been submitted for a degree at any other University.

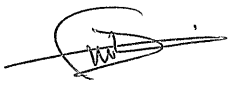

Durmus Turkmen
University of Leicester
Engineering Department

SUMMARY

This thesis describes an experimental study of the compressive failure of T800/924C carbon fibre-epoxy laminates exposed in hot-wet environments.

The specimens were immersed in boiling water so that the moisture equilibrium level was reached in a period of few weeks. The moisture level and moisture diffusion through the thickness of the laminate were measured experimentally and compared with theory (Fick's Law).

Uniaxial compression tests were carried out in a Celanese test rig and the failure mechanisms were studied under various environmental conditions. Fracture characteristics were identified using optical and scanning electron microscopy. The critical failure mechanisms observed were in-plane and out-of-plane fibre microbuckling. At test temperatures higher than 50°C the failure mode switched from in-plane to out-of-plane microbuckling. As the temperature increased the shear strength and stiffness of the resin were considerably reduced. This decreased the amount of side support for the fibres and reduced the strain level at which fibre microbuckling occurred.

Finally, recent theoretical models were employed to predict the compressive stress-strain response and strength of unidirectional laminates. It was found that although the theoretical models do not exactly predict the compressive strength of the laminate, they are sufficiently accurate for the cases examined.

ACKNOWLEDGEMENTS

This work carried out in the Engineering department of the University of Leicester, with the support of the Pamukkale Universitesi, Turkey.

I would like to thank my supervisors, Dr.C. Soutis and Prof. A.R.S. Ponter for their support and guidance during the course of this research. I would like to thank Dr. D. Kelly and Mr. H. Demirer for helpful discussion.

I am grateful to members of technical staff of the Engineering Department at Leicester who have helped at various stages during the project. They include, Mr. C.J. Morrison, Mr. D. Pratt, Mr. H. Sharma Mr. G.R. O'Connor, Mr. A. Lightfoot, Mr.G. Clark, Mr. A. Forryan, Mr. A.S.Wale, Mr. A. Payne and the photographers Mr.P.M. Smith an Mr. G. McTurk.

COMPRESSIVE BEHAVIOUR OF CFRP LAMINATES EXPOSED IN HOT-WET ENVIRONMENTS

CONTENTS

Appendices, references, tables and figures are placed at the end of each chapter.

NOTATION

E_{11}	Elastic modulus in fibre direction
E_{22}	Elastic modulus in transverse direction
V_f	Fibre volume fraction
E_m	Young's modulus for matrix
E_f	Young's modulus for fibre
G_m	Shear modulus for matrix
σ_c	Compressive strength
τ	Shear strength
τ_y	Shear yield stress
τ_f	Shear failure stress
τ_a	Applied shear stress
γ_y	Shear yield strain of material
γ_f	Shear failure strain
ε_1	Strain in direction 1 (from rosette straingauge)
ε_2	Strain in direction 2 (from rosette straingauge)
P	Applied load
w	Net width between the two notches
h	The thickness of the test specimen
D_c	Moisture diffusion coefficient for finite plate
D_∞	Moisture diffusion coefficient for infinite plate
u/d :	Unidirectional
m/d	Multidirectional
W_w	Wet specimen weight
W_d	Oven dry specimen weight

$M\%$	Average moisture content absorbed by the material
$M_\infty\%$	Moisture equilibrium level
W	Specimen width
l	Specimen length
R_c	Resin system constant
E	Activation energy of diffusion process
G_c	Ideal gas constant
T	Absolute temperature
H_D	Vickers average hardness dry condition
H_W	Vickers average hardness wet condition
T_g	Glass transition temperature
T_{dg}	Dry glass transition temperature
T_{wg}	Wet glass transition temperature
c	Constant dependent on the constraint
ℓ/k	The slenderness ratio
ℓ	Specimen gauge length
k	Radius of gyration of the cross section
t_o	Specimen thickness
G_{12}	Shear modulus
σ_f	Failure stress under uniaxial compression
$\bar{\phi}$	Initial fibre misalignment
ϕ	Kink band inclination angle
β	Boundary orientation angle
λ_k	Kink length
ν	Poisson's ratio
ν_m	Poisson's ratio for matrix
α	Resin constant

G_c	Composite shear modulus
CFRP	Carbon Fibre Reinforced Plastics
SEM	Scanning Electron Microscopy
IITRI :	Illinois Institute Technology Research Institute
RH	Relative humidity
RT	Room temperature
M_1	Percentage of moisture absorption in t_1 time
M_2	Percentage of moisture absorption in t_2 time
pp	Polypropylene
u/d	Unidirectional
m/d	Multidirectional

CHAPTER ONE

1. INTRODUCTION

Composite materials exhibit high specific strength and stiffness and are widely used in the aerospace, automotive and sports industries. They exhibit several failure mechanisms under static loading: matrix cracking, delamination, fibre breakage (tension) and fibre microbuckling (compression). In order to predict their compressive and tensile response at different temperatures and humidities the failure mechanisms must be well understood. It is necessary to understand how temperature affects the basic properties of the materials. Obviously, strength and stiffness are two properties that are of fundamental importance in structural design. However, because of the large temperature difference between elevated temperature cure of graphite/epoxy and the ambient cold of space, thermal expansion is also important.

Several investigators [1-3] have studied moisture absorption through the thickness of laminates at various environmental conditions. While it is well known that the epoxies used as matrix materials in fiber reinforced composites absorb small amounts of moisture, experience has shown that the combined effects of high temperature and humid environments represent a more severe threat to long-term structural integrity in advanced composite structures. Early tests indicate that the graphite fibers do not absorb a measurable amount of water [4]; consequently, absorption of moisture is limited to the resin matrix of composite material. Hygrothermal effects, can influence the overall composite behaviour, as it is the complex interaction between the fibres and matrix that gives rise to the structural capability of resin matrix composites. Browning et *al.,* [4], evaluated the effects of absorbed moisture on the mechanical properties of neat epoxy resin and a derived graphite/epoxy composite. The glass transition temperature, elastic modulus of the neat resin, and the strength and elastic modulus for unidirectional and quasi-isotropic composite laminates were determined as a function of absorbed moisture and temperature. A method for predicting moisture content and through-the-thickness profile for laminates exposed to a constant humidity and temperature was developed. The test data obtained indicated that moisture and temperature effects on the neat

resin translate directly to matrix controlled properties of the composite material and can lead to change in failure mode, while fiber controlled properties show very little environmental sensitivity. Several other investigators [5-10] examined the compressive behaviour of carbon fibre reinforced plastic (CFRP) laminates in hot-wet environments. They observed that the strength and stiffness properties are reduced considerably. Potter et *al.*, [6-7] found that failure is by microbuckling of the 0^{o} layers. At room temperature failure is by in-plane microbuckling while at high temperature the failure mode is out-of-plane microbuckling.

In early work on this subject, Rosen [11] developed an elastic microbuckling analysis in order to predict the compressive strength. His model over-estimates the failure strength of the composite suggesting that fibre microbuckling is a plastic phenomenon. The combined effect of fibre misalignment and plastic matrix were suggested by Argon [12] to reduce predictions of compressive strength to more acceptable values. Budiansky [13] has argued that fibre microbuckling is highly sensitive to fibre misalignment. Budiansky [13] and Hahn [14] have attempted to model fibre microbuckling by taking into account fibre misalignment and matrix/fibre debonding. First generation models of microbuckling failure from notched laminates under uniaxial compressive load have been developed by Soutis et al.[15].

In the present study, T800/924C carbon fibre-epoxy composite laminates are exposed in boiling water and their moisture content is considered. The changes of compressive strength are determined by performing uniaxial compression tests in hot-dry and hot-wet conditions using the Celanese test rig [16]. The results presented indicate that exposure to hygrothermal environments reduces the strength properties substantially and causes the failure mode to change from in-plane fibre microbuckling at room temperature to out-of-plane at temperatures greater than $50^{o}C$.

This experimental study has also been carried out to examine the failure mechanisms in unidirectional $[0]_{4s}$ glass polypropylene (Plytron) composite laminates under uniaxial compressive loading at 20 ^{o}C, $50^{o}C$, $80^{o}C$, $100^{o}C$ and $120^{o}C$ hot-dry conditions.

The compressive failure mode is examined in some detail using optical and scanning electron microscopy (SEM). Recent theoretical methods are employed to predict compressive stress-strain response and strength.

Regarding this study a number of papers have been published in the open literature. Copies of these papers are attached at the end of chapter seven in Appendix A.

REFERENCES

1. Copley, S.M. and Collings, T.A., The Determination of Through-thickness Moisture Distribution and Diffusion Coefficient in Fibre Reinforced Plastic Laminates, *RAE, Tech. Rep.* 81105, 1981.

2. Curtis, P.T., A Basic Computer Program to Calculate Moisture Content in Resins and FRC, *RAE, Tech. Mem. Mat.*375 June, 1981.

3. Copley, S.M. A Computer Program to Model Moisture Diffusion and Its Application to Accelerated Aging of Composites, *RAE Tech. Rep.* 82010, Jan.1982.

4. Browning, C.E., Ilusman, G.E., and Whitney, J.M., Moisture Effect in Epoxy Matrix Composites, *Composite Materials Testing and Design (Fourth Conference), ASTM STP 617*, American Society for Testing and Materials, Philadelphia, pp. 48-496, 1977.

5. Joshi, M.K., The Effect of Moisture on the Shear Properties of Carbon Fiber Composite, *Composites,* Vol.14 No.3, p.196, July, 1983.

6. Potter, R.T. and Purslow, D., The Environmental Degradation of Notched CFRP in Compression, *Composites,* Vol. 14, No.3, p.207, July, 1983.

7. Purslow, D. and Potter, R.T., The Effect of Environment on the Compression Strength of Notched CFRP Fractographic Investigation, C*omposites,* Vol.15, No 2, p.112, April 1984.

8. Shen, C.H. and Springer, G.S., Moisture Absorption and Disabsorption of Composite Materials, *J. Composite Materials* Vol. 10, p2. 1976.

9. Hyer, M.V., Herakovich, C.T., Milkovich, S.M. and Short, J.S., Temperature Dependence of Mechanical and Thermal Expansion Properties of T300/5208 Graphite/epoxy, *Composites,* Vol.14 No. 3, p.276, July 1983

10. Lou, A.Y. and T.P.Murtha, T.P., Environmental Effects on Glass Fibre Reinforced PPS Stampable Composites. *J. Composite Materials*. Vol. 21, p.910, 1987.

11.Rosen, B.W. Mechanics of Composite Strengthening, *Fibre Composite Materials,* American Society of Metals, pp 37-75, 1965.

12.Argon, A.S., Fracture of Composites, *Treatise of Materials Science and Technology,* Vol.1, Academic Press Newyork, 1972.

13.Budiansky, B., Micromechanics, *Computers and Structures*, Vol.16, No.1, pp. 1-12, 1983.

14.Hahn, H.T. Compressive Failure Mechanisms in Composite Structures, *NASA,* CR-3988, 1986.

15.Soutis, C., Fleck, N.A. and Smith, P.A., The Compression Fatigue Behaviour of a Notched Carbon Fiber Epoxy Laminate, *Int. J. Fatigue,* Vol.13, No.4, pp. 303-312., 1991.

16. Standard Test Method for Compressive Properties of Unidirectional or Crossply Fibre Resin Composites, *ASTM Standard D 3410-87, American Society for Testing and Materials*, Philadelphia, PA, 1992.

CHAPTER TWO

LITERATURE REVIEW

2.1 Introduction

In recent years, carbon fibre composite materials have evolved from an available alternative to a likely candidate for the role of a primary structural material in high performance aircraft applications. As the design expertise required to exploit the potential of composite materials for diversified practical and state of the art applications has increased, so has the need for assessing the impact of environmental conditions such as temperature, moisture and compressive loading on these material systems. Understanding the response of carbon fibre/epoxy composites to dynamic hygrothermal environments is not only essential for the prudent use of these materials, but also to assure integrity and life durability for confident use.

While it is well known that the epoxies used as matrix materials in fibre reinforced composites absorb small amounts of moisture, experience has shown that the combined effects of high temperature and humid environments represent a more severe threat to the long-term structural integrity of advanced composite structures. Early tests[1] indicate that the graphite fibres do not absorb a measurable amount of water; consequently, absorption of moisture is limited to the resin matrix of composite materials. Hygrothermal effects, however, can influence the overall composite behaviour, as it is the complex interaction between the fibres and matrix that gives rise to the structural capability of resin matrix composites.

A number of recent investigations [2-7] document the effects of adverse environmental conditions on graphite epoxy composites for simple lay-up

configurations and states of stress. Primary interest, however, has been placed upon static performance.

Browning et *al.,* [1], evaluated the effects of absorbed moisture on the mechanical properties of neat epoxy resin and a derived graphite/epoxy composite. One primary consideration for evaluating the static performance of composite materials is assessing the impact of environmental conditions on the elastic modulus. Shen and Springer considered this subject in their study [2]. The influence of environmental cycling on the mechanical properties of graphite/epoxy composites was studied by Lundemo and Thor [3].

2.2 Compressive Failure of Unidirectional Laminates

Unidirectional composite laminates are rarely used in structural components but are usually combined with plies of varying orientation in a multidirectional laminate. However, it is the 0^{O} layers in such a laminate that carry most of the applied load and from a structural design view point it is important to know the failure stress of these layers and how they relate to the stress in a totally unidirectional laminate.

In compression testing, unidirectional plates are sensitive to Euler buckling, specimen misalignment in the testing fixture, the quality of material and non-uniform loading. There are several types of specimens that can be used to enable the measurement of the compressive strength of unidirectional (u/d) composites; e.g., sandwich beams (flexural test), end-loaded and shear loaded specimens. The Celanese compression test rig (ASTM D3419/75) is used to load specimens by shear.

The measurement of the compressive properties of unidirectional laminates presents problems due to their highly anisotropic nature and to the complexity of the failure mechanisms. Failure may occur as a result of the three competing failure modes: Euler buckling (bending), fibre microbuckling and interlaminar shear failure.

One of the most serious problems in compression testing of composite laminates is premature failure caused by global buckling. Some test methods utilize thick laminates to avoid global buckling. However, they create other problems, including debonding between specimen end tab interfaces and mid-plane delamination

due to high interlaminar stresses. Piggott et *al.*,[8-9] employed experimental data to suggest some empirical failure criteria, which postulated different modes of failure depending on the relative strengths of the fibre, matrix and interface. The primary feature of these empirical criteria are their reliance on a linear relation between fiber volume fraction and compressive strength, which is not found in any usual analytical model of microbuckling or kinking. Steif [10] assumed that kinking evolved from fiber fracture caused by microbuckling. He concentrated on the analysis of microbuckling of bundle of initially misaligned fibres. Fibres were assumed to break in tension during bending. The fiber breaking strain was found to depend significantly on the magnitude of the initial waviness, but to be largely independent of the matrix shear modulus and the matrix shear strength, indicating that fibre bending was the dominant influence . Recently, Schapery [11] has incorporated a previously developed method of characterizing nonlinear, inelastic behaviour of composites to study kink banding in polymer composites under compression. He postulated that a band of wavy fibres becomes a kink band when local matrix cracking occurs. The corresponding value of axial stress equals or exceeds the predicted critical stress for buckling. The kink band angle is fixed through the requirement of matrix cracking, however, the compressive strength was found to be a weak function of kink band angle.

Wisnom [12] performed a two-dimensional finite element analysis of an ASTM D 3410 IITRI specimen and similar shear-loaded specimen. This analysis studied the magnitude of shear stress induced by the end tabs. A nonlinear constitutive relation for the matrix in shear resulted in decrease in the tangent shear modulus under load, reducing the predicting microbuckling load. The author concluded that the stress concentrations from tabs may cause premature matrix yield and failure, and that measured strength values under predicted the true compressive strength of many composite materials. Chamis and Sinclair [13] employed finite elements to assesS the effects of the end attachments in the IITRI fixture. Authors studied the effects of eccentricities introduced by the end conditions and progressive end-tab debonding. They concluded that the standard IITRI specimen is not susceptible to buckling unless significant misalignment or end-tab debonding is present.. Eccentricities on the order of one ply thickness were found to have negligible effect, but eccentricities on the

order of twenty ply thickness were significant. When global buckling occurs, the stress-strain curves recorded by the back-to-back gauges deviate to opposite directions because one gauge is under compression and another changes from compression to tension [14]. Berg and Salama [15] argued that the kink band must be inclined in order to permit the buckled fibres to undergo both compression and shear deformation.

2.3 Compressive Failure of Composite Laminates in Hot -Wet Environments

Carbon fibre reinforced plastics, when exposed to humid environments for a sufficient length of time, can absorb approximately 2% by weight of water [16]. It is known that hot and humid environments can degrade some aspects of the material performance, in particular the compressive strength [17-18]. Experimental results show that temperature and humidity have a marked influence on the compressive strength and that there is a clear interaction between temperature and moisture content. The compressive strength decreases with increasing moisture content and with increasing temperature for the T300/976 composite system [18]. At $20^{O}C$ and $120^{O}C$ the moisturized specimens do not regain their strength after drying. The shear strength is also decreased with increasing temperature. The moisture content does not affect the shear strength at elevated temperature ($120^{O}C$ and $175^{O}C$). The modulus of the matrix will be reduced as either the amount of absorbed water or temperature increases. Reduction in matrix modulus will promote failure of the composite by out-of-plane fibre microbuckling [19]. The compressive failure takes the form of a shear crack (fibre microbuckling) that initiates at the free edge or a material defect and extends at an angle of $5\text{-}20^{O}$ to the horizontal axis, across the width of the specimen.

Hendrick and Whiteside [20] have presented the effects of environmental factors on the epoxy matrix of boron and graphite epoxy composite systems. The mechanisms by which these factors produce a reduction in matrix controlled strength and stiffness properties such as transverse tension, shear and longitudinal compression are described.

Haque and Jeelani [21] have reported the influence of moisture and temperature effect on the compressive properties of T-300/epoxy, thermosetting and APC-2 thermoplastic composites. They found that the compressive strength and modulus of APC-2 thermoplastic composite are comparatively higher than those of T-300/epoxy composite. APC-2 also sustains higher compressive strength in the presence of moisture as compared to T-300/epoxy. The degradation of the compressive modulus is mostly temperature dependent. The effect of moisture at 100°C is negligible for both materials.

Zhou and Lucas [22] have studied T300/924 unidirectional graphite epoxy prepreg specimens placed into distilled water at various temperatures. They examined the specimens under optical and scanning electron microscopes after three months immersion. Cracks develop on the surface of the specimens. The crack depth increased with time. At 4300h, the average crack depth emanating from the surface into the laminate is about 0.5 mm. When the specimens were left in distilled water for up to 35 days no crack was observed on the surface and only Fickian diffusion exists. Naeem [23] compared moisture absorption of vinylester composite with polyester(272) composite; the specimens were fully submerged in distilled water and tested in 95% relative humidity at various temperatures. He found that the vinylester composite absorbed less amount of moisture than the polyester composite because the vinylester resin has relatively few ester groups available for hydrolysis, and also the methyl group which shields the ester linkage increases resistance to hydrolysis. Vinylester 470-36 tended to absorb more moisture than 411-45 because of its higher crosslink density and more ester groups for hydrolysis. There was not any sign of microcracking on the surface or inside the material with 411-45 and 470-36. However, polyester samples had microcracks on the surface after immersion in a water bath at 70°C for 14 days.

T300/5208 Graphite/epoxy stiffness properties have been studied under uniaxial compressive loading [24-25]. Sinclair and Chamis [24] have tested the unidirectional composite materials under uniaxial compressive loading by using the Illinois Institute of Technology Research Institute (IITRI) modified Celanese Test Method. The experimental determination of longitudinal compressive strength was sensitive to

possible tab debonding and load misalignment. They argued [24] that, even if tab debonding and misalignment are present the test data can still be used in conjunction with theoretical analysis to determine a reasonable value for longitudinal strength. Hyer *et.al* [25] have tested T300/5208 unidirectional graphite epoxy laminates in the temperature range of -157°C to 121°C. They found that most properties exhibit nearly linear temperature dependence. But the transverse modulus and the axial coefficient of thermal expansion both showed high non-linear temperature dependence, with order of magnitude changes observed in the above temperature range. The matrix dominated property (E_{22}) exhibits a very strong temperature dependence at low temperature, the matrix dominated thermal expansion coefficient is almost independent of temperature.

AS4/3501-6 graphite /epoxy matrix dominated properties, i.e., transverse tensile and in plane shear properties, decrease with increasing temperature and moisture content for a fixed strain rate [26]. The ultimate shear strain decreases slightly with strain for graphite epoxy system.

XAS-914 Carbon Fibre Reinforced (CFRP) unidirectional coupons were tested in compression at a temperature range of -70°C-120 °C [27]. It has been shown that the compressive failure of unidirectional XAS-914 laminates involve fibre microbuckling and that a shear failure is not attainable even at -70 °C. The compressive failure of unidirectional CFRP has been shown to be nonlinear and this is attributed to elastic fibre microinstability which is initiated by initial fibre waviness. The room temperature failure mode of XAS-914 system was always by fibre microbuckling.

Composites made of unidirectional aramid fibre reinforced CIBA-GEIGY-epoxy resin have been studied[28]. The environmental chamber was maintained at different relative humidities (50%, 70%, or 100%) and at different temperatures, ranging from 50° to 76° C. Each specimen was kept in an appropriate chamber until the desired maximum saturation level (maximum moisture content M_m) was reached. The composites with untreated fibres reached maximum saturation earlier than composites with treated fibres. The maximum moisture contents attained was 4 to 5 percent. This level was reached during exposure to air at 100 percent relative

humidity. After moisturization, the specimens were tested at room temperature. Compressive strengths were measured with a Celanese fixture at loading rate of 0.05mm/sec. After redrying, the composites containing treated as well as untreated fibres regained nearly all their strengths. Thus neither moisture nor surface treatment appear to affect significantly the compressive strength of the aramid composite system.

The influence of water absorption becomes more severe for glass fibre reinforced composites since it is known that moisture attacks the glass fibre matrix interface, especially in the presence of high temperature. Lou and Murtha[29] studied a long glass fibre reinforced material, AG20-40, and a short glass fibre reinforced material, AG10-20. As a neat resin, polyethylene sulfide shows good property retention after extended exposure to hot water[29]. This good resin property should carry over as a matrix material in composite performance. When composite specimens were exposed to hot water, there were no measurable changes in specimen dimensions and low weight gains were observed. Good retention of modulus and strength is observed up to 121^{o}C with a fairly rapid reduction occurring above this temperature. A 65% and 75% strength retention is obtained for AG20-40, and AG10-20, respectively, when the composite specimens were exposed in hot water at 149^{o}C for two weeks. Property retention after extended hot/wet exposure is extremely important for glass fibre reinforced composites since moisture has been known to attack the fibre/matrix interface.

2.4 Review of Theoretical Models

Various investigators[30-44] have studied the compression failure mechanisms of composite laminates. In spite of the importance of the compressive strength properties of laminates in aircraft design, there is not at present a universally accepted theoretical model for the prediction of the compressive strength. This problem is complex, not only because of the mechanics but also because of the different failure modes that can occur. In fact, many factors exist in the compressive response of composite materials and they can trigger a number of different failure modes. These factors occur at the structural level (laminate level), and the microstructural level

(fibre-to matrix level). Related to these factors, the state of applied load, fibre waviness, fibre volume fraction, voids, fibre tilting, fibre misalignment and stress concentrations all have been shown to play a role in determining the predominant failure mode governing compressive failure. Therefore, these variables need to be considered in experimental work.

In order to predict the compressive strength of unidirectional laminates many researchers have suggested a number of models. In 1964 Rosen [30] modelled compressive failure of unidirectional composite materials without requiring the use of empirical factors like Dow and Gruntfest's model[31]. His analysis was based on the idea that the fibres behave as slender columns supported by an elastic foundation which is the matrix material. Two possible modes were assumed:

a) the fibres buckle out-of phase with each other (extension mode), and

b) the fibres buckle in phase (shear mode).

For the extension mode, the deformation of the matrix material between the fibres is extension in the direction perpendicular to the fibres. For the shear mode, shear deformation occurs in the matrix material. By using an energy approach, Rosen obtained the following equations for the compressive strength.

For the extension mode

$$\sigma_c = 2V_f\left(\frac{V_f E_m E_f}{3(1-V_f)}\right)^{\frac{1}{2}} \qquad (1)$$

and for the shear mode

$$\sigma_c = \frac{G_m}{1-V_f} \qquad (2)$$

where σ_c is the compressive strength of the unidirectional composite material

V_f is the fibre volume fraction

E_m is the Young's modulus for the matrix

E_f is the fibre Young's modulus and

G_m is the shear modulus for the matrix.

For composites of practical structural interest, which have fibre volume fractions greater than 20%, the shear mode predicts the lower strength. However equations 1 and 2 grossly over-estimate the compressive strength of most graphite/epoxy composites. Schuerch [32] independently proposed the same model as Rosen and arrived at the same results for composites that are not subjected to inelastic deformation prior to failure. He tested boron-magnesium laminates and obtained good correlation between theory and experiment.

Lanir and Fung [33] investigated theoretically the prebuckling and postbuckling behaviour of a cylindrical fibre surrounded by a matrix material. They pointed out that buckling of the fibre is possible if it is not supported by the surrounding matrix and initial fibre-matrix debonding decreases buckling load. They also pointed out that in common composite materials the buckling of fibres will have no significant effect on the overall behaviour of the linear elastic range but fibre buckling will significantly affect the fibre behaviour of the composite when loaded in the plastic range.

Argon [34] asserted that the combined effect of fibre misalignment and yielding of the matrix is the reason that measured compressive strength is considerably lower than the prediction of the Rosen's buckling model of individual fibres. If a fibre is at a small angle away from the compression axis there will be resolved shear stress in the matrix between the fibres. When this shear stress exceeds the shear strength of the composite, failure occurs. The shear strength of the composite is taken to be approximately equal to the matrix shear strength between the fibre and matrix and it is assumed to be greater than the matrix yield strength.

Evans and Adler [35] presented a detailed treatment of the kink banding process due to microbuckling using a thermodynamic analysis. The kink morphology can be characterized by three parameters: kink band orientation angle (ϕ), the kink band angle (β) and the kink length (λ_k). They derived the relation $\phi=2\beta$ by minimizing the strain energy in the kink band zone and found that fibre kinking was the dominant failure mechanism for unidirectional laminates. The authors[35] obtained a value for

the preferred kink band orientation by minimizing the plastic work done on the matrix during fibre rotation.

The evidence is now compelling that non-linear deformation of the matrix, together with the presence of small initial fiber misalignments, are essential features of the kinking process. On the basis of a one dimensional theory which assumes inextensible fibers and neglects fibre bending resistance, Budiansky and Fleck [36] found small fiber misalignments of the order of 2° can account for the observed compressive strengths. Wisnom[37] incorporated the matrix nonlinearity and fibre misalignment into a numerical model to asses the effects of lateral constraint by the grips on composite failure. The motivation for his investigation came from experimental results (Haeberle and Mathews[38] and Pearson[39]) that showed misalignments of 3° to cause a reduction of less than 5% in the compressive strength, as compared to the decrease of 75% predicted by the misalignment model. Wisnom attributed this behaviour to lateral constraint imposed by the grips in the experiments. The numerical model with constraint predicted a failure stress of 1800 MPa for the same XAS/914 material; this stress was relatively independent of misalignment up to 4 degrees, and was higher than the experimental values of about 1600 MPa. Yurgatis et. *al.,* [40] suggested that small random fiber misalignments on the order of 1 or 2 degrees do have a significant effect on the compressive strength. XAS- and AS-4 carbon fiber failures were by microbuckling under uniaxial compressive loading[40].

Argon [34] reported the influence of matrix plasticity and misalignment of fibres on kinking. He identified the shear strength of composite material as the most important parameter affecting the compressive strength. In this model fibre kinking occurs in a $\beta = 0°$ band within which fibres have suffered an initial fibre misalignment angle $\bar{\phi}$. The compressive strength was given by:

$$\sigma_c = \frac{\tau_y}{\bar{\phi}} \qquad (3)$$

where σ_c is the compressive strength, τ_y is the shear yield strength and $\bar{\phi}$ is the initial fibre misalignment. Budiansky[41] extended this result for an elastic-perfectly plastic composite response, and found

$$\sigma_c = \frac{\tau_y}{\gamma_y + \bar{\phi}} = \frac{G}{1 + \bar{\phi}/\gamma_y} \qquad (4)$$

where G is shear modulus of composite.

Batdorf and Ko [42] have shown that this failure is due to small initial fibre misalignments that are virtually unavoidable in practical construction. But such misalignments must in addition have other effects on the mechanical behaviour of composites. One effect is reduction in the initial compressive stiffness, which is shown to depend on the degree of fibre misalignment and elastic shear modulus of the composite. A second effect is a nonlinearity in the compressive stress-strain curve arising from two sources:

a) the reduction in shear stiffness of the composite with increasing shear strain and

b) the reduction in compressive stiffness due to increasing fibre tilt.

For an elastic perfectly plastic composite, Batdorf and Ko derived the following equation in a similar way to Budiansky's prediction. They argued that the shear strain has an additional effect on the compressive strength of the composite. This relationship was:

$$\sigma_c = \frac{\tau_f - \tau_a}{\bar{\phi} + \gamma_f} \qquad (5)$$

where τ_f is shear the failure stress, τ_a is applied shear stress and γ_f is the yield strain of the material.

In 1988 Steif [43,44] presented a model for the compressive failure of fibre reinforced composite with brittle, weakly bonded constituents. He extended the beam on an elastic foundation model of Rosen[30] to allow for slippage at the fibre matrix interface. Using equilibrium conditions, he derived an explicit formula for the

compressive strength in terms of interfacial shear strain and the degree of fibre misalignment. This theory predicts strengths that are lower than classical models (e.g. equation 2) predict, but the lower strengths are obtained by assuming a misalignment amplitude.

Swanson [45] attempted to explain the dependence of compressive failure strain on laminate lay-up and his model was based on a beam-column on an elastic foundation equation given by Hahn and Williams [46] but also included the effects of lamination. The model predicted that the apparent strength of the axial plies depends on the total laminate lay-up, and in particular on shear stiffness, matrix strength, the fibre strength and initial waviness. The model was used to explain the data on the compressive strengths of various laminates presented in [47].

In summary, the compressive failure mechanisms of fibre reinforced composite materials have been investigated for more than 30 years. Advanced carbon fibre composite systems have been examined, assuming the following possible compressive failure models: fibre buckling, transverse tension, fibre kinking, matrix yielding and delamination. Virtually all compressive failure models are still controversial, in that not everyone agrees that a particular model is the correct model. Thus a unified theory that can be applied to various composite systems and failure modes does not exist at present. Nevertheless, the various micromechanical models available in the literature can predict with some success the critical compressive strength. Furthermore, they can successfully suggest the critical parameters that influence the compressive load capability of unidirectional composite laminates.

2.5 Aims of Present Work

The aims of the current research program were to:

i) study the moisture absorption of T800/924C system exposed in boiling water (accelerated ageing),

ii) measure the compressive properties of unidirectional (u/d) laminates tested in hot-dry and hot-wet conditions,

iii) examine the failure mechanisms in compression by using optical microscopy and Scanning Electron Microscopy (SEM), and finally

iv) verify the correctness of existing fibre microbuckling theories.

REFERENCES

1. Browning, C.E., Ilusman, G.E., and Whitney, J.M., Moisture Effect in Epoxy Matrix Composites, *Composite Materials Testing and Design (Fourth Conference), ASTM STP 617*, American Society for Testing and Materials, Philadelphia, pp. 48-496, 1977.

2. Shen, C.H. and Springer, G.S., Environmental effects on the Elastic Moduli of Composite Materials. *Journal of Composite Materials,* Vol. 11, pp. 250-264, July 1977.

3. Lundemo, C.Y and Thor, S.C., Influence of Environmental Cycling on the Mechanical Properties of Composite Materials, *Journal of Composite Materials* Vol. 11, pp. 276-283, July 1977.

4. Copley, S.M. and Collings, T.A The determination of through-thickness moisture distribution and diffusion coefficient in fibre reinforced plastic laminates, *RAE, Tech. Rep.* 81105, 1981.

5. Curtis, P.T. A basic computer program to calculate moisture content in Resins and FRC, *RAE, Tech. Mem. Mat.*375 June, 1981.

6. Copley, S.M., A computer program to model moisture diffusion and its application to accelerated aging of composites, *RAE Tech. Rep.* 82010, Jan.1982.

7. Joshi, M.K., The effect of moisture on the shear properties of carbon fibre composite, *Composites,* Vol.14 No.3, p.192, July, 1983.

8. Piggott, M.R., and Harris, B. Compressive Strength of Carbon, Glass and Kevlar-49 Fibre Reinforced Polyester Resins, *J.Mater. Sci.* 15 pp. 2523-2538, 1980.

9. Piggott, M.R., A theoretical Frame work for the Compressive Properties of Aligned fibre Composites, *J.Mater. Sci.* Vol.16, pp. 2837-2845, 1981.

10. Steif, P. S., A Simple Model for Kinking in Fibre Microbuckling Composites: Part I&II , *Journal of Composite Materials,* Vol. 26, pp.549-569, 1990.

11. Schapery, R.A., Prediction of Compressive Strength and kinkbands in Composites using a Work Potential, *Journal of International Solids and Structures,* Vol 32, No 6/7, pp.739-765, 1995.

12. Wisnom, M.R., Effect of Shear Stress in indirect compression tests of Unidirectional Carbon-fibre/epoxy, *AIAA J.* Vol.29, pp 1692-1697, 1991.

13. Chamis, C.C. and Sinclair, J.H., Longitudinal Compressive Failure Modes in Fiber Composites: End Attachment Effects on IITRI Type Test Specimens, *J. Comp. Tech. Res.* Vol.7, pp. 129-135., 1985.

14. Tan, S.C. and Knight, M., An Extrapolation Method for the Evaluation of Compression Strength of Laminated Composites, *Compression Response of Composite Structures, ASTM STP 1185*, pp. 323-337, 1994.

15. Berg, C.A. and Salama, M., Fatigue of Graphite Fibre-reinforced Epoxy in Compression. *Fiber Science and Technology,* Vol.6, pp. 79-118, 1973.

16. Barker, A.S. and Balasundaram, V. Compression Testing of CFRP Exposed the Humid Environments, *Composites,* Vol. 18. No 3, pp.217-222, July, 1987.

17. Potter, R.T. and Purslow, D. The Environmental Degradation of Notched CFRP in Compression, *Composites,* Vol.14, No.3, p.207, 1983.

18. Tang, J.M. and Springer, G.S.. Effect of moisture and temperature on the compressive and short beam shear properties of fiberite T300/976 fabric. *J. Reinforced Plastic and Composites,* Vol. 7, p.120, 1988.

19. Joshi, O.M. and Judge, C.H. The absorption of Moisture in Some Cast Epoxy Resins and Their Carbon Fibre Composites, *RAE Tech. Memorandum* Mat/STR 1008, January 1983.

20. Hendrick, I.G. and Whiteside, J.B., Effects of Environment on Advanced Composite Structures, *AIAA Paper* No. 77-463, 1977.

21. Haque, A. and Jeelani, S. Environmental Effects on the Compressive Properties: Thermosetting vs. Thermoplastic Composites, *Journal of Reinforced Plastics and Composites,* Vol. 11, pp. 146-157, February 1992.

22. Zhou, J. and Lucas, J.P., The Effects of a Water Environment on Anomalous Absorption Behaviour in Graphite/epoxy composites, *Composite Science and Technology*, Vol. 53, pp. 57-64, 1995.

23. Naeem, M. The Resistance of Glass Reinforced Thermosetting Polymers to Thermo-humid Conditions, *Ph.D. Thesis* Loughborough University, 1985.

24. Sinclair, J.H. and Chamis, C.C., Compressive Behaviour of Unidirectional Fibrous Composites, *Compression Testing of Homogenous Materials and Composites, ASTM-STP 808*, pp. 155-174, 1983.

25. Hyer, M.V., Herakovich, C.T., Milkovich, S.M. and Short, J.S., Temperature Dependence of Mechanical and Thermal Expansion Properties of T300/5208 Graphite/epoxy, *Composites,* Vol.14 No. 3, p.276, July 1983.

26. Daniel, I.M., Yaniv, G. and Peimanidis, G., Hygrothermal and Strain Rate Effects on Properties of Graphite/Epoxy Composites. *Journal of Engineering Materials and Technology,* Vol. 110, pp.169-173, April 1988.

27. Port, K.F. The Compressive Strength of Carbon Fibre Reinforced Plastics, *RAE Technical Report,* 82083, 1982.

28. Verpoest, I and Springer, G.S., Effect of moisture on the compressive and interlaminar shear strength of aramid-epoxy composites. *J. Reinforced Plastics and Composites*, Vol. 7, 1988.

29. Lou, A.Y. and Murtha, T.P., Environmental effects on glass fibre reinforced PPS stampable composites. *J. Composite Materials.* Vol. 21, p.190, 1987.

30. Rosen, B.W. Mechanics of Composite Strengthening, *Fibre Composite Materials ASM*,Metal Park, Ohio, pp. 37-75, October 1964.

31. Dow, N.F. and Gruntfest, I.J., Determination of Most-Needed, Potentially Possible Improvements in Materials for Ballistic and Space Vehicles, *General Electric Technical Information Series* R60sd389, June 1960.

32. Schuerch, H., Prediction of Compressive Strength of Uniaxial Fibre Composite Materials, *AIAA Journal*, Vol.34 No. 4, pp.102-106, 1966.

33. Lanir, Y and Fung, Y.C.B., Fibre Composite Columns Under Compression, *Journal of Composite Materials*, Vol. 6, No. 3, pp.387-401, July 1972.

34. Argon, A.S., Fracture of Composites, *Treatise on Materials Science and Technology,* Vol. 1, pp. 79-114, 1972.

35. Evans, A.G., and Adler, W.F., Kinking as a Mode of Structural Degradation in Carbon Fibre Composites. *Acta Metallurgica,* Vol. 26, pp. 725-738, May 1978.

36. Budiansky, B. and Fleck, N.A., Compressive Failure of Fiber Composites, *Journal of Mechanics and Physics of Solids.* Vol.41, No.1, pp.183-212, 1993.

37. Wisnom, M.R., Nonlinear Analysis of Misaligned Unidirectional Carbon Fibre-epoxy Compression Specimen, *Composite Engineering*, Vol 3, pp. 547-556, 1993.

38. Haeberle, J.G. and Mathews, F.L., Studies on Compressive Failure in Unidirectional CFRP Using an Improved Test Method, *Proceedings ECCMIV Studgard*, pp. 517-523, 1990.

39. Pearson, A. E. Capabilities of Compression Test Methods for Evaluating Unidirectional Carbon Fibre Reinforced Composites, *Proceedings of the 36th International SAMPE Symposium*, Elsevier, Amsterdam, pp. 1079-1093, 1991.

40. Yurgatis, S.W. and Strenstein, S.S., Experiments to Revel the Role of Matrix Properties and Composite Microstructure in Longitudinal Compression Strength, *Compression Response of Composite Structures, ASTM-STP 1185,* pp. 193-204, 1994.

41. Budiansky, B., Micromechanics, *Computers and Structures,* Vol. 16 No 1-4, pp. 3-12, 1983.

42. Batdorf, S.B. and Ko, W.C. Stress-strain behaviour and failure of uniaxial composites in combined compression and shear-I&II *Internal report, School of Engineering and Applied Science, University of California*, Los Angeles, CA 90024 June 1987.

43. Steif, P. S., An Exact Two Dimensional Approach to Fibre Microbuckling, *International Journal of Solid and Structures,* Vol. 23, No. 9, pp. 1-12, 1987.

44. Steif, P. S., A Simple Model for the Compressive Failure of Weakly Bonded, Fibre Reinforced Composites, *Journal of Composite Materials,* Vol. 22, pp.819-828, 1988.

45. Swanson, S.R., A micro-mechanics for In-situ Compression Strength of Fibre Composite Laminates, *ASME, Journal of Engineering Material and Technology,* Vol. 114, pp. 8-12, January 1992.

46. Hahn, H.T., and Williams, J.G., Compression Failure Mechanisms in Unidirectional Composites, *Composite Materials Testing and Design, (7th Conference), ASTM STP 893*, pp. 115-139, 1986.

47. Swanson, S.R. and Colvin, G.E., Compression Failure in Reduced Adhesion Fibre Laminates, *ASME, Journal of Engineering Material and Technology,* Vol. 115, pp.187-192, April 1993.

CHAPTER THREE

EXPERIMENTAL PROCEDURE FOR STATIC TESTS

3.1. Introduction

This chapter describes the experimental methods employed to study the shear and compressive behaviour of carbon fibre-epoxy (T800/924C) and glass-epoxy (Plytron) unidirectional (u/d) composite laminates.

In the present study, a modified Iosipescu test method was employed to measure the shear properties[1]. The Iosipescu specimen was originally proposed for the shear strength measurement of metals [2]. It has, however, gained popularity for the determination of shear modulus and strength of unidirectional, cross-ply and woven fabric continuous fibre reinforced composites as well as sheet moulding materials.

Compression test methods originally designed for metals cannot in most cases be applied to composites, therefore new test methods had to be developed. These methods include the Celanese [3], the Illinois Institute of Technology Research Institute (IITRI) method[4] and the sandwich beam compression test loading technique[5]. The Celanese method, first standardized by the ASTM in 1975 remained as the only composite material compression testing standard until 1987 when the IITRI and sandwich test methods were added to the ASTM standard D3410.

The Celanese and IITRI methods rely on shear to transfer the load from the testing machine through fixture grips into the specimen via tabs. Tab region failures are quite common due to stress peaks near tab ends. These are more severe for fatigue loading and hot/wet conditions. Debonding due to interlaminar shear stresses

and fibre breaks due to high axial stresses are often noticed [6]. Although stress concentrations can be reduced by using compliant (±45 glass/epoxy) tabs with low taper angles (7°-10°), special care is needed for bonding tapered tabs and achieving valid failure modes.

In the present study, untabbed straight-sided specimens are tested using the RAE modified Celanese test rig [7]. The spark-eroded grip inserts of the apparatus have been specially textured so that no damage occurs in the composite.

3.2. Composite Materials

i) Carbon fibre-epoxy system

The laminates used in this work were manufactured from a T800/924C carbon fibre-epoxy pre-impregnated tape which was 0.125 mm thick. The T800 fibres are continuous high strength fibres pre-impregnated with Ciba-composites 924C epoxy resin, the fiber volume fraction was approximately 65%. Sheets of prepreg material were cut into 250 mm by 300 mm plies and laid up by hand. Sixteen plies were used to manufacture unidirectional composite plates which resulted in a cured laminate of approximately 2 mm thickness.

All laminates were cured in an autoclave at a temperature of 170^{o}C for an hour and postcured for four hours at 190^{o}C at the Royal Aerospace Establishment (RAE), Farnborough. An ultrasonic C-scanning was used to check the quality of the molded laminates. Test specimens were kept at an ambient laboratory air environment prior to use.

ii) Glass fibre-polypropylene system (Plytron)

Plytron consists of continuous glass fibre in a thermoplastic matrix of polypropylene (65 vol.% resin content). It comes under the ICI (Imperial Chemical Industries) trade name 'Plytron' and is produced in 240 mm wide prepreg for laminate assembly. An elevated temperature compression moulding technique was employed to manufacture $[0_4]_s$ and $[(\pm 45)_2]_s$ glass/pp laminates. Sheets of the prepreg material were cut to 260 mm by 240 mm using a guillotine and laid together by hand. Eight plies were used in the composite plates which resulted in a cured laminate thickness of

approximately 3.8 mm. Teflon coated porous bleed fabric and absorbent cloth were used to sandwich the laminate during compression moulding which resulted in the removal of excess polymer matrix. The manufacturer's standard compression moulding cycle was followed which produced laminates of acceptable quality.

3.3 Mechanical Tests (Specimen Design and Test Equipment)

3.3.1 Shear test

Iosipescu test specimens were cut from the composite panels with the fibers oriented in the longitudinal direction by using a diamond tipped saw. Each specimen was ground on the long edges to a width of 12.7 mm. The Iosipescu specimen dimensions shown in Figure 1 are 50.8 mm long, 12.7 mm wide with a nominal thickness of 2 mm [1].

A rosette strain gauge orientated at $\pm 45^{\circ}$ to the longitudinal axis of the specimen was glued, and centered between the notches. By this technique the shear strength, shear strain and shear modulus of the material can be measured.

Iosipescu[2] observed that by cutting 90° notches on each edge of the test specimen, the shear-stress distribution in the specimen could be altered from the parabolic shear-stress distribution present in constant cross-section beams, to a constant shear-stress distribution in the region between the two notches. The shear stress, τ is simply equal to the shear force divided by the net cross-sectional area of the specimen.

$$\tau = \frac{P}{wt} \qquad (1)$$

Where P is the applied load, w is the net width between the two notches and t is the thickness of the test specimen, figure 1.

The specimen was loaded by using an Iosipescu shear test fixture which is shown with an environmental unit in figures 2. Shear strains are measured with a rosette strain gauge which averages the strains over a finite area in the test section (figure 3). The shear strain γ_{12} is determined from the strain gauge as,

$$\gamma_{12} = \varepsilon_1 - (-\varepsilon_2) \qquad (2)$$

where the strain in strain gauge leg 1 is tensile (ε_1) and in leg 2 is compressive ($-\varepsilon_2$).

Two sets of specimens were tested under various environmental conditions. The first set of specimens was tested at elevated temperatures (20 °C, 50 °C, 80 °C and 100 °C) and in dry conditions. The other specimens were immersed in boiling water before testing, until reaching 1.42% moisture content by weight. Then these specimen were tested at 20 °C, 50 °C, 80 °C and 100 °C, and 95% relative humidity (RH).

Shear properties of Plytron were measured from tensile tests of ± 45 plies by using the CRAG test method[7].

All specimens were allowed about 15 minutes to reach equilibrium with their surroundings, prior to testing; load was applied continuously and failure occurred within between 60-90 seconds.

3.3.2 Compression tests of unidirectional specimens

The specimen geometry used for the unidirectional compression tests was based on CRAG test methods [7]. At least five test specimens were prepared from $[0_8]_s$ 2 mm thick composite laminates. The specimens had a constant rectangular cross section and the thickness variation was less than 2%. The dimensions of the specimens were 10 mm wide and 110 mm long and with a gauge length of 12 mm; the gauge length must be short enough to prevent Euler buckling but sufficiently long to allow stress decay to uniaxial compression. The specimens were instrumented with 2 mm long strain gauges on either side of the gauge section to measure strain and any bending.

The specimens were tested under uniaxial compressive loading at hot-dry and hot-wet (20°C, 50°C, 80°C and 100°C with 95% RH) conditions; the specimens tested in hot-wet conditions contained 1.42% by weight moisture.

The tests were performed using the modified Celanese test jig, figure 4, at a constant compression rate of 1 mm/min on a screw-driven machine of load capacity

50 kN. Figure 5 shows the Celanese compression test unit with an environmental chamber, the serrated grip (figure 6) faces of the Celanese rig were replaced by spark eroded inserts (figure 7) to eliminate adhesively bonded tabs on the specimen ends; tab misalignments, unequal tapers and variation or irregularity in the thickness of tabs or adhesive layers are problems which may cause premature failure in the composite and are all avoided in the present investigation.

The new grip inserts were cut from quench hardened 817M40 CrNi Mo steel and their faces were spark-eroded to produce a surface roughness of approximately 20 Ra (average roughness 20 μm). Figure 7 shows a spark-eroded grip with a conical collet. The new grips were used to test u/d T800/924C composite laminate at hot-dry and hot-wet environmental conditions.

The specimens were strain gauged with back to back foil strain gauges enabling bending strains to be determined as well as the elastic modulus, E_{11}. For some specimens the uniaxial strain gauges were replaced with a 90° rosette to obtain the Poisson ratio, υ_{12}.

In order to measure the compressive strength of the unidirectional laminates as a function of temperature and humidity the Celanese rig was further modified. Extra inspection ports were drilled on the Celanese alignment sleeve (Figure 5). A hot air blower for hot-dry tests and steam pipe with hot air blower for hot-wet tests were attached to the environmental chamber sleeve. Symmetric air flow was achieved and the specimen was heated evenly. It took less than 5 min. to reach 100°C and the environmental conditioning chamber was capable of maintaining the temperature to within $\pm 3°$. The specimens were kept at hot-dry and hot-wet environments for about 10-15 min. before being tested. The temperature and humidity of the environment was monitored regularly by a Testotherm hygrometer positioned in the centre of the specimen and lightly touching its surface.

3.4 Damage Evaluation Techniques

Optical microscopy and scanning electron microscopy (SEM) were used to identify the mechanisms of damage that occurred during compression testing.

From the damaged area of selected compression test specimens of carbon and glass fibre coupons were cut 2 cm long. The coupons were encapsulated in a plastic mold using a slow curing epoxy resin. The encapsulated coupons after cure were removed from the plastic mold and mounted on a MOTOPOL automatic, variable speed polishing machine .

Specimens were polished in four stages. The first stage is grinding, where the coupons are ground flat using sequentially finer emery paper from 220 to 4000 grids. The second stage is called planar grinding. In this stage METLAP 10 was used with 15 micron METADI Diamond Slurry liquid. The third stage is sample integrity stage; Metlap 4 with 9 micron and TEXMET with 3 micron METADI Diamond Slurry are used, respectively. Finally TEXMET is used with MICROPOLISH liquid. After each stage the coupons were thoroughly rinsed under running water for 15 seconds. After the last stage the coupons were dried by a hot air blower [8].

The polished fracture surfaces were examined using an OLYMPUS optical microscope (Model VANOX-T AHMT).

Some other coupons were also cut from the failed specimens and examined under the scanning electron microscope (SEM) in order to observe the damage mode at a higher magnification. To facilitate observation by the scanning electron microscope, the carbon fibre specimens were made conductive by coating them with a thin gold film, which was applied by sputter coating of thickness of 5 nm. They were then studied and photographed with an International Scientific Instruments model DS-130. A beam voltage of 15 kV was used and the minimum working distance possible was 15 mm. Working magnifications to study patterns of fibre microbuckling were 70-500x; to study the details of a single or group of fractured fibres 1 k-15 kx magnification was required.

REFERENCES

1. Walrath, D.E. and Adams, D.F., The Iosipescu Shear Test as Applied to Composite Materials, *Experimental Mechanic,* Vol.23, No.1, p.105, 1983.

2. Iosipescu, N. New Accurate Procedure for Single Shear Testing of Metals, *Journal of Materials,* Vol.2, No.3, pp. 537-566, 1967.

3. Standard Test Method for Compressive Properties of Unidirectional or Crossply Fibre Resin Composites, *ASTM Standard D 3410-87, American Society for Testing and Materials*, Philadelphia, PA, 1992.

4. Hofer, Jr., K.E. and Rao, P.N., A New Static Compression Fixture For Advanced Composite Materials, *Journal of Testing and Evaluation*, Vol.5, No.4, pp 278-283, July 1977.

5. Shuart, M.J. An Evaluation of Sandwich Beam Compression Test Method for Composites, Test Method and Design Allowable for Fibrous Composites, ASTM STP 734. C.C Chamis, Ed., *American Society for Testing and Materials*, pp 152-165, 1981.

6. Chaterjee, S., Adams, D. and Oplinger, D.W., 'Test Methods for Composites a Status Report', *Compression test methods.* Volume II. *DOT/FAA/CT-93/17,* II, June 1993.

7. Curtis, P.T., CRAG Test Methods for the Measurement of the Engineering Properties of Fibre-reinforced Plastics, *RAE Technical Report 88012*, 1988.

8. Buehler Microstructural Analysis Reference Manual *Buehler U.K. Ltd. University of Warwick Science Park Coventry,* 1992.

9. Lee and M. Munro., Evaluation of Testing Techniques for the Iosipescu Shear Test for Advanced Composite Materials, *Journal of composite materials* Vol 24, p.418, April 1983.

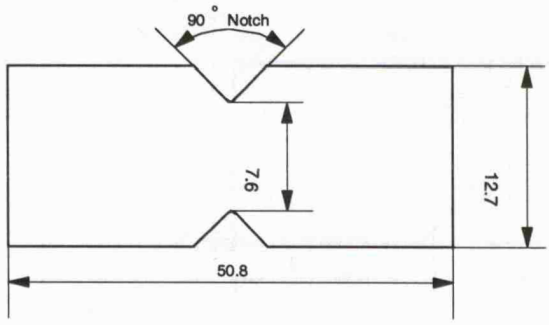

Figure 1 Iosipescu test specimen[9].

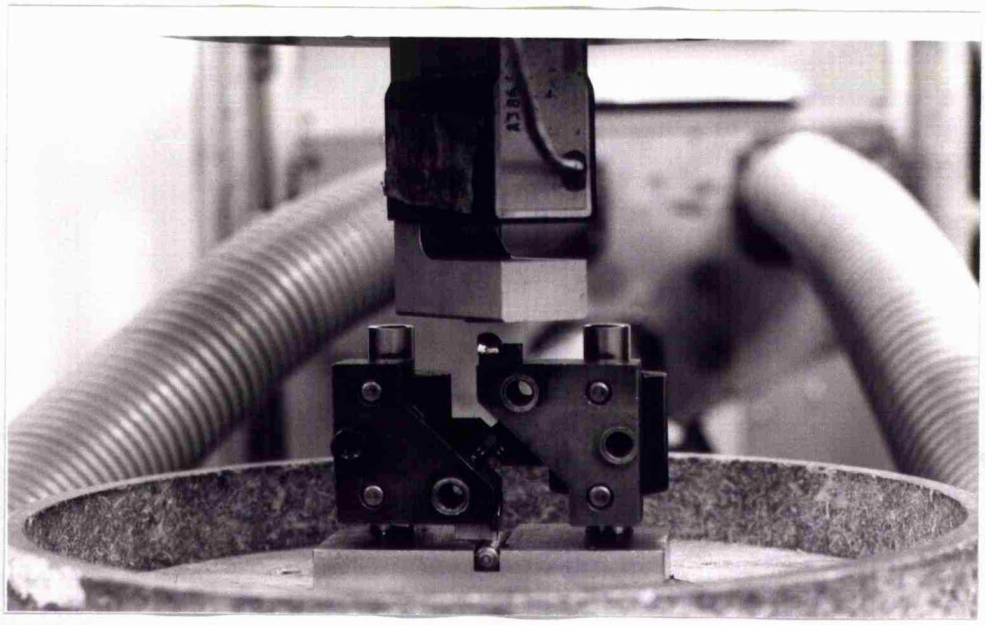

Figure 2 Iosipescu shear test fixture with an environmental unit.

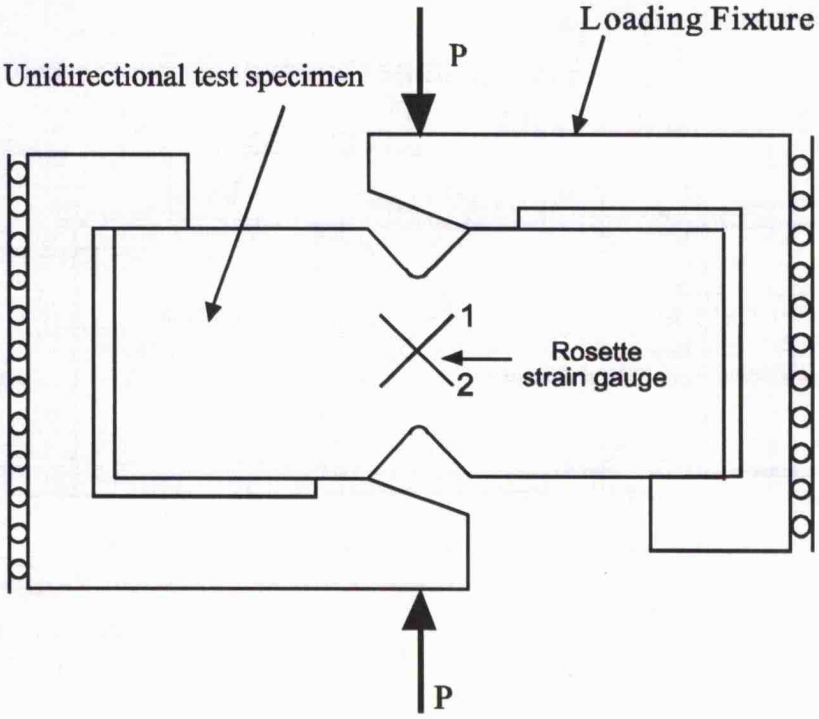

Figure 3 A schematic representation of the loading fixture for the Iosipescu Shear test

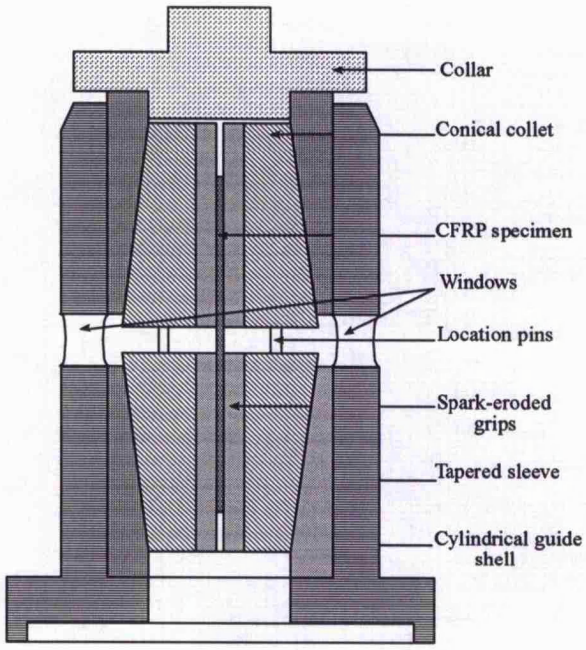

Figure 4 Modified Celanese compression-test fixture

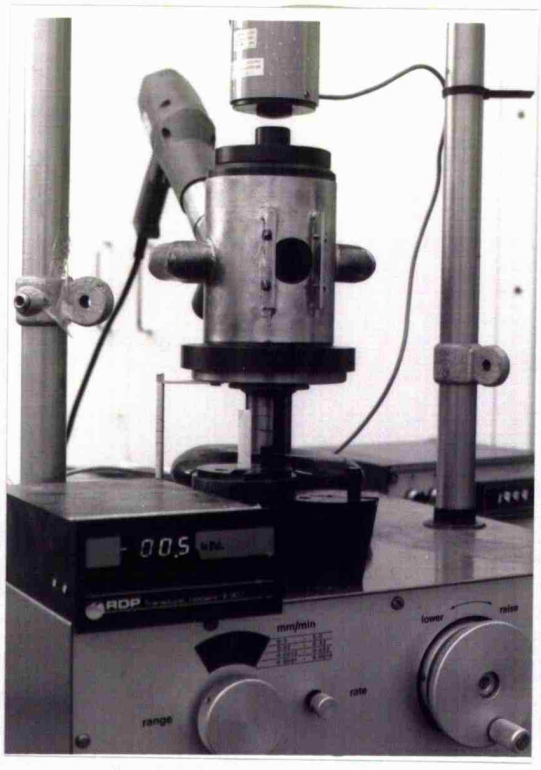

Figure 5 Celanese rig with an environmental unit

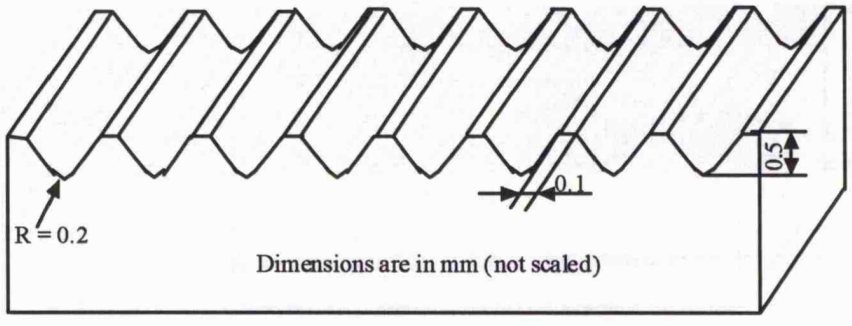

Figure 6 Conventional serrated grip faces (V grips).

Figure 7 Spark-eroded grip insert in a Celanese conical collet.

CHAPTER FOUR

MOISTURE ABSORPTION IN T800/924C CFRP LAMINATES

4.1 Introduction

Carbon fibre reinforced plastics (CFRP) are increasingly being used in the manufacture of aircraft structural components. Since, in such a service environment, fibre composite structures are exposed to atmospheric moisture and temperature variation due consideration must be given to their effect on mechanical properties. When an organic matrix composite is exposed to humid air or to water both the moisture content and the temperature of the material may change with time. These changes, in turn, may affect the thermal and mechanical properties, resulting in a decrease in performance. Therefore, to utilize the full potential of composite materials their response to environmental exposure must be known.. It is known that hot and humid environments can degrade some aspects of the material performance, in particular the compressive strength [1,2]. In order to account for moisture effects in the design of composite structures, it is necessary to predict both the total moisture content and the profile of the moisture distribution through the laminate thickness as a function of the service environment. Water absorption by the epoxy resin leads to a reduction in the glass transition temperature and to a softening of the resin with a loss of stiffness and strength which causes fibre microbuckling and premature laminate failure [3].

The rate at which water is absorbed by a composite depends on the nature of the matrix, the orientation of fibres with respect to the direction of water penetration, the temperature difference in water concentration between the composite and the wet environment, the applied stress and whether the absorbed water interacts with or damages the composite. The time necessary for water to penetrate to the centre of the composite depends on the rate of water absorption and the material thickness. It has been found by other workers[4-5] that hot and humid conditions reduce the compressive strength considerably. The degradation becomes more extensive as the conditions become more severe. The quantity of water absorbed by a laminate is therefore of considerable importance, in particular to designers when setting design limits for structures operating in moist environments.

The aim of this section is to evaluate the water of the relatively new T800/924C carbon fibre-epoxy system. A computer program has been developed in [6] to calculate both the quantity of water absorbed by the composite laminates and the profile of the moisture distribution through the laminate thickness during exposure to boiling water (accelerated ageing). The numerical results are compared with experimental measurements.

4.2 Theoretical Background of Moisture Diffusion, Fick's Law

Most of the evidence in the literature suggests that water is absorbed by a bulk diffusion mechanism in the resin and for flat plates the rate of moisture absorption $\partial M / \partial t$, through the thickness direction (z) can be described by Fick's second law[7]:

$$\frac{\partial M}{\partial t} = D_c \frac{\partial^2 M}{\partial z^2} \qquad (1)$$

where D_c is known as the diffusion coefficient. It should be remembered that the two main characteristics of Fickian behaviour are: i) the absorption curve should be linear initially and ii) the moisture content should reach a saturation level (M_∞) at large values of $(\text{time})^{1/2}$. Equation 1 can be solved using a finite difference method [6]. A

FORTRAN finite difference program [6] is used for the solution of equation 1 the profile of the moisture distribution through the laminate thickness is determined. The structure of the FORTRAN program is given as a flow chart in figure 1.

When the laminate is exposed to a humid environment it will reach an equilibrium level, where the moisture level throughout the laminate is the same. In order to predict mathematically the content and distribution of moisture in a laminate it is necessary to know the equilibrium level M_∞ (i.e. the maximum amount of moisture that can be absorbed by a laminate at a given humidity) and the diffusion coefficient D. To measure these data normally requires exposure times of over six months, even for relatively thin laminates of say 1 mm thick [6]. In this work the conditioned specimens were immersed in boiling water so the equilibrium level was reached in a period of a few weeks. The moisture equilibrium level depends only on the concentration of moisture or relative humidity of the environment and it is generally accepted to be independent of temperature.

The measurement of M_∞ and D are explained in the following sections.

4.3 Calculation of the Diffusion Coefficient (D)

The moisture diffusion coefficient can be obtained experimentally or by using the Arrhenius Equation[3].

a) Experimental procedure for water absorption.

Test specimens were cut from the T800/924C $[0_8]$ unidirectional (u/d) and $[(\pm 45,0_2)_3]_s$ multidirectional (m/d) composite panels (2 mm x11 mm x110 mm u/d and 245 mm m/d specimens). After cutting, the width of the specimens were ground to 10 mm (u/d) and 50 mm (m/d) by a surface grinder which contains a very high percentage of pure aluminum oxide and has a roughness of 60 grit medium grade. They were then dried in an oven at 50°C. The specimens were immersed in distilled boiling water (accelerated ageing) and removed at various time intervals to determine

their weight. To do this they were placed under cold water for about five minutes to cool down and stabilize at room temperature (RT). They were then removed and excess water on the surface was wiped off using a paper tissue. The specimens were weighed with an accuracy of 0.001g and values recorded in order to calculate the average moisture content, using the expression

$$M\% = \frac{W_w - W_d}{W_d} x100 \qquad (3)$$

where W_w is the current wet specimen weight ,

W_d is the oven dry specimen weight,

and M(%) is the average moisture content absorbed by the material.

The time between removing the specimens from the boiling water, weighing and returning the specimen to the boiling water was kept to approximately 10 min.

It is necessary to find the moisture equilibrium level in order to calculate the diffusion coefficient. The equilibrium level is the condition reached by a material when there is essentially no further change in its average moisture content due to the surrounding environment. When a composite laminate is exposed to boiling water, the moisture from the water is picked up on its surfaces before diffusing through to the inner plies. The surfaces of the laminate are always in equilibrium with the humid environment, *i.e.* surface wetting can be achieved much faster than any loss of moisture from the surface due to diffusion into the inner plies; hence the surface plies of the laminate must contain moisture at a level equal to that of the equilibrium level (M_∞) of the material. When the moisture diffusion is plotted against specimen thickness at different stages in the process the results give rise to the same moisture concentration.

Several unidirectional (2 mm x10 mm x110 mm) and multidirectional (3 mm x50 mm x245 mm) m/d T800/924C specimens were immersed in boiling water; the results of average moisture content against time are plotted in Figs 2a and 2b respectively. In these figures, dotted lines show Fickian diffusion which were calculated by using a FORTRAN program published by Copley [6].

It can be seen from Figures 2a and 2b that the moisture equilibrium level M_∞ (for u/d laminate after about 36 days and m/d laminate after 70 days) was found to be approximately 1.42%.

The analytical solution of equation 1, that can be obtained by the method of separation of variables [8], yields the amount of moisture uptake which varies with time as

$$M(t) = M_o + (M_\infty - M_o)\frac{4}{h}\sqrt{\frac{Dt}{\pi}} \qquad (4)$$

where M_o is initial amount of moisture in the solid, M_∞ is the final amount at equilibrium, and 'h' is the laminate thickness. From equation 4 it is clear why the initial part of the plot of M(t) versus the square root of time should be a straight line. The diffusivity can be now determined using the value of M for two different values times:

$$D_c = \pi\left(\frac{h}{4(M_\infty - M_o)}\right)^2\left(\frac{M(t_2) - M(t_1)}{\sqrt{t_2} - \sqrt{t_1}}\right)^2 \qquad (5)$$

Equation 5 is often considered with M_o=0. The diffusivity can now be determined by using equation 5 and the slope of Figs. 2a and 2b for the unidirectional and $[(\pm 45/0_2)_3]_s$ multidirectional laminate, respectively.

The slope $M/\sqrt{t}$ is obtained from using the complete specimen(finite plate) and therefore includes moisture diffused through all six surfaces. This gives a greater

slope than would have been obtained for an infinite plane sheet as moisture had diffused through six sides instead of two. To give a better estimate of the true one dimensional coefficient D_∞ a correction factor given by Shen and Springer [9] is used:

$$D_\infty = D_c\left(1+\frac{h}{W}+\frac{h}{\ell}\right)^{-2} \qquad (6)$$

where w(mm) and ℓ (mm) are the specimen width and length, respectively. This equation assume that the diffusion is isotropic.

b) Arrhenius equation [3]

The moisture diffusion coefficient can be estimated from Arrhenius equation, i.e

$$D_\infty = R_c \exp(-\frac{E}{G_c T}) \qquad (7)$$

where R_c is a constant for the resin system related to diffusion coefficient ($mm^2\ s^{-1}$),

E is the activation energy of the diffusion process ($kJ\ mol^{-1}$),

G_c is the ideal gas constant ($J\ K^{-1}\ mol^{-1}$) (E/G_c=4000 for 924C epoxy resin system)

and T is the absolute temperature (K).

In equation 7 D_∞ depends on temperature but is independent of humidity level.

The equilibrium moisture level could be theoretically determined from

$$M_\infty = \alpha RH \qquad (8)$$

where α is resin constant and RH= relative humidity. Once the resin constants R_c and α are known for the resin system examined, D_∞ and M_∞ can be obtained and using equation 1 and the moisture distribution through the laminate thickness can be found.

For the T800/924C system the resin constants α and R_c have been estimated for measurement of M_∞, D_c (given by equation 5) and found equal to 0.0142 and 0.038 respectively. These values provided the input to the computer program.

4.4 Measurement of Through Thickness Moisture Distribution

Three unidirectional (2 mm x10 mm x30 mm) and three $[(\pm 45,0_2)_3]_s$ multidirectional (3 mm x50 mm x20 mm) T800/924C specimens were immersed in boiling water. After 10, 20 and 36 days (for unidirectional) and 10, 20 and 70 days (for multidirectional) specimens were removed for sectioning and moisture content measurement. Upon removal from the boiling water they were wiped with a paper tissue before being weighed.

After obtaining the average moisture content, the specimens were sliced in order to measure the moisture absorption through the thickness of the laminate. A sharp knife was used for slitting the specimens.

A blade was connected to a metal bar which was attached to a milling machine chuck. It was set-up parallel to the vice edges, and the specimen was placed in the vice. The milling machine bed was displaced by 0.266 mm for each slitting operation time which is equal to the two ply thickness. After slitting, each slice was weighed immediately. All slices were kept in an oven at 50°C for four hours and then weighed again and the moisture content through the half thickness of the specimen was derived. The values obtained are plotted in Figures 3a and 3b.

The diffusion coefficient and equilibrium moisture content (M_∞=1.42%) are used with the computer finite difference program developed in [6] to estimate the through thickness moisture distribution, Figures 3a and 3b. The program models one-dimensional moisture diffusion in materials which exhibit Fickian diffusion characteristics; it is interactive and it accepts either a diffusion coefficient and surface moisture level or the environmental conditions, i.e., temperature and humidity. From

figures 3a and 3b, it is clear that although Fick's law does not exactly model the actual diffusion, it is sufficiently accurate for the cases examined.

4.5 Prediction of Glass Transition Temperature (T_g)

The glass transition temperature T_g was calculated by using the micro hardness test technique[10]. A 50 mm x20 mm x3 mm T800/924C multidirectional dry specimen was put on a heating block which was connected to a temperature controller. When the specimen reached the setting temperature it was left for about 15 minutes for the temperature to reach the same level throughout its thickness. Then micro hardness tests were conducted at various temperature levels by using the Mitutoyo Micro Hardness Tester. For each temperature level 10 readings were taken from the Tester and the lowest values were taken for plotting; the highest values were fibre rich areas. The average hardness was calculated for each environmental condition and the values were then plotted against temperature (Figure 4).

The same procedure was followed to determine T_g of a wet specimen with a 1.42% moisture level. Micro hardness tests were performed at various temperatures and 95% RH. The results are presented in Figure 4. The hardness test results can be described by the following equations.

$$H_D = 53.7 - 8.9x10^{-2}T_{dg} \qquad (9)$$

$$H_W = 44.9 - 5.67x10^{-2}T_{wg} \qquad (10)$$

where H_D and H_w are the average hardness (Vickers) for dry and wet conditions, respectively. T_{dg} is the dry glass transition temperature and T_{wg} is the wet glass transition temperature..

The glass transition temperature for the T800/924C dry specimen is approximately 190°C. The hardness of the materials should be the same ($H_D = H_w$) at

the glass transition temperature level, for any environmental condition (dry or wet), then Equations (9-10) can be written as

$$8.9T_{dg} - 5.67T_{wg} = 8.8x10^2 \qquad (11)$$

From Equation (10) the wet glass transition temperature, T_{wg} can be determined (T_{wg}= 136°C).

4.6 Concluding Remarks

The diffusion coefficient and the equilibrium moist content are measured and used with a computer program developed in [6] to estimate through thickness moisture distribution. It is found that although Fickian diffusion does not exactly model the actual moisture absorption, in the T800/924C composite system, it is sufficiently accurate for the cases examined. Further work is required to study the effect of stacking sequence on the moisture diffusion.

Moisture content can affect glass transition temperature of the composite laminate. The glass transition temperature of the T800/924C composite system has been reduced by about 50°C when the laminate has a 1.42% by weight moisture content by weight

REFERENCES

1. Potter R.T. and .Purslow, D. The Environmental Degradation of Notched CFRP in Compression *Composites,* Vol.14, No.3, pp.206-225,1983.

2. Barker, A.J. and Balasundaram, V. Compression Testing of Carbon Fibre-Reinforced Plastics Exposed to Humid Environments, *Composites*, Vol.8, No.3, pp.217-226, 1987.

3. Browning, C.E., Husman, C.E. and Whitney, J.M. Moisture Effects in Epoxy Matrix Composites, *AFML-TR-77-41*, 1977.

4. Verpoest, I and Springer, G.S. Effect of Moisture on the Compressive and Interlaminar Shear Strength of Aramid-epoxy Composites. *J. Reinforced Plastics,* Vol. 7, p.23, 1988.

5. Ramani, S.V. and Nelson, H.G. Effect of Moisture on the Fatigue Behaviour of Graphite/epoxy Composite Laminates *NASA Tech. Memo.* 78546, 1979.

6. Copley, A Computer Program to Model moisture Diffusion and Diffusion Coefficient in Fibre Reinforced Plastic Laminates, *RAE. Rep. 81105*, 18 Aug. 1981.

7. Crank, J. The Mathematics of Diffusion, 2nd edition, *Oxford, Clarendon Press* 1975.

8. De Wilde, W.P. and Frokovic, P. The Modelling of Moisture Absorption in Epoxies: Effects at Boundaries, *Composites,* Vol.25, No.2, pp.119-127, 1994.

9. Shen, C. and Springer, S.G., Moisture absorption and desabsorption of composite materials, *J. Comp. Mater.,* Vol.10, pp.2-20, 1976.

10. Whitney, B and Tsai, S.W. Effects on Environment of the Compressive Strength of Laminated Epoxy Matrix Composites, *AFML-TR-79-4179,* December 1979.

Table 1 Moisture diffusion coefficient for a (2x10x110 mm) U/D and a (3x50x245 mm) M/D T800/924C laminate

	U/D	M/D
$D_c = \pi(\frac{h}{4(M_\infty)})^2(\frac{M_2 - M_1}{\sqrt{t_2} - \sqrt{t_1}})^2$	$1.25x10^{-6}$	$1.1x10^{-6}$
$D_\infty = D_c(1+\frac{h}{w}+\frac{h}{l})^{-2}$	$8.42x10^{-7}$	$9.3x10^{-7}$

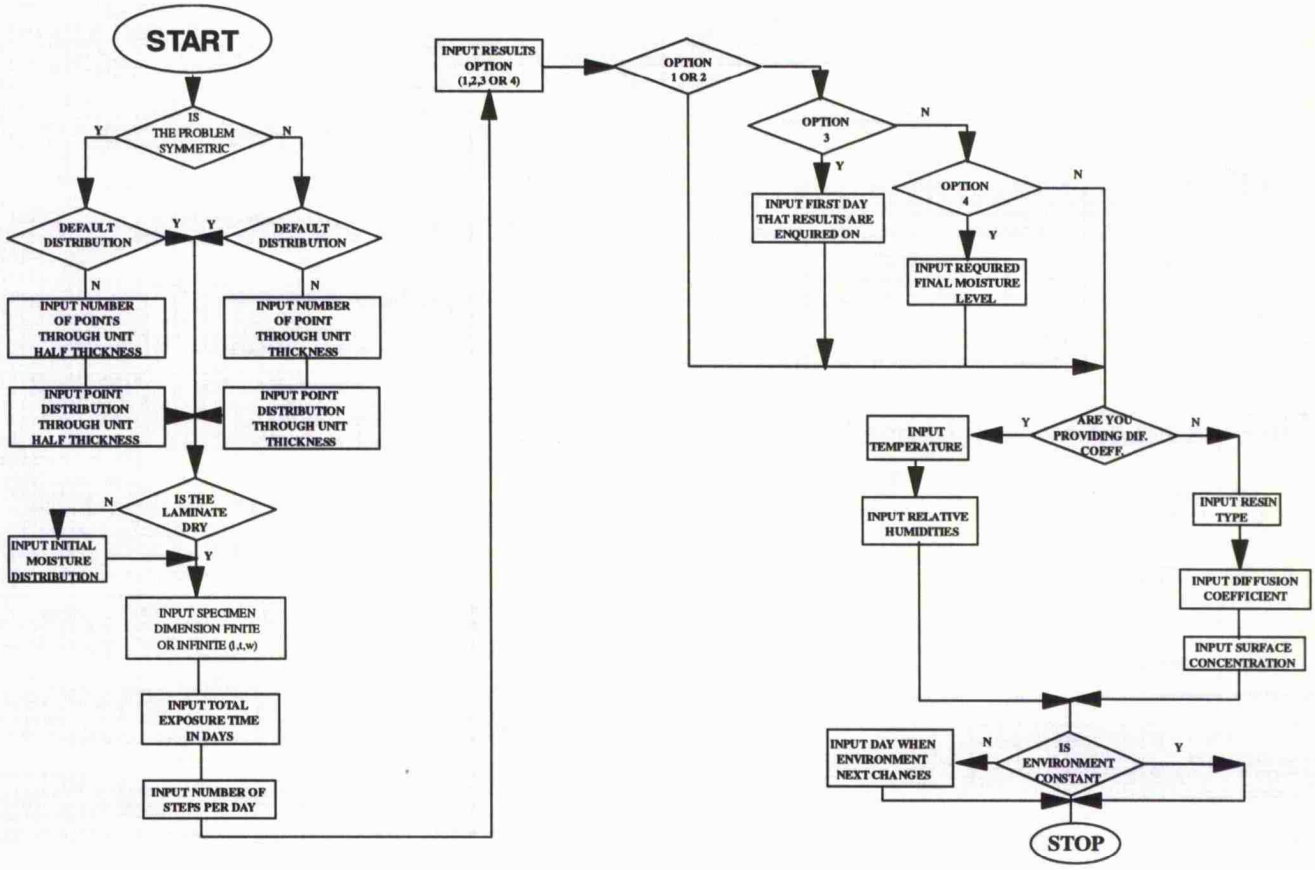

Figure 1 Flow chart of subroutine input[6].

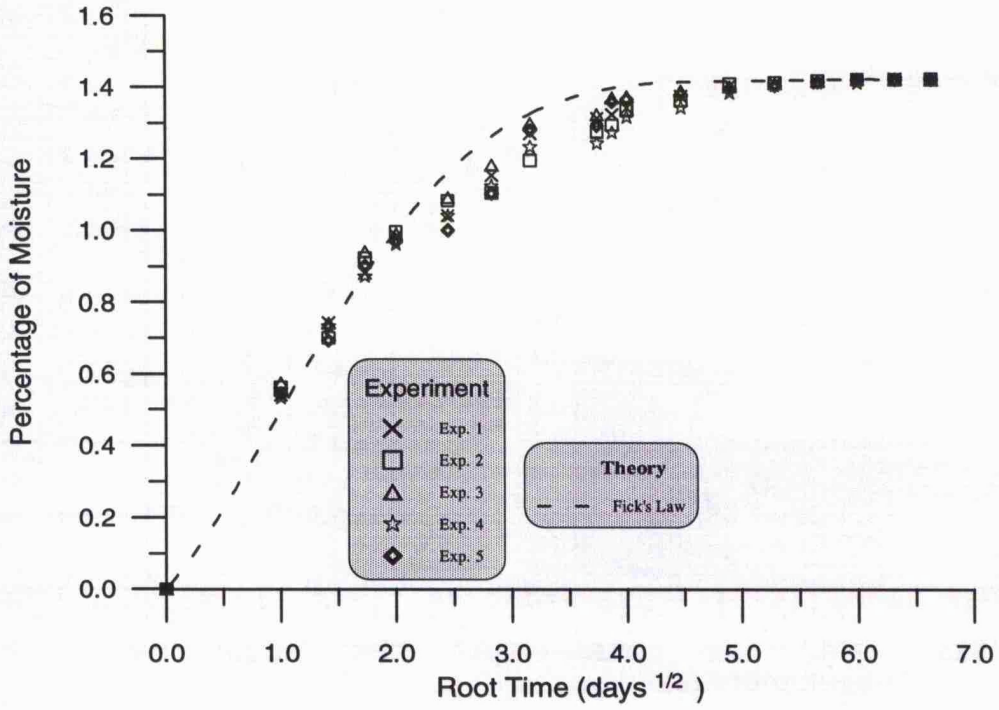

Figure 2.a Moisture uptake in T800/924C U/D specimens immersed in boiling water (2x10x110 mm)

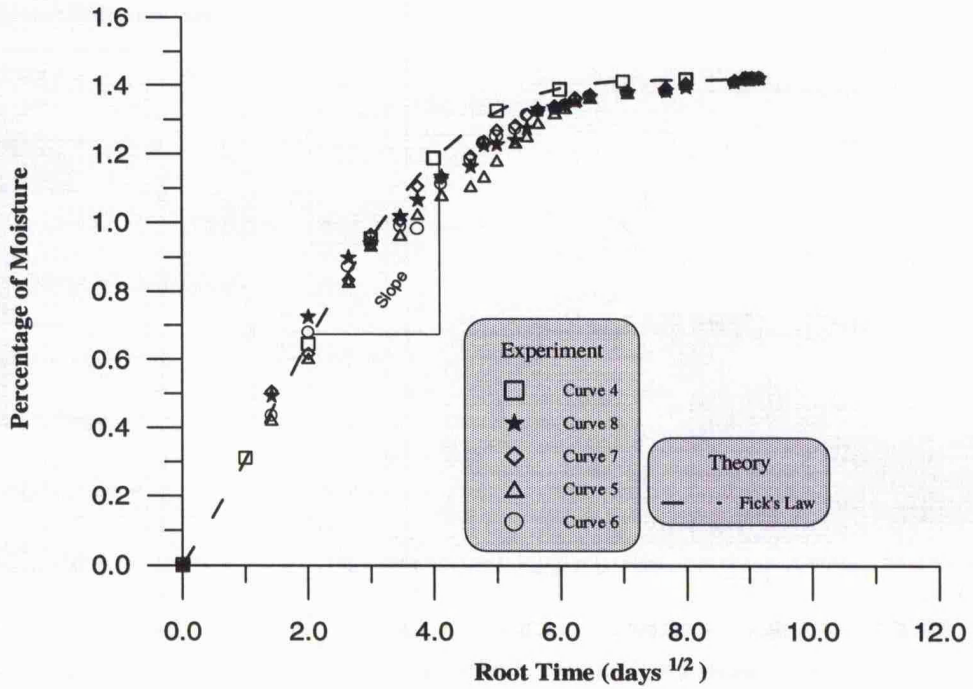

Figure 2. b Moisture uptake in T800/924C $[(\pm 45,0_2)_3]_s$ specimens immersed in boiling wa (3x50x245 mm).

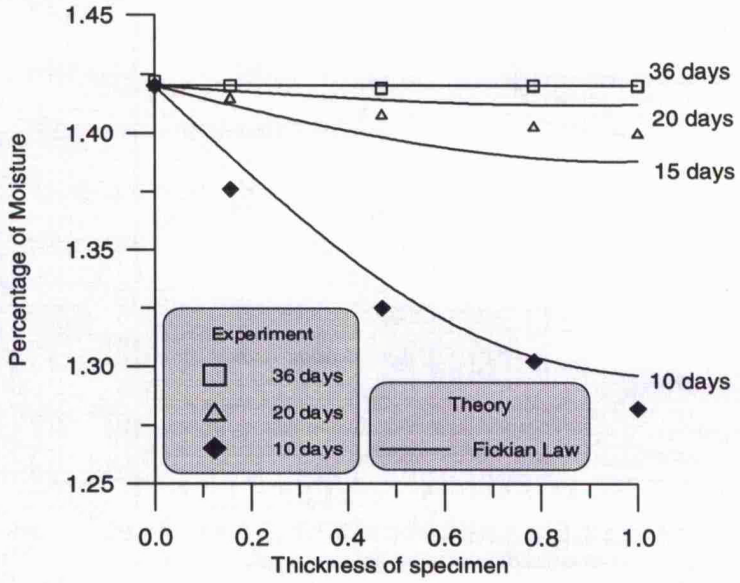

Figure 3 a Moisture absorption through the thickness of a T800/924C u/d specimen (2x10x30 mm)

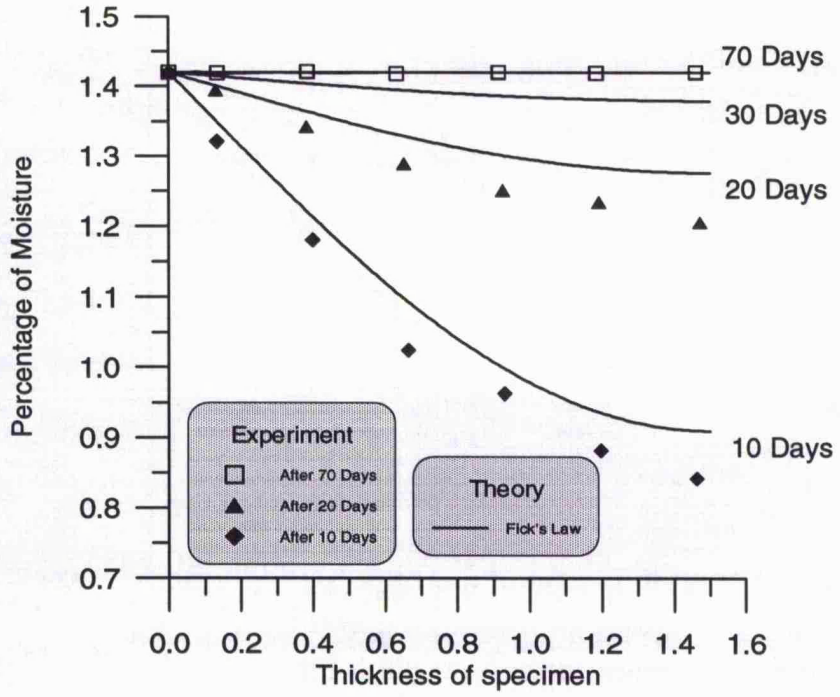

Figure 3 b Moisture absorption through the thickness of a T800/924C m/d specimen ($[(\pm 45,0_2)_3]_s$, 3x50x20 mm)

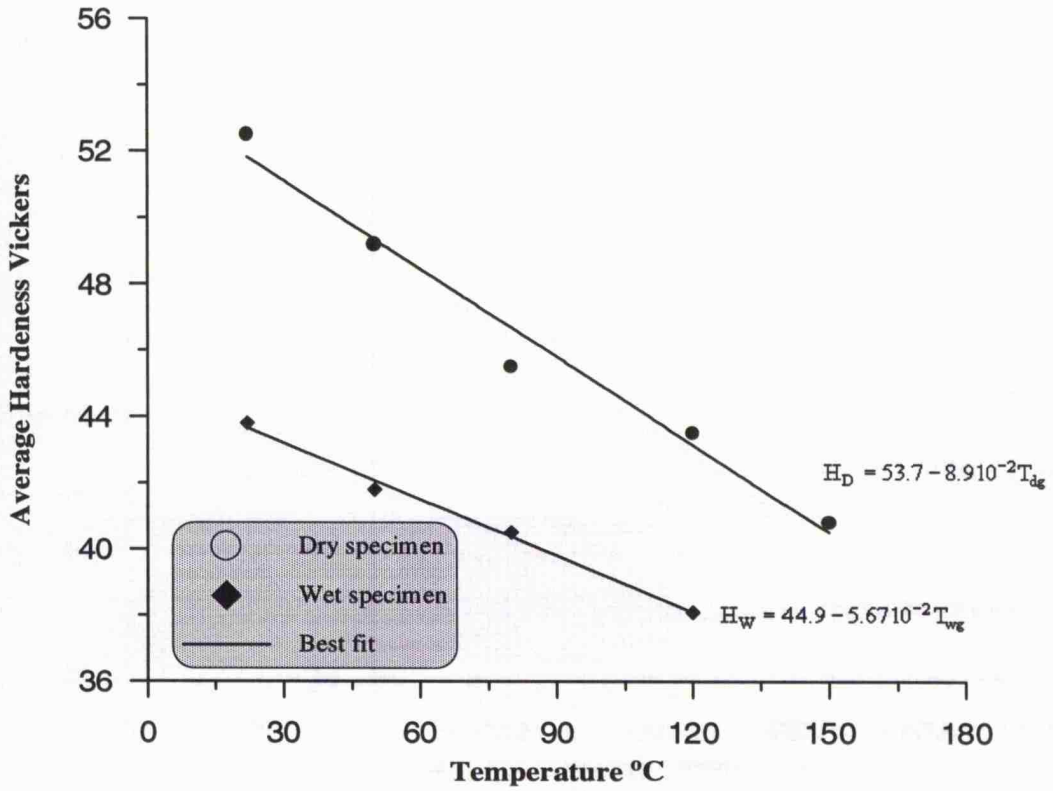

Figure 4. Hardness test results for dry and wet T800/924C specimens.

CHAPTER FIVE

MEASUREMENT OF UNIAXIAL COMPRESSIVE STRENGTH UNDER VARIOUS ENVIRONMENTAL CONDITIONS

5.1 Introduction

Composite materials exhibit high specific strength and stiffness. This makes them attractive for aerospace, automotive and sport industries. There is a concern, however, that the mechanical properties of these materials may suffer when they are exposed to high temperatures and moisture for long periods of time. The majority of composite laminates are based on carbon and glass fibres with a matrix of either epoxy or polyester resin. Polyester based matrix materials are weaker in compression than in tension due to fibre microbuckling [1]. Microbuckling nucleates locally (e.g. at voids, free edge, resin rich regions) and propagates under little additional load through the laminate, along a narrow zone within the 0^{o} plies causing a loss in structural integrity. It is suggested [2-5] that failure induced by fibre microbuckling is dependent on the shear strength/modulus of the polymer matrix. To evaluate the validity of these models the present study investigates the effect of resin ductility, by varying the test temperature and moisture content, on the compressive strength of unidirectional carbon and glass fibre epoxy laminates.

The compressive properties of carbon-epoxy (T800/924C) and glass-polypropylene (Plytron) composite systems, are presented under various environmental conditions (hot-dry and hot-wet). Fracture characteristics are identified using optical and scanning electron microscopy. Shear strength results are also

discussed for the T800/924C composite; existing models suggest that the compressive strength is a function of shear yield stress and initial fibre misalignment.

5.2 T800/924C Carbon fibre/Epoxy Composite Laminate

5.2.1 Shear strength properties of T800/924C unidirectional laminate

At least five specimens were tested under shear loading in hot-dry (20°C, 50 °C, 80 °C and 100 °C, and dry) and hot-wet (20°C, 50 °C, 80 °C and 100 °C, with 95% RH) conditions to measure the shear properties of the a T800/924C unidirectional composite. The tests were performed using the a Wyoming test fixture (Iosipescu test) and the specimens failed in 60-90 seconds using a screw driven machine of load capacity 50 kN.

a) Shear strength data in hot-dry and hot-wet conditions.

The hygrothermal state affects the stress-strain behaviour of composite materials in two different ways; the properties of the constituents may vary with temperature and moisture concentration, and fabrication residual stresses are altered by the hygrothermal state. Since the fibres are usually the least sensitive to environment, hygrothermal effects are most noticeable in matrix dominated properties, e.g., transverse tensile, transverse compressive, and in-plane shear properties.

Effects of temperature on the shear strength properties response of the T800/924C composite system are presented in Table 1. It can be seen that the coefficient of variation for strength is less than 5%. The stress-strain curves are presented in figure 1. From this figure the secant shear moduli were measured at 0.5% applied shear-strain. The shear modulus and shear strength decrease gradually with increasing temperature while the failure strain increases. The matrix dominated properties such as in-plane shear modulus and the corresponding strength, degrade by 20% at 100°C.

The effects of moisture on the shear properties of the T800/924C laminate was measured and the results are shown in Table 2. The shear strength is further reduced

(by 24%) when the laminate contains 1.42% moisture by weight and is tested at 100°C and 95% RH. The temperature and humidity effects on the shear strength of unidirectional laminates are presented in figure 2.

b) Failure modes

Axial splitting and delaminations were observed in the 0° test specimens. Cracks initiate at the notch roots and propagate parallel to the fibres on the opposite side to the inner loading points (figure 3). The shear stress concentration at the notch tip is primarily responsible for the crack initiation, and growth [6]. The cracks relieve the localized stress concentrations at the notch tips. After axial splitting, a damage zone appears at approximately 85° to the crack planes at 50°C as shown in figure 3. The damage zones in specimens tested at 100°C consist of numerous short interfacial cracks and extensive fibre breakage and bending as shown in figure 4.

Subsequent to the two intralaminar failure modes the material continued to sustain load with increasing non linearity until interply failure occurred at the inner load points with subsequent progressive crushing.

5.2.2 Compressive strength properties of T800/924C unidirectional laminates

At least five specimens were tested under uniaxial compressive loading in hot-dry (20°C, 50 °C, 80 °C and 100 °C, and dry) and hot-wet (20°C, 50 °C, 80 °C and 100°C, with 95% RH) conditions. The tests were performed using a modified Celanese test jig (with spark-eroded grip inserts) at a constant compression rate of 1mm/min on a screw driven machine of load capacity 50 kN; strength properties and failure modes are discussed in the following sections..

a) Strength data for hot-dry and hot-wet conditions.

The effect of temperature in dry test conditions on the compressive strength/stiffness properties of the T800/924C unidirectional laminate is presented in Table 3. The results quoted in Table 3 are based on the average of five specimens tested at each temperature level; the coefficient of variation is less than 6%.

T800/924C carbon fiber epoxy displays a non-linear stress strain behaviour under compressive loading, with the reduction in stiffness becoming more pronounced with increasing temperature. The room temperature response of a selected specimen is shown in figure 5. The longitudinal strain on the two faces of the coupon (back-to-back strains) is initially the same but as the applied load is increased the strains diverge indicating bending. Such bending cannot be totally avoided in compression testing. It may be the result of an initial imperfection in the specimen. The mean line plotted through the strain points exhibits an initial straight portion with an elastic (secant) modulus of 166.5 GPa, followed by a continuously curved portion with a tangential modulus at failure approximately 10% less than that of the linear part. This non-linear stress-strain response is attributable to elastic fibre microinstability that is initiated, as soon as compression loading commences, by any initial fibre waviness or misalignment. The average failure strength is 1395 MPa and the mean failure strain 0.93%; the maximum compressive strain on one face of the specimen at failure (i.e., the sum of the direct and bending strains) is approximately 1%. If this value of 1% is used in conjunction with the projected mean stress-strain response of figure 5, it is evident that it represents a failure stress of 1500 MPa. Similar results were obtained in [7] from straight-sided specimens with carefully bonded aluminum tabs. This suggests that the spark-eroded grip inserts used in the present study introduce the compressive load successfully into the specimen, without causing any damage on the faces of the composite and hence premature failure is avoided [8]

The compressive stress strain responses for T800/924C u/d laminate tested at high temperatures are shown in figure 6, data are plotted up to the ultimate strength. The elastic modulus and Poisson's ratio were measured for each temperature level from the stress-strain curve at 0.25% applied strain.

It can be seen from Table 3 that high temperature has a marked influence on the composite's compressive behaviour. At an operating temperature of 100 ^{o}C dry the strength has been reduced by more than 30% (figure 7), the failure strain has dropped from 0.93% to 0.728% (figure 8) and the elastic modulus has changed from 166.5GPa to 137 GPa (figure 9). The Poisson's Ratio has slightly increased with increasing temperature (figure 10). The compressive strength and stiffness have been reduced

due to the reduction of shear properties. In uniaxial compression a reduction in matrix strength properties means reduced support for the fibres, which promotes premature failure of the composite by fibre microbuckling [9]

The compressive strength is further reduced (by 53%) when the laminate contains 1.4% by weight moisture and is tested at 100°C and 95%RH. It can be seen from the results shown in Table 4, that the compressive strength (σ_c) is only 20% of the elastic shear modulus; remember that Rosen's analysis of fibre buckling predicts that σ_c is equal to the shear modulus. This suggests that a plastic-buckling analysis is required in order to estimate strength more accurately. The results quoted in Table 4 are based on the average of five specimens tested at each environmental condition; the coefficient of variation is less than 5%. The results are also plotted in figure 11, which shows the compressive strength-temperature relationship in hot-dry and hot-wet environmental conditions

b) Failure Modes

i) Hot-dry conditions

Failure occurred predominantly within the gauge section as shown in figure 12. All specimens failed suddenly and catastrophically. After failure the load dropped essentially to zero. Most of the tested specimens show secondary fibre micro buckling. A typical example is shown in figure 13. Longitudinal splits and fibre/matrix debonding do not occur gradually but take place suddenly and concurrently with the final failure. Fibre microbuckling is considered as the critical damage mechanism, which causes the catastrophic fracture. The specimens which were tested at dry conditions generally fail along a $\pm 20°$-$30°$ ($=\beta$) line from the transverse direction; secondary fibre microbuckling is also inclined at a similar angle, figure 13. Figure 14 shows an optical micrograph which illustrates in-plane fibre microbuckling in a specimen tested at room temperature; it grows across the specimen width at an angle $\beta \approx 25°$ to the horizontal axis.

A typical view at low magnification of the fracture surface is shown in figure 15. The fracture is transverse and is accompanied by extensive longitudinal cracking in the

direction of fibres within, and at the boundaries of the plies. The latter cracks are delaminations. The microscopic surface of the fracture is stepped. Figure 16 shows such a step observed under the SEM examination. This feature is typical of failure of the fibres by microbuckling, which, as a rule, is the main mode of failure in compression [10].

Purslow [10] has noted that the height of the step is a multiple of half the wavelength for fiber buckling. A detailed micrograph of the fracture surface at relatively high magnification is shown in figure 17. The fracture propagated through the individual fibres from the tensile to compressive side in a direction perpendicular to the buckling axis. The fracture direction and height common to all the fibres in a step indicate localized crack propagation. Thus, the buckling axis can be used for determination of the direction of crack propagation through a region of the fracture and possibly for identification of the local failure origin. The arrow in figure 17 indicates the direction of bending and crack propagation through the region shown.

In the case of specimens tested at temperatures higher than 50°C, as figure 18 shows, fracture occurs in the middle of the specimen and is almost perpendicular to the loading axis. Subsequent examination by scanning electron microscopy (SEM) revealed that the fibres underwent out-of-plane microbuckling. The strain at which this failure mode initiates is reduced with increasing temperature and at 100°C is only 75% of the strain required to initiate in-plane microbuckling. Thus, any weakening of the matrix or fibre/matrix interface arising from elevated temperatures increases the probability of out-of-plane buckling (figure 18) of the fibres which results in degraded compressive strength. Figure 18 is taken from the secondary fibre microbuckling region through the thickness. Figures 19 a&b show SEM views of the fracture surface of a unidirectional compressive specimen tested at 50°C. Similar fracture characteristics were observed in specimens tested at 100°C

ii) Hot-wet conditions

The specimens which were tested in hot-wet conditions generally failed along a $\pm 15\text{-}20^{\circ}$ ($=\beta$) line from the transverse directional; primary and secondary fibre microbuckling were observed, except in specimens tested at 100°C hot-wet. In a

100°C hot-wet test the specimen failed at almost $\beta \approx 0$, figure 21. Figure 20 shows overall fracture of unidirectional specimens. They were tested in hot-wet conditions and contained 1.42% by weight moisture. Figure 21 shows a failed unidirectional specimen which illustrates secondary fibre microbuckling and splitting. Optical microscopy was used to examine the failure through the thickness. In the case of specimens tested in hot-wet conditions damage occurs in the centre of the specimen and grows almost perpendicular to the loading axis. Subsequent examination by scanning electron microscopy revealed that the fibres underwent out-of-plane microbuckling. From room temperature to 100°C all failures are out-of-plane microbuckling as shown in figure 22 a&b. The strength properties of the specimens tested in hot-wet conditions are substantially reduced, see Table 4. This is attributed to the reduction in matrix strength properties and weakening of the ply interface with increasing temperature and environmental conditioning. Thus, in compression the matrix and interface play a key role in providing side support to the fibres and consequently resistance to fibre buckling.

SEM examination revealed that the morphology of the fracture surface was significantly affected by the absorption of moisture. There is an increase in the amount of fibre/matrix debonding in the specimens that absorbed moisture (1.42% by weight) and were tested at elevated temperature and humidity (95% RH). This is due to weakening of the fibre matrix bond. The fractographic surface of a room temperature wet compression specimen studied by SEM is shown in figure 23a. Figures 23b and c show in more detail the fractured surface. Under compressive testing longitudinal cracks propagate along the fibre/matrix interfaces and along the layers of resin between adjacent plies. Fibre matrix debonding due to humidity can be seen in figures 23b and c. Humidity can also change fiber fracture surface. Fibres do not clearly show tension compression behaviour (as in hot-dry tests) on their fracture surfaces as shown figure 23 c. Typical fracture surfaces of specimens tested at 80°C and 100°C are shown in figures 24-25 (with M_∞=1.42%) tested at 95% RH environment. Moisture plasticises the matrix and reduces the glass transition temperature (Tg) by about 40 °C and causes the resin to swell. Moisture and temperature cause a large reduction in strength and increase in plasticity. Figures 24-

25 b and c show that in the hot-wet specimen the matrix has parted cleanly from the fibres over most of the fracture. Moisture between fiber and matrix causes fibre matrix debonding.

5.3 Plytron (Glass/polypropylene)

5.3.1 Celanese compression tests of $[0]_{4s}$ laminates at high temperatures

a) Stress strain data

Compression tests were carried out to investigate the mechanics of uniaxial compressive failure in unidirectional $[0]_{4s}$ plytron laminates at various temperatures: room temperature, 50°C, 80°C, 100°C and 120°C (the specimen design and test technique with an environmental unit were described in chapter three). Compressive failure in all specimens is catastrophic and quite localized, (Figure 26). A kink band structure (fibre microbuckling) occurs without warning and immediately leads to laminate breakage. Fracture is within the specimen gauge length implying that the test is successful. A plot of the applied axial stress as a function of average axial strain measured by back-to-back strain gauges is shown in figure 27, for a typical specimen tested at room temperature. The mean compressive strength is 317 MPa, which is less than 60% of the tensile strength. The average failure strain and the Young's modulus (measured at 0.25% applied strain) are 0.98% and 29.5 GPa, respectively. The effect of temperature on compressive properties of the unidirectional laminate can be seen in Table 5 and also the results are plotted in Figure 28.

The values quoted in Table 5 are based on the average of five specimens tested at each temperature level. The results demonstrate that temperature has a marked influence on the compressive strength. At operating temperature of 120°C the strength has been reduced by more than 60% and the failure strain has dropped by approximately 50%. This is because the modulus and strength of the matrix has reduced substantially with increasing temperature. In uniaxial compression, reduction in matrix strength properties means reduced side support for the fibres, which promotes premature failure of the composite by fibre microbuckling. The tensile properties of plytron are tabulated in tables 6-8 for comparison purposes. It can be

seen that the compressive strength is more temperature dependent than the tensile strength[11]. More details are given in [11]. In general, the tensile strength of a composite depends more on its fibre reinforcement, but compressive strength relies more upon its matrix material.

The compressive properties of a laminate tested at 120°C were as follows: the elastic modulus was reduced by 38%, the tensile stress reduced by 66% and the failure strain reduced by 52%. The normalized longitudinal stiffness can be written as a linear function of temperature i.e,

$$\frac{E_{11}}{E_{11}^{RT}} = 1 - K(\theta - \theta_o) \quad (K=3.73\ 10^{-3}) \qquad (1)$$

where E_{11} is the elastic modulus in the loading direction, θ is the testing temperature in the range (20°-120°C) and θ_o is the room temperature (20°C), Figure 29. The normalized longitudinal strain is written as,

$$\frac{\varepsilon_{11}}{\varepsilon_{11}^{RT}} = 1 - K(\theta - \theta_o) \quad (K=5.1\ 10^{-3}) \qquad (2)$$

where ε_{11} is strain in loading direction, Figure 30. Finally, the normalized longitudinal stress can be written in terms of temperature as,

$$\frac{\sigma_f}{\sigma_f^{RT}} = 1 - K(\theta - \theta_o) \quad (K=6.47\ 10^{-3}) \qquad (3)$$

where σ_f is the failure stress under uniaxial compression, Figure 31.

b) Compressive fracture modes

Sections from failed specimens (cut from the edge and across the width) were mounted in a resin block, polished and photographed under an optical microscope. The specimens were examined in order to determine the failure mode at each environmental condition. From the optical microscopy pictures the kinking length ℓ_k, boundary orientation angles β_1 and β_2 and the inclination angle ϕ were measured for

the above environmental conditions and their values are summarized in the appendix I. It can be seen that the fibre boundary orientation angle β_1 depends on temperature. Some specimens showed some secondary microbuckling, figure 32. Damage to the room temperature unidirectional specimens involves fibre movement in the plane of the laminate (in-plane fibre microbuckling) along a 20^0-25^0 line from the transverse axis, figure 33. In figure 33 the optical micrograph shows that the fibres break at two points, which create a band inclined at $\beta_1 \approx 25^o$ to the horizontal axis (or 65^o to the fibre axis). It was observed in all specimens that angle β_1 remains constant. The microbuckle once started either from the free edge or from a pre-existing material imperfection such as a void or a resin rich region or a fibre misalignment, keeps its orientation and propagation. Berg and Salama [12] argued that kink bands must be inclined in order to permit the buckled fibres to undergo both compressive and shear deformation. The reason is that microbuckling along planes which permit shear displacement as buckling proceeds requires smaller compressive stress than does buckling on a plane that does not permit shear displacement. (i.e. planes perpendicular to the fibre axis.) The broken fibre segments in figure 33 are approximately 35-40 fibre diameters long and have rotated by almost 30^o from the loading axis ($\phi=30^o$). Once failure has occurred, the kink inclination angle ϕ can increase rapidly if the load is not immediately removed. These values are similar to those reported by Hahn [13] for S-glass epoxy composite. For a carbon fibre epoxy system examined in [7], β_1 was found equal to 5^o-15^o, $\phi=30^o$ and w=8-10 fibre diameters. Whether the angle of kink band inclination and the kink band width are of significance is still unclear. Scanning electron micrographs of the fracture surface of a selected glass polypropylene specimen are shown in figures 34 a&b. The surface exhibits well defined steps and it is evident from figure 34b that each fibre fails in bending.

In the case of specimens tested at temperatures higher than 50°C damage was confined to out-of-plane deformation in an almost 90^o kink band across the specimen width (figure 35). The kink band width measured 40-60 fibre diameters. Failed specimens show features quite distinct from those observed in specimens in which fibre buckling occurred in-plane, figure 33. Out-of-plane fibre microbuckling (fibres rotated in the x-z plane) is shown in figure 36. The strain level at which out-of-plane

microbuckling initiates is reduced with increasing temperature and at 120°C is less than 50% of the strain required to initiate in-plane microbuckling. Thus the out-of-plane microbuckling has been precipitated by lower matrix strength/stiffness and a weaker ply interface reduction of fibre/matrix bond in the hot specimen. Clearly, any weakening of the matrix properties or fibre/matrix interface arising from elevated temperature increases the probability of out-of-plane buckling of the fibres.

5.4. Conclusions

Untabbed straight-sided T800/924C carbon-epoxy and Plytron specimens give acceptable failure modes and locations when tested with special grip insert in a modified Celanese test rig provided. The faces of the grip inserts are spark-eroded to produce a surface finish of approximately 20 Ra. No damage to the surface plies is observed in specimens with uniform thickness and specimen preparation costs are substantially reduced. The strength/stiffness properties and failure modes are comparable to those obtained from specimens with carefully bonded aluminum tabs. With spark-eroded grips, tabs are not required in compression testing.

The strength properties of T800/924C have dropped more than 20% at an operating temperature of 100°C-dry. The compressive strength is further reduced (by 53%) when the laminate contains 1.42% by weight moisture and is tested at 100°C and 95% RH. At operating temperature of 120°C-dry the compressive strength of plytron has been reduced by more than 60% and the failure strain has dropped by approximately 50%. Moisture and temperature cause a large reduction in strength and increase plasticity. This is attributed to the reduction in matrix strength properties and weakening of the ply interface with increasing temperature and environmental conditioning.

Most of the T800/924C carbon-epoxy specimens show secondary fibre microbuckling in hot-dry and hot-wet conditions. In the case of specimens tested in various environment conditions damage occurs in the centre of the specimens and out-of-plane fibre microbuckling grows almost perpendicular to the loading axis. Under compressive testing longitudinal cracks propagate along the fibre/matrix

interfaces and along the layers of resin between adjacent plies. Humidity can also cause matrix/fibre debonding.

The compressive failure of unidirectional glass/pp laminates occurs due to fibre microbuckling, regardless of temperature. In the case of specimens tested at above approximately 50°C the failure mode changes from in-plane to out-of-plane microbuckling, which initiates at lower applied strains. Failure initiation depends also on material imperfections, such as voids, resin rich regions and fibre misalignment.

The progressive decrease in strength with increasing temperature is associated with a reduction in matrix shear strength properties with increasing temperature. Thus, in compression the matrix and interface play a key role in providing side support to the fibres and consequently resistance to fibre microbuckling. In currently used composites the strength of carbon and glass fibres has been substantially increased while polymeric matrices have changed very little in strength due to demands for high toughness of composite. As a result, the fibres fail by microbuckling before their compressive strength is reached.

REFERENCES

1. Harper, J.F. and Heumann, T.O., Failure Mechanisms in Uniaxial Compression in Fibre Composites, *4th International Conference on Fibre Reinforced Composite,* Proceeding of the Institution of Mechanical Engineers, pp.231-235, 27-29 March 1990 Liverpool.

2. Collings, T.A., Harvey R.J., and Daizel A.W., The Use of Elevated Temperature in the Structural Testing of FRP Components for Simulating the Effect of Hot and Wet Environmental Exposure, *Composites*, Vol.24, No.8, pp.625-634, 1993.

3. Argon, A.S., Fracture of Composites, *Treatise on Materials Science & Technology*, Vol 1, Academic Press, New York, pp. 79-114, 1972.

4. Evans, H.T., Compression Failure Mechanisms in Composite Structures. NASA CR-3988, 1986.

5. Evans, A.G. and Adler, W.F., Kinking as a Mode of Structural Degradation in Carbon Fibre Composites. *Acta Metallurgica*, Vol.22, pp.725-738, 1977.

6. Barnes, J.A, Kumasa, M. and Hull, D. Theoretical and Experimental Evaluation of the Iosipescu Shear Test. *Composite Science and Technology*, Vol.28, p.251-268, 1987.

7. Soutis, C., Measurement of Static Compressive Strength of Fibre/epoxy Laminates, *Composite Science and Technology*, Vol.42, pp. 373-392, 1991.

8. Soutis, C. Turkmen, D. and Morrison, C.J., Compressive Failure of Unidirectional Composites at Elevated Temperature Using Untabbed Specimens, *ECCM CTS2*, pp 169-177, 1994.

9. Soutis C. and Turkmen D., High Temperature Effects on the Compressive Strength of Glass Fibre-reinforced Composites, *Proceedings of the Ninth International Conference on Composite Materials (ICCM/9),* Madrid, 12-16, pp 581-588, July 1993.

10. Purslow, D., 'Some Fundamental Aspect of Composites Fractography' *Composites*, p.241, October 1981.

11. Turkmen, D. High Temperature Effects on the Compressive Behaviour of Glass/Polypropylene Laminates, *University of Leicester Engineering Department* Report 92-3, Jan. 1992.

12. Berg, C.A. and Salama, M., Fatigue of Graphite Fibre-Reinforced Epoxy in Compression, *Fibre Science & Technology*, vol.6, pp.725-738, 1973.

13. Hahn, H.T, Compression Failure mechanisms in Composite Structures, *NASA CR-3988*, 1986.

Appendix I

Fibre microbuckling geometry observed in plytron at various temperatures.

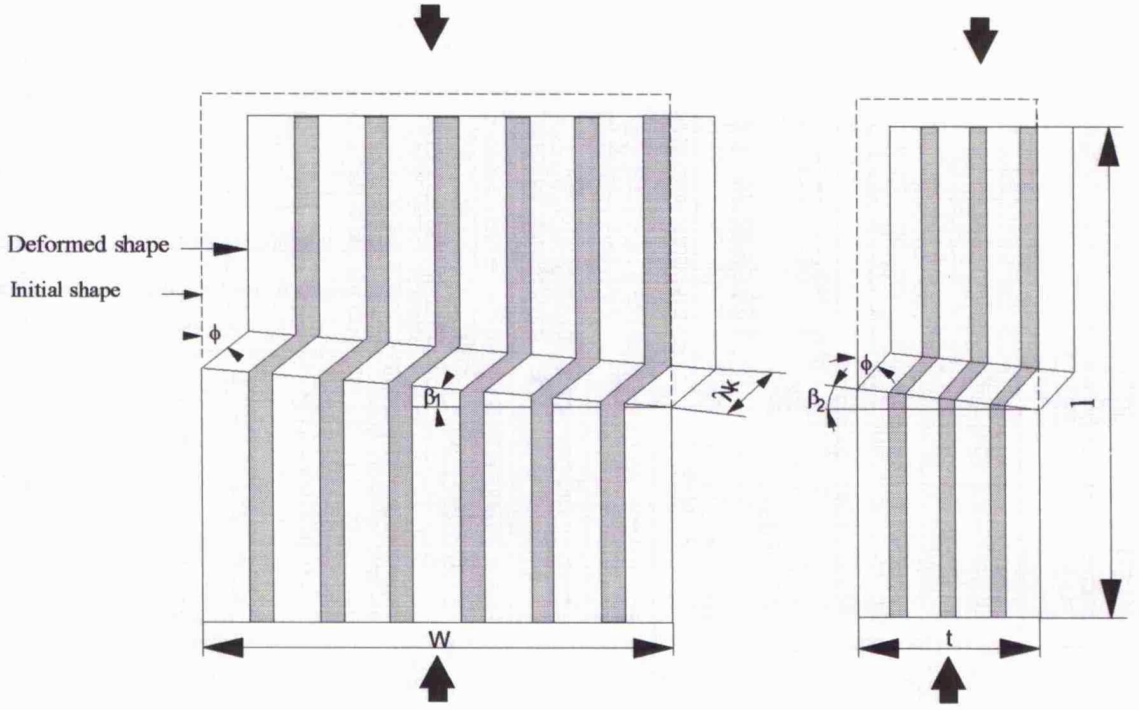

w=specimen width and t=specimen thickness.

At room temperature

$\phi = 30^\circ$	$\phi = 24^\circ - 33^\circ$
$\beta_1 = 24^\circ$	$\beta_2 = 24^\circ$
$\lambda_k = 0.88 - 1.00$ mm	$\lambda_k \cong 1$ mm
$d_f \cong 25\ \mu m$	
$\lambda_k / d_f = 35 - 40$	

At 50°C

$\phi = 18^\circ$	$\phi = 24^\circ - 35^\circ$
$\beta_1 = 18^\circ$	$\beta_2 = 16 - 18^\circ$
$\lambda_k = 1 - 1.50$ mm	$\lambda_k \cong 1 - 1.8$ mm
$d_f \cong 25\ \mu m$	
$\lambda_k / d_f = 40 - 72$	

At 80°C

$\phi = 30°$	$\phi = 25° - 30°$
$\beta_1 = 5°$	$\beta_2 = 25°$
$\lambda_k = 1 - 1.50$ mm	$\lambda_k \cong 0.8 - 1.4$ mm
$d_f \cong 25\ \mu m$	
$\lambda_k / d_f = 35 - 60$	

At 100°C

$\phi = 50°$	$\phi = 50° - 55°$
$\beta_1 = 18°$	$\beta_2 = 28°$
$\lambda_k = 1 - 1.20$ mm	$\lambda_k \cong 1 - 1.5$ mm
$d_f \cong 25\ \mu m$	
$\lambda_k / d_f = 40 - 60$	

At 120°C

$\phi = 50°$	$\phi = 50° - 55°$
$\beta_1 = 3°$	$\beta_2 = 30°$
$\lambda_k = 1 - 1.40$ mm	$\lambda_k \cong 1 - 1.5$ mm
$d_f \cong 25\ \mu m$	
$\lambda_k / d_f = 40 - 60$	

10. TABLES

Table 1 T800/924C u/d specimens tested by using an Iosipescu test rig at various temperatures (hot-dry)

Test temperature. °C	Average shear strength MPa	Coefficient of strength variation %	Average Shear Strain %	Average Shear Mod. G_{12}^{+}, GPa
20	111	3.1	6.4	6.05
50	104.6	1.85	6.77	5.79
80	98	1.92	7.43	5.42
100	88.8	2.37	6.39*	4.9

* Strain gauge failure

$^{+}$ Shear modulus measured from secant modulus at 0.5% applied shear strain

Table 2 Pre-soaked T800/924C u/d specimen (with 1.42% moisture by weight) tested in shear at hot-wet conditions (using Iosipescu test rig)

Test temperature. °C	Average shear strength MPa	Coefficient of variation %
20	102.4	1.48
50	96.8	2.35
80	90.6	0.9
100	84.55	0.8

Table 3 T800/924C u/d specimen tested under uniaxial compression at hot-dry conditions.

Test Temp. °C	Ave. Failure Strength. MPa	Coefficient of strength variation %	Average fail. strain %	Poisson's Ratio ν_{12}*	Young's m. (E_{11}) GPa*
20	1395	2.27	0.925	0.353	166.5
50	1230	1.07	0.842	0.359	154
80	1137	4.85	0.742	0.361	148
100	973	5.5	0.728	0.37	137

*Measured from secant modulus at 0.25% axial strain * Strain-gauge failure

Table.4 T800/924C u/d specimen tested under uniaxial compression at hot-wet condition (pre-soaked specimen with 1.42% moisture)

Test temperature and humidity °C-95%RH	Average Failure Strength MPa	Coefficient of. Variation %
20	1060	2.4
50	930	2.3
80	828	2.25
100	654	4.15

Table 5 Compressive strength properties of a $[0]_{4s}$ glass polypropylene laminate at various temperatures.

Temperature °C	20	50	80	100	120
Modulus E_{11} (GPa)	29.5	27	25.3	23	20
Strength σ_f (MPa)	317	234	177	148	108
Strain to failure ε_f (%)	0.98	0.85	0.68	0.54	0.47

Table 6 Tensile strength properties of a $[0]_{4s}$ glass polypropylene laminate at various temperatures.

Temperature °C	20	50	80	100	120
Modulus E_{11} (GPa)	29.5	26.4	23.4	22	20
Strength σ_f (MPa)	550	470	411	350	280
Strain ε_f (%)	1.92	1.80	1.72	1.6	1.4

Table 7 Tensile strength properties of a $[90]_{4s}$ glass polypropylene laminate at various temperatures.

Temperature °C	20	50	80	100	120
Modulus E_{22} (GPa)	4.1	2.4	1.5	1.4	0.96
Strength σ_f (MPa)	21.3	16.36	11.3	8.84	6.68
Strain to failure ε_f (%)	0.75	1.17	1.44	1.67	2.38

Table 8 Shear strength properties of glass polypropylene system at various temperatures.

Temperature °C	20	50	80	100	120
Shear Modulus G_{12} (GPa)	2	1	0.86	0.4	0.3
Shear Strength τ_f (MPa)	56	48	38	33	28
Shear strain to failure γ_f (%)	19.5	25.88	32.6	38.76	44.93

FIGURES

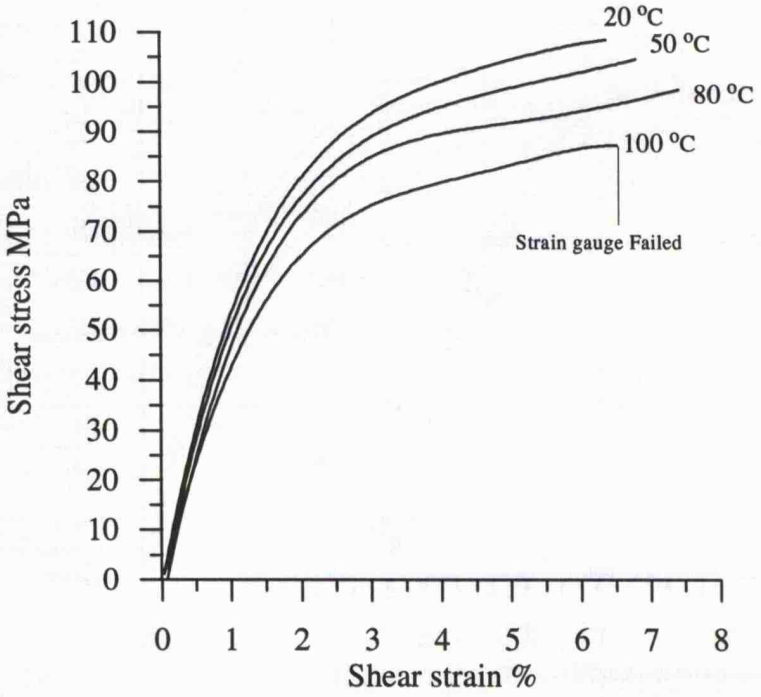

Figure 1 Shear response of a $[0_8]_s$ T800/924C laminate at various temperatures (hot-dry)

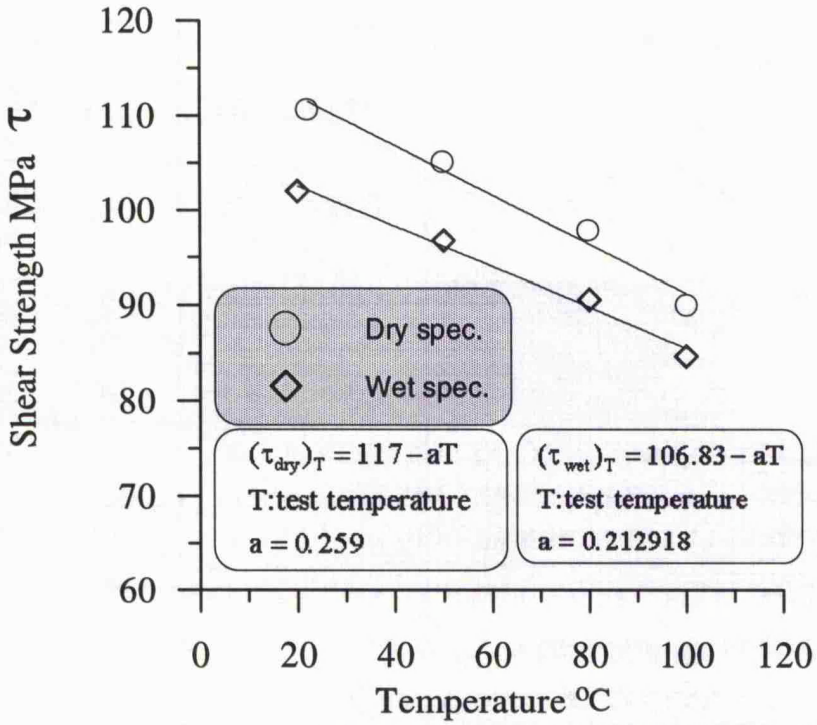

Figure 2 Shear strength versus temperature for a T800/924C $[0_8]_s$ laminate at hot-dry and hot-wet conditions.

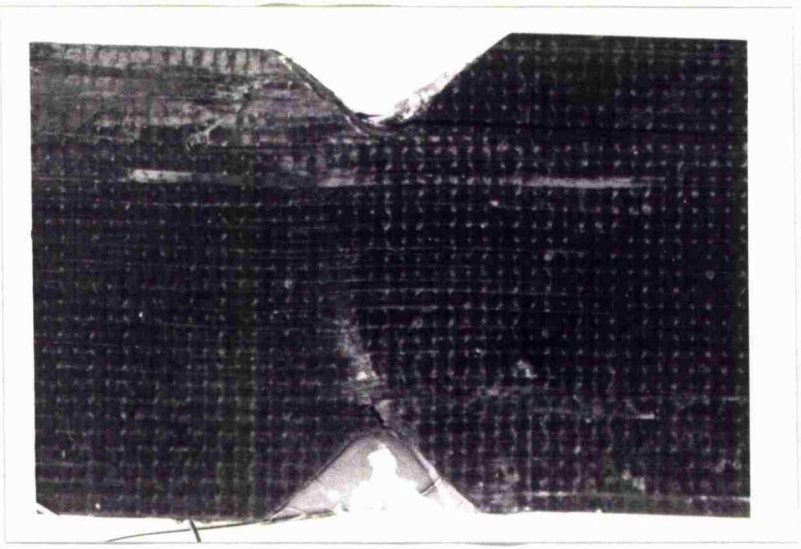

Figure 3 Overall shear failure of a T800/924C unidirectional specimen tested at 50°C-dry splitting and fibre breakage can be seen.

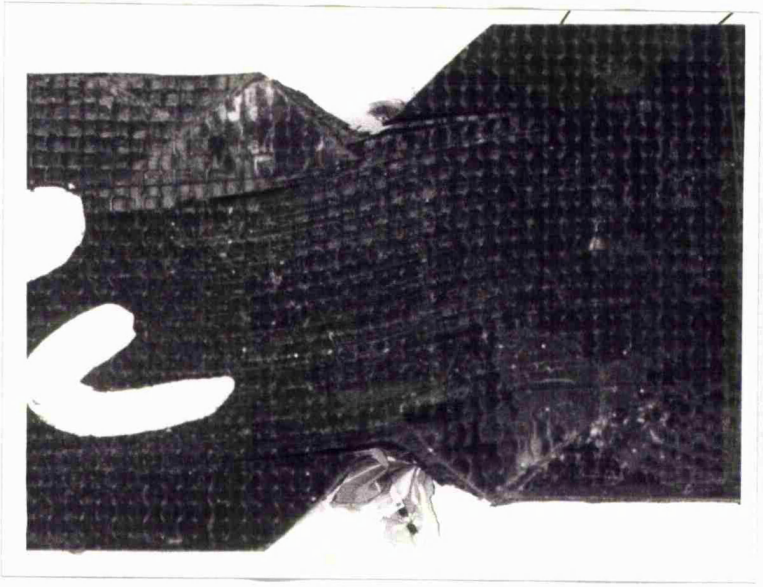

Figure 4 Overall shear failure of a T800/924C unidirectional specimen tested at 100°C-dry

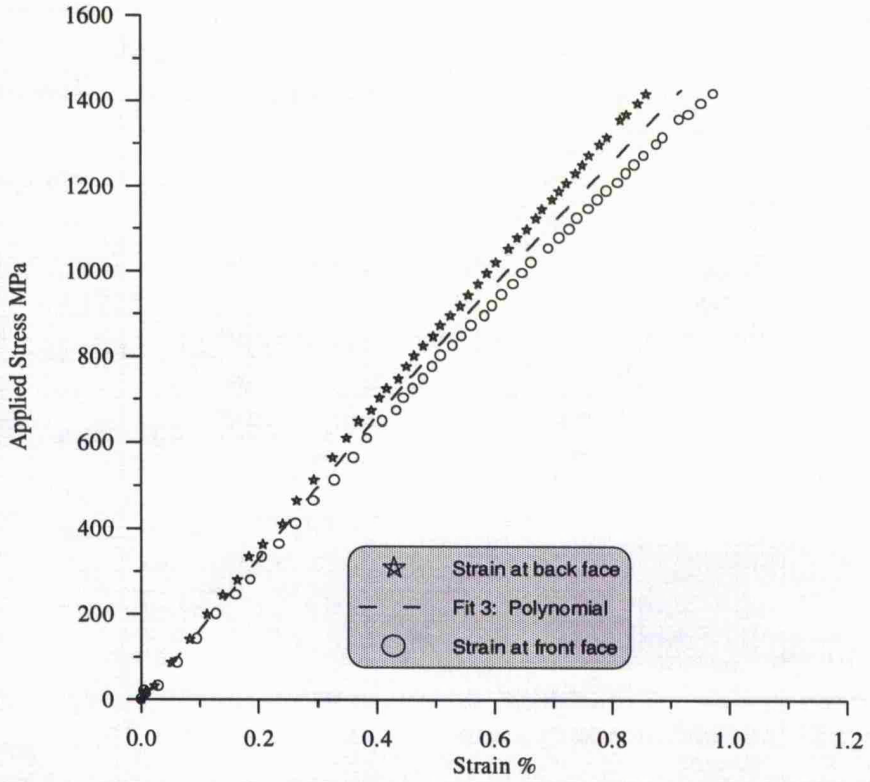

Figure 5 Compressive stress-strain response of a $[0_8]$s T800/924C laminate tested at room temperature (Dry conditions)

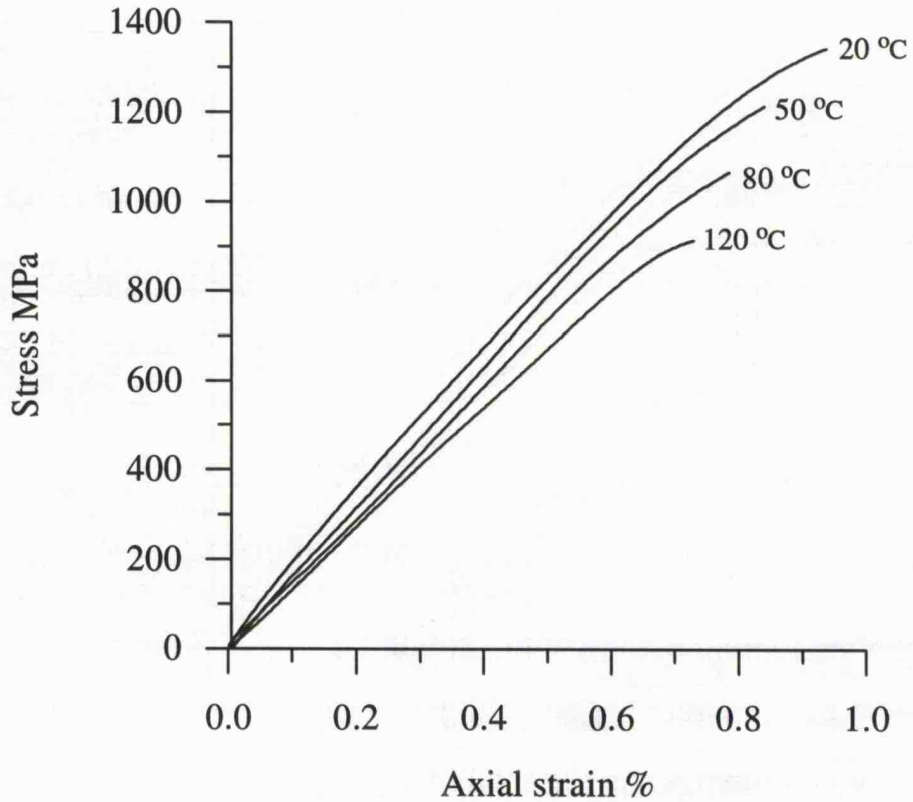

Figure 6 Compressive stress-strain response of a $[0_8]_s$ T800/924C laminate at various temperatures (hot-dry).

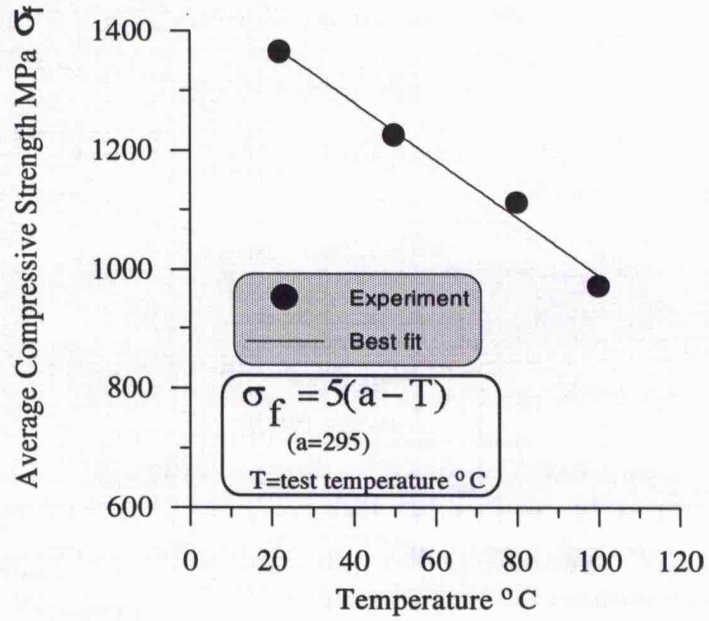

Figure 7 Compressive strength versus temperature for T800/924C laminates (hot-dry)

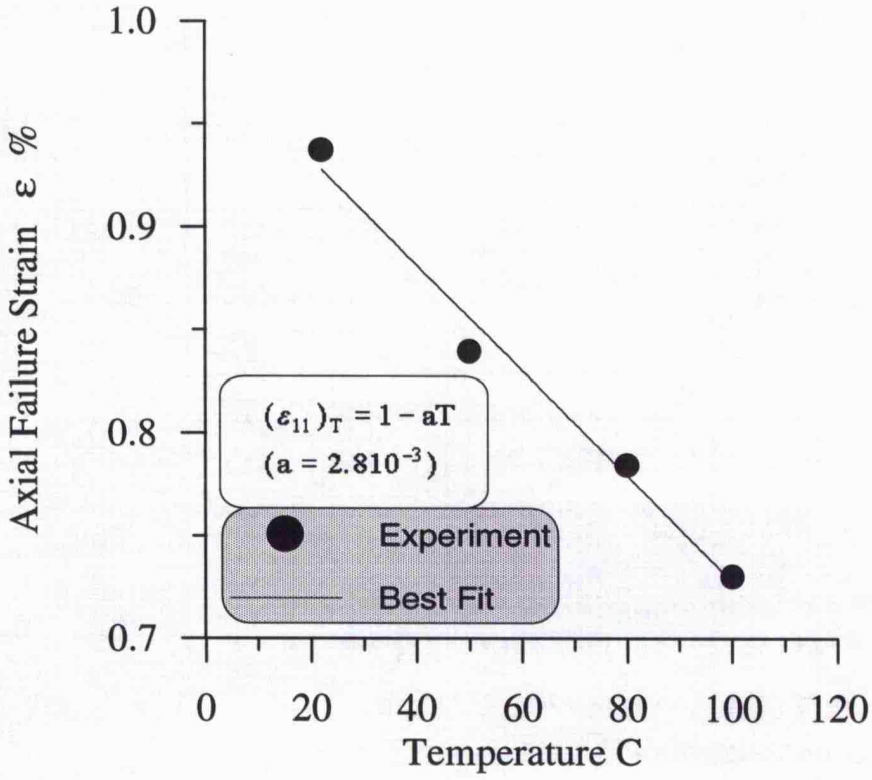

Figure 8 Axial failure strain versus temperature for T800/924C laminates (hot-dry)

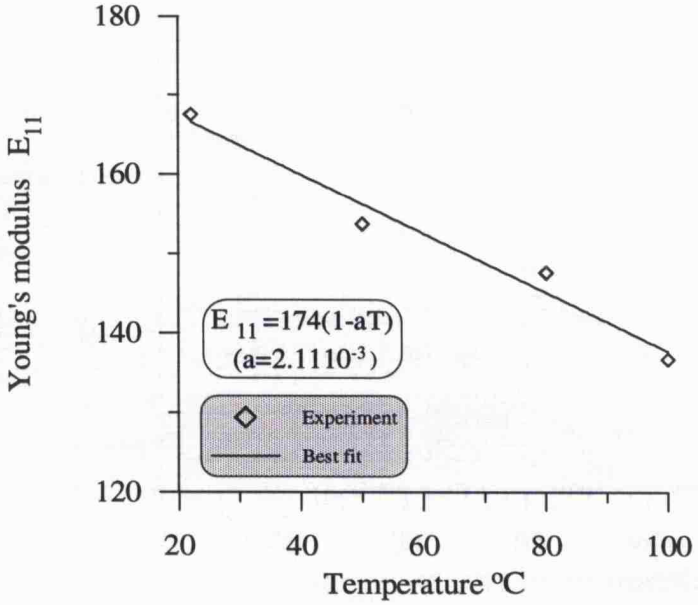

Figure 9 Young's modulus versus temperature for T800/924C laminates (hot-dry)

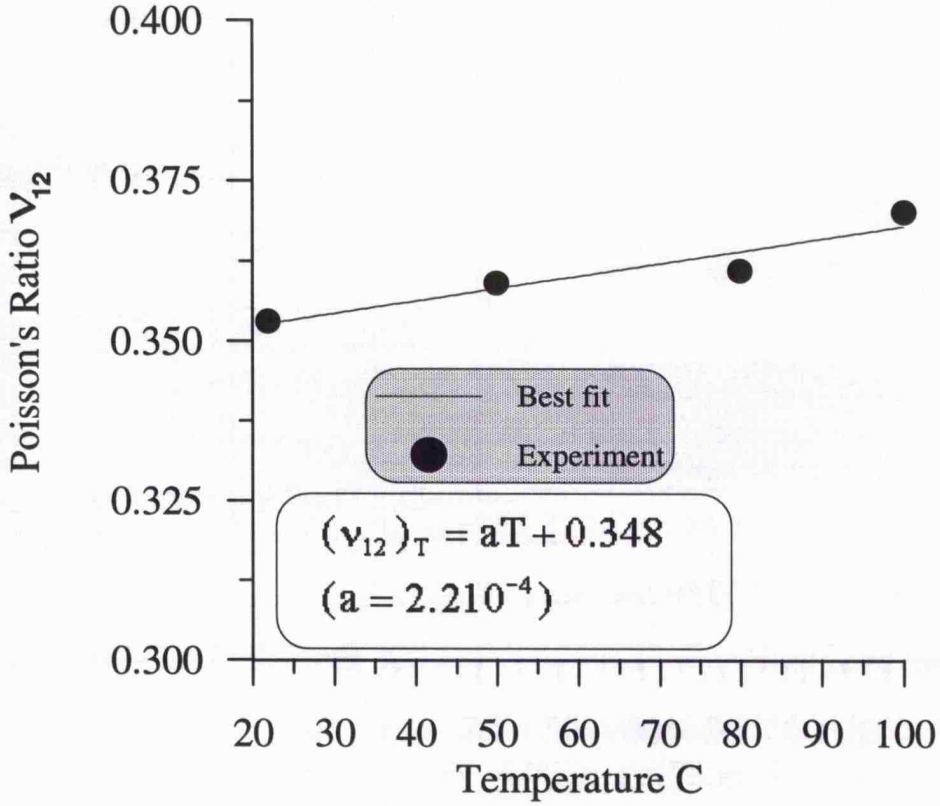

Figure 10 Poisson's ratio versus temperature for T800/924C laminates (hot-dry)

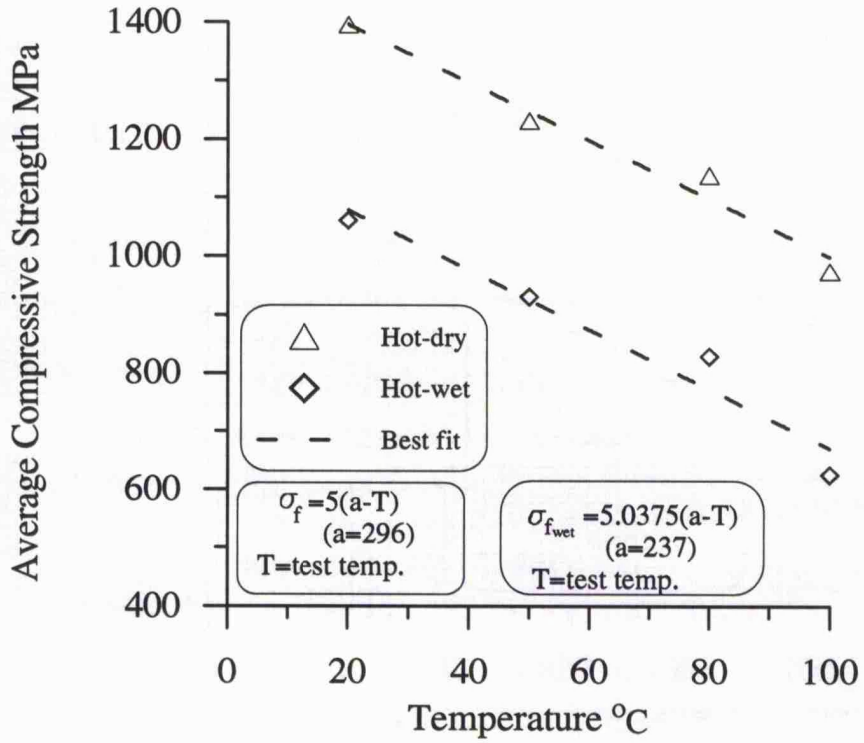

Figure 11 Compressive strength versus temperature for T800/924C laminate tested at hot-dry and hot-wet (95% RH) conditions

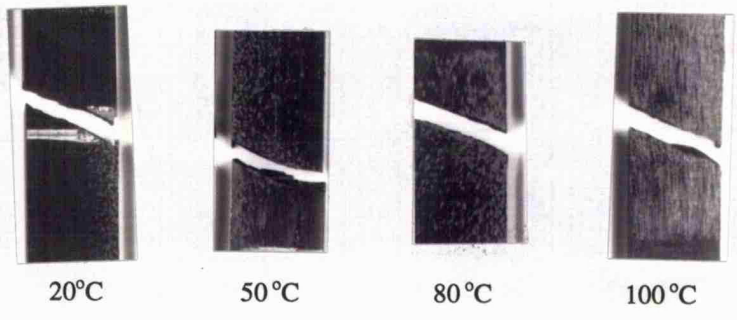

Figure 12 Overall failure of T800/924C unidirectional specimens tested at various temperature under uniaxial compressive loading.

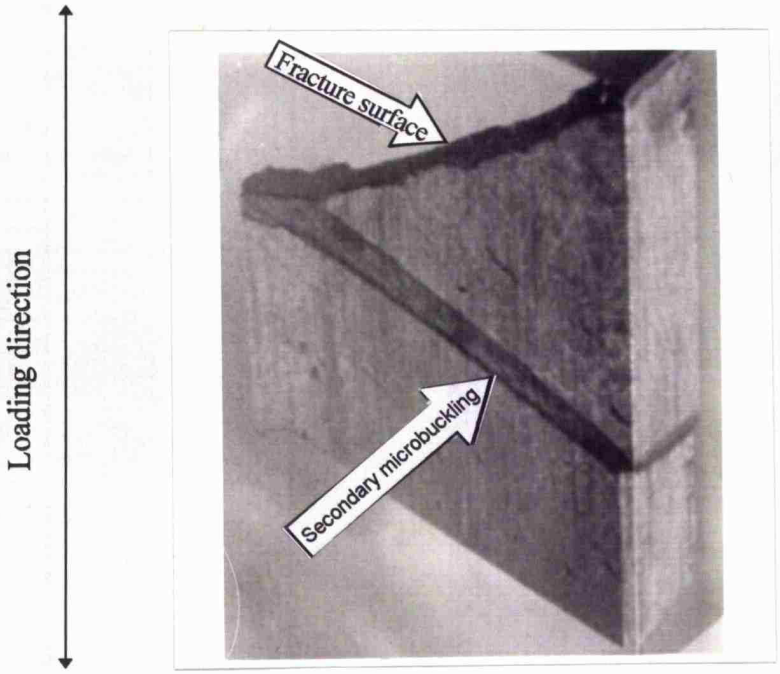

Figure 13 Overall failure of a T800/924C unidirectional specimen. A secondary fibre microbuckling zone has been developed (100°C dry).

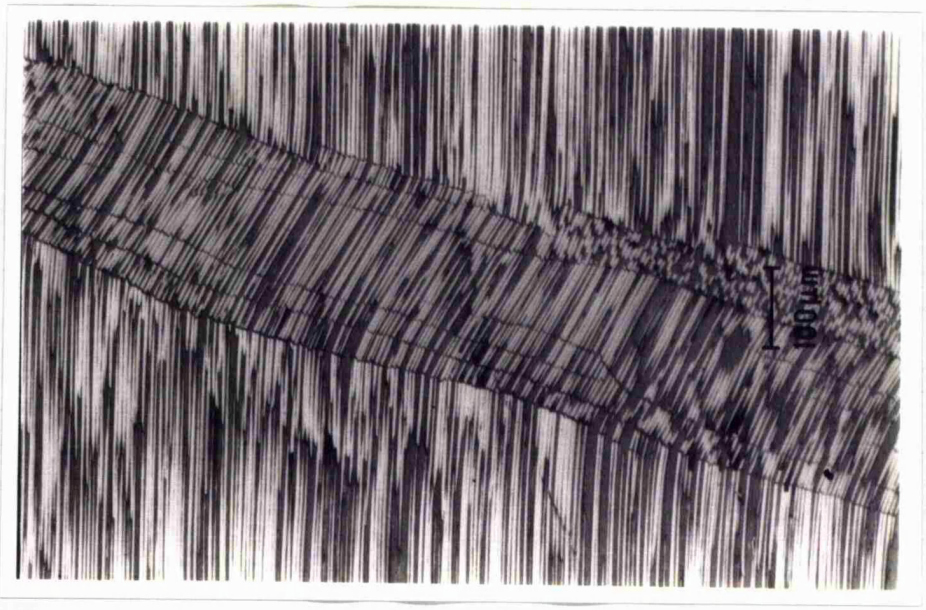

Figure 14 In-plane fibre microbuckling mode at room temperature.

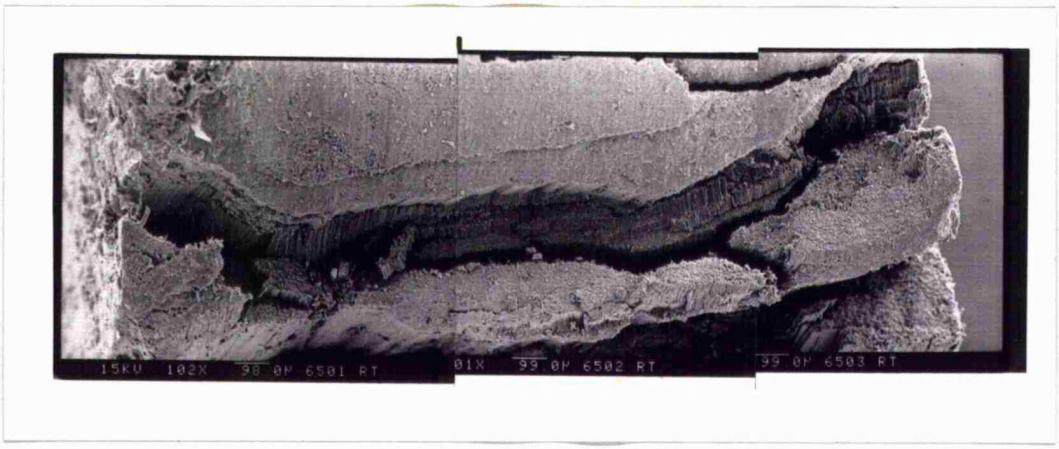

Figure 15 Typical fracture surface under uniaxial compressive loading at room temperature (dry).

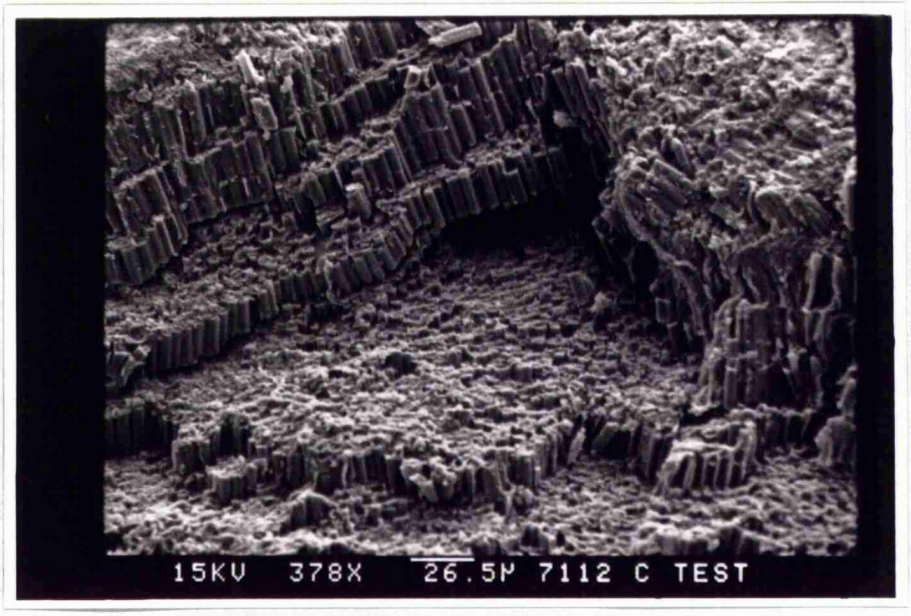

Figure 16 Fracture surface of a T800/924C specimen after fibre microbuckling failure (room-dry).

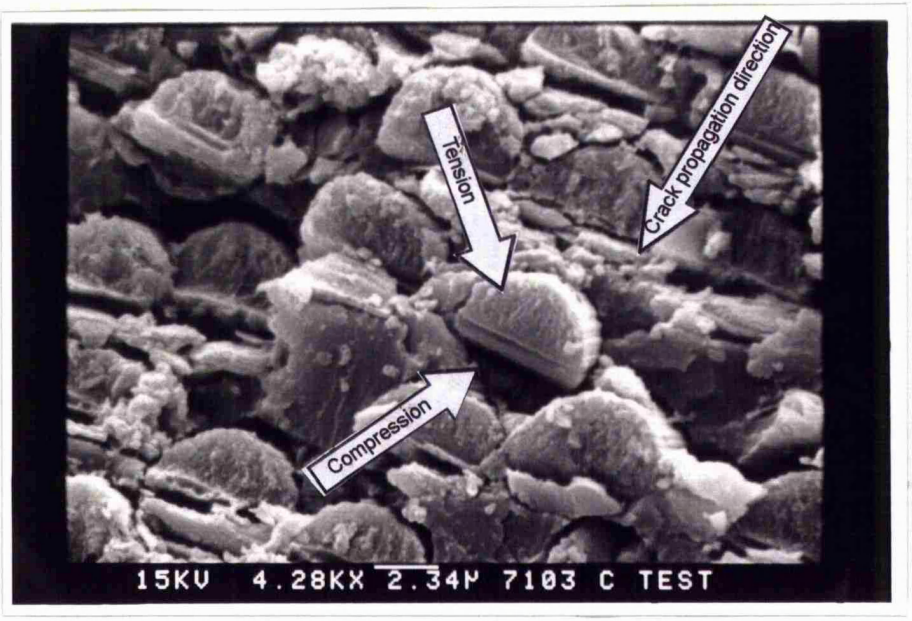

Figure 17 Higher magnification of the fracture surface shown in Fig.16. Compression and tension regions on individual fibres are shown (RT-dry).

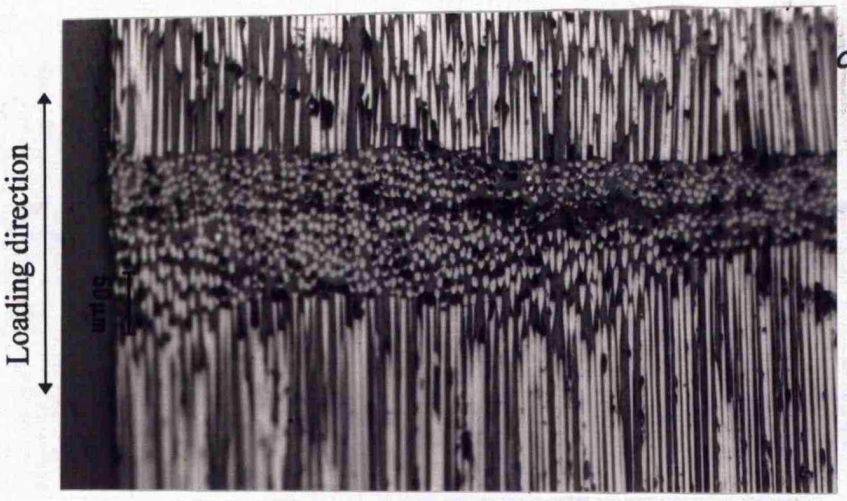

Figure 18 Out-of-plane fiber microbuckling at 100°C dry conditions.

a)

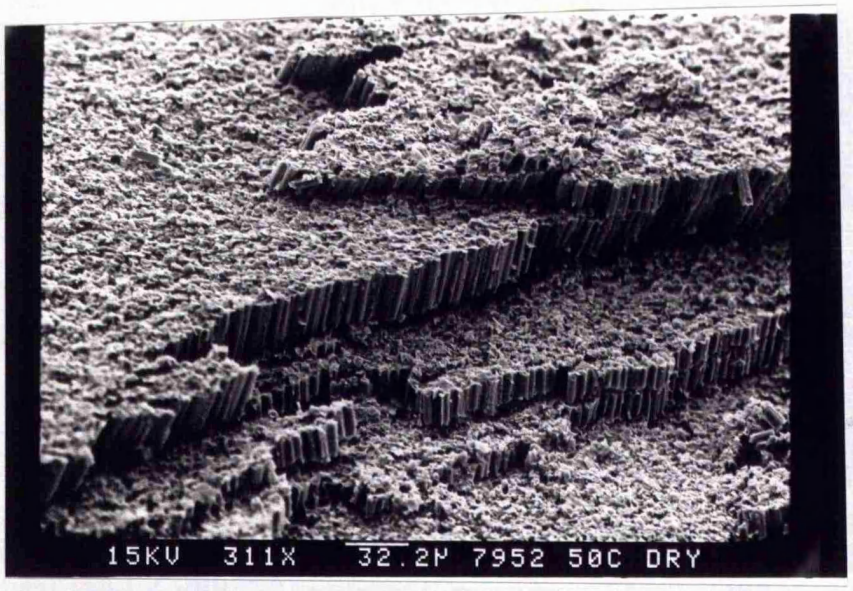

b)

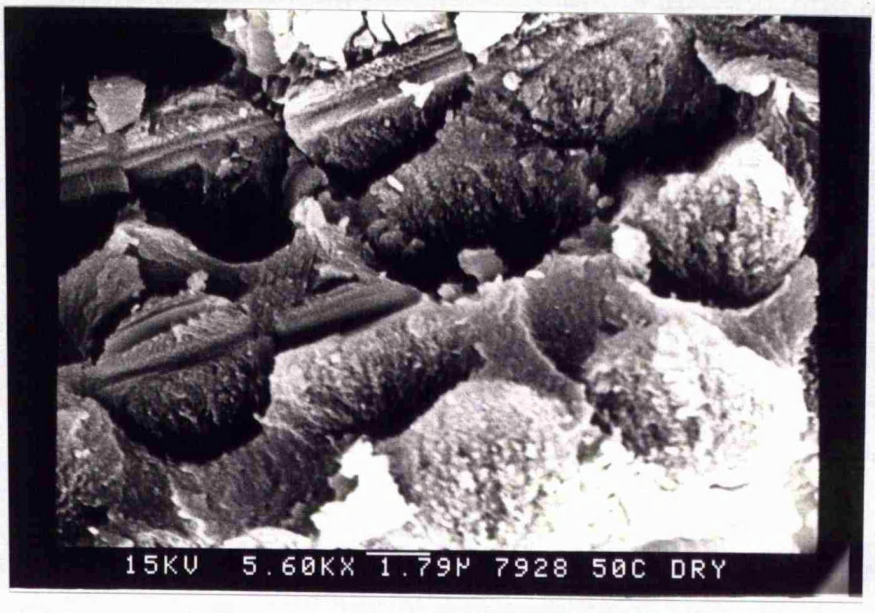

Figure 19 Typical fracture surface of uniaxialy compressed specimen at 50°C (dry). a) low magnification b) higher magnification of fracture surface.

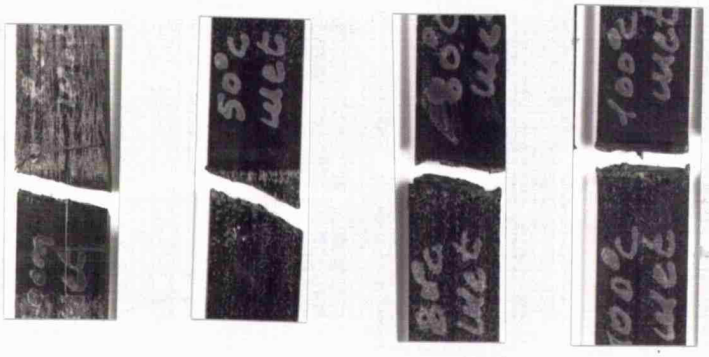

Figure 20 Overall failure of T800/924C specimens tested in hot-wet conditions under uniaxial compressive loading.

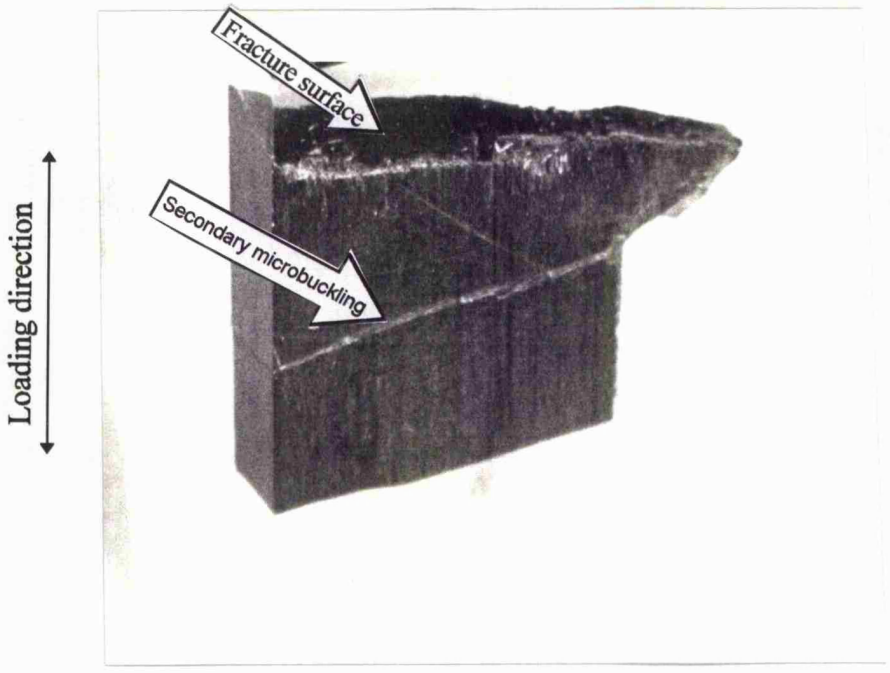

Figure 21 Overall view of the fracture surface of a T800/924C unidirectional specimen. Primary and secondary fibre microbuckling zones can be seen (100°C hot-wet).

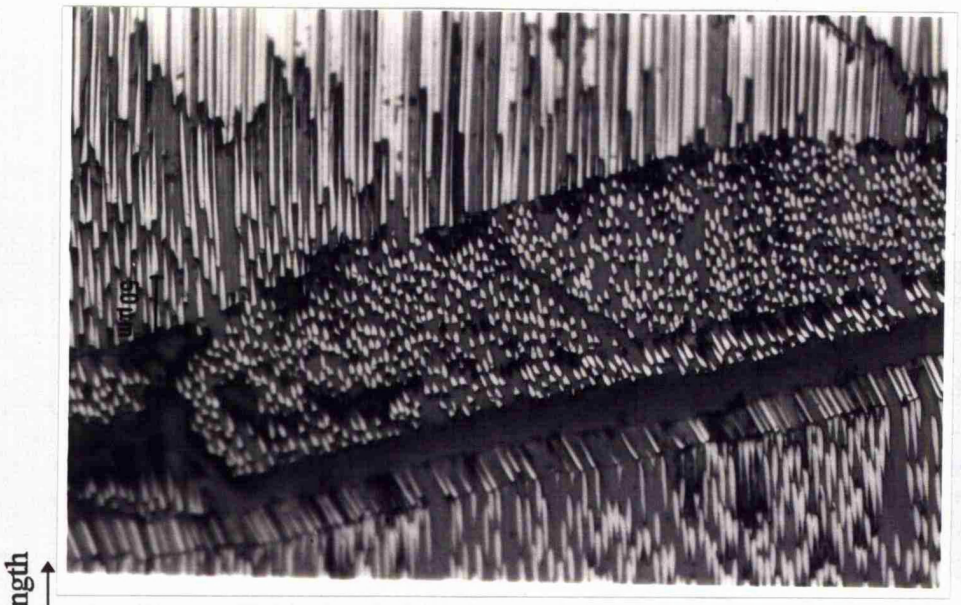

length

width

a)

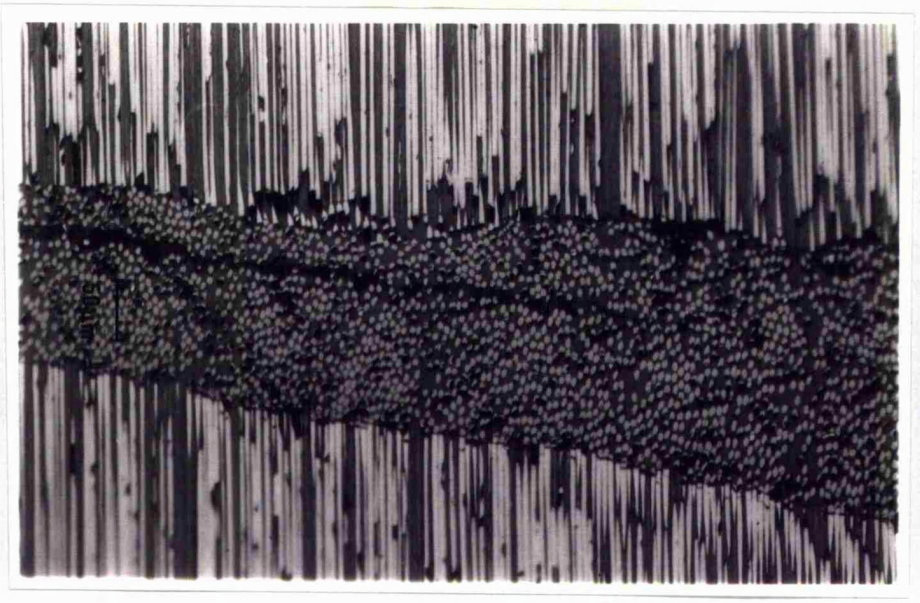

b)

Figure 22 Out-of-plane fiber microbuckling at hot-wet conditions a) Room temperature b) 100°C

a)

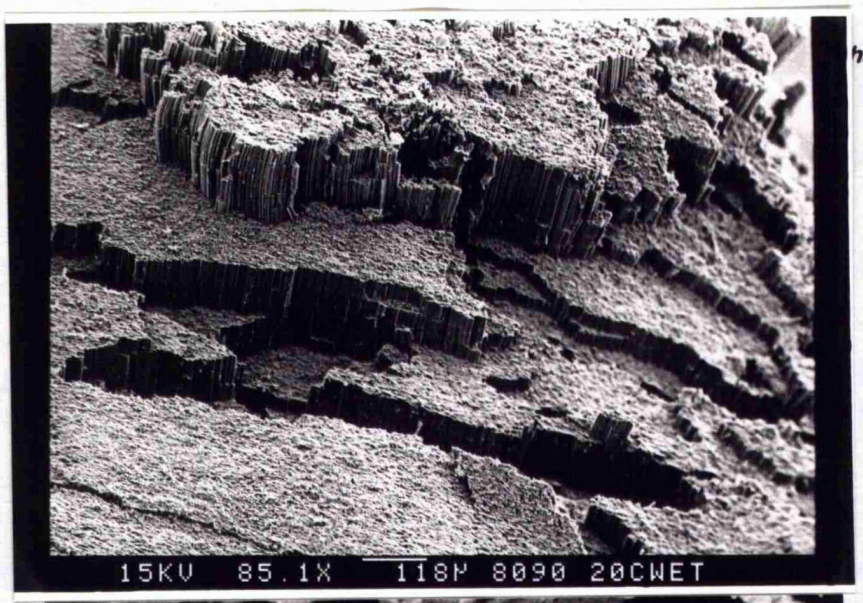

b)

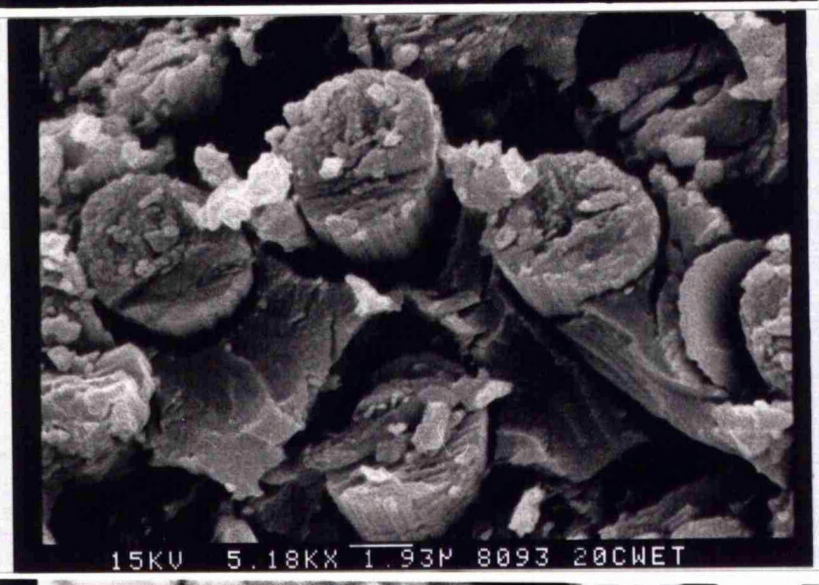

c)

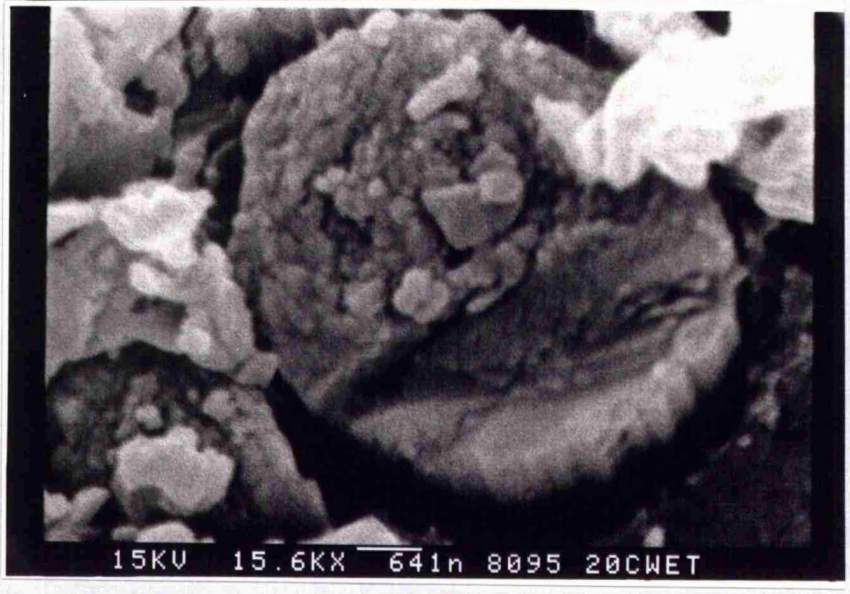

Figure 23 Fracture surface at room temperature (with 95% RH) a)Step fracture surface b)detail of fiber-matrix interface c)fracture surface of a single fibre

a)

b)

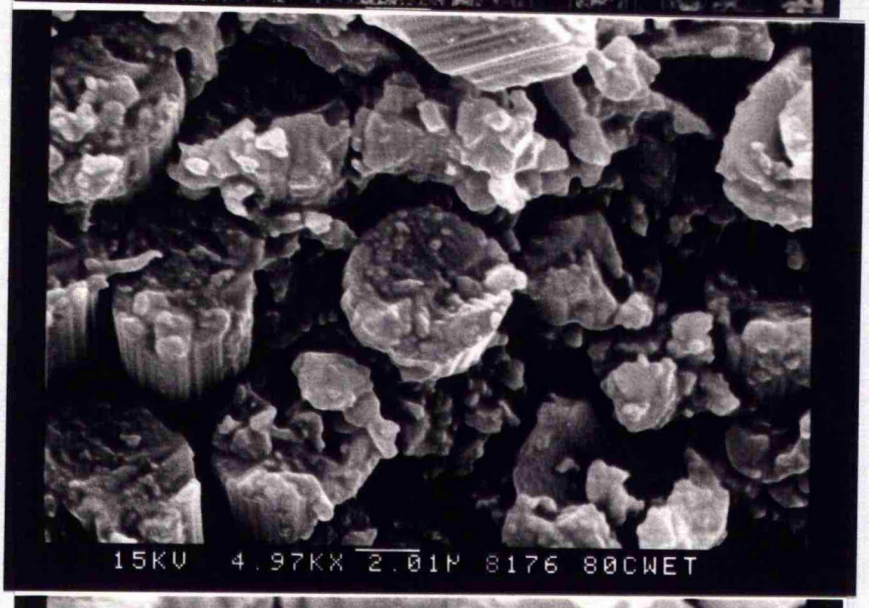

c)

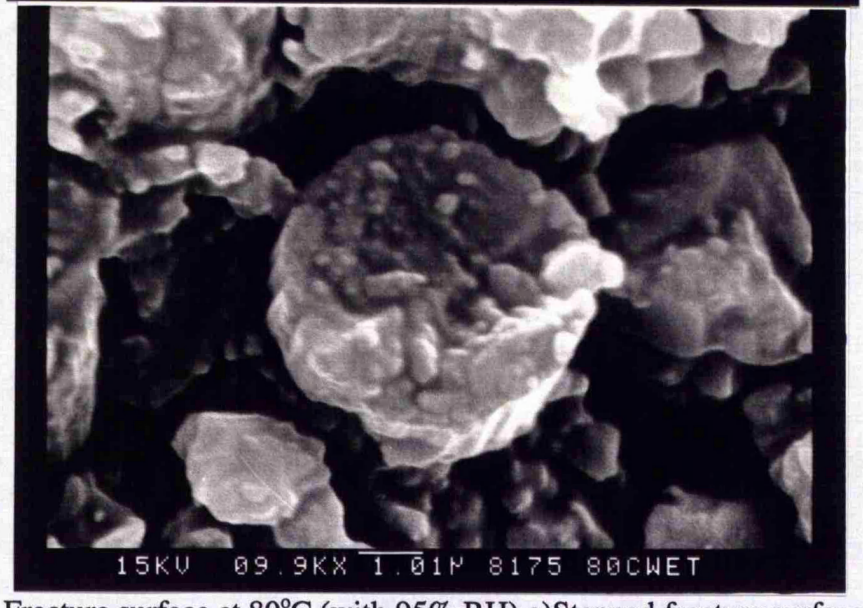

Figure 24 Fracture surface at 80°C (with 95% RH) a)Stepped fracture surface b)detail of fiber-matrix interface c)fracture surface of a single fibre

a)

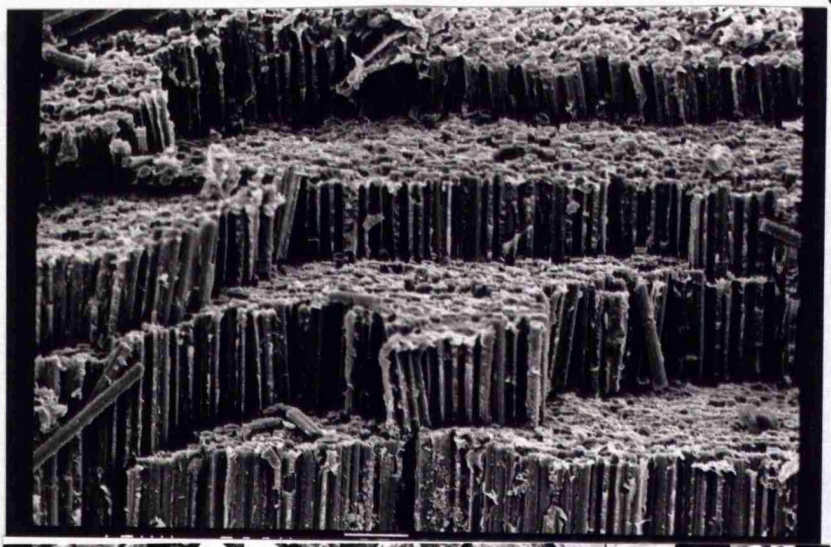

b)

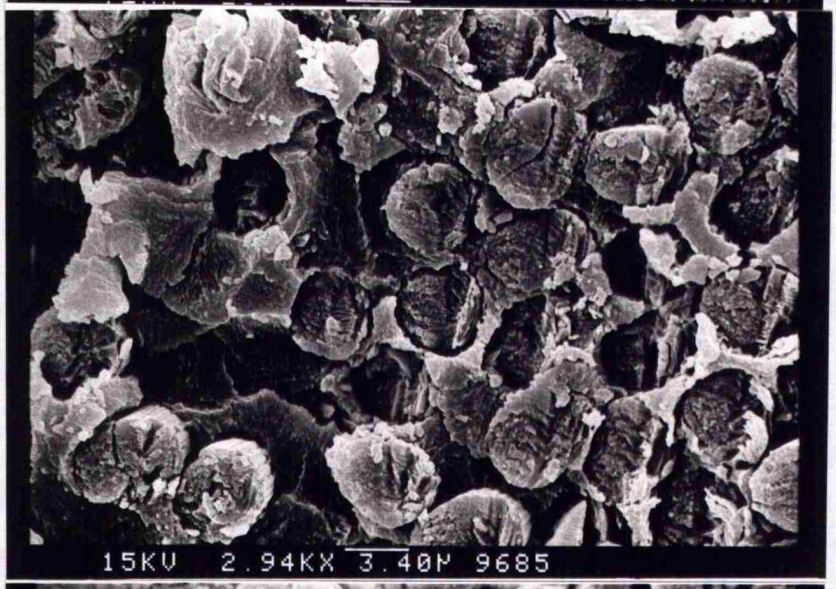

c)

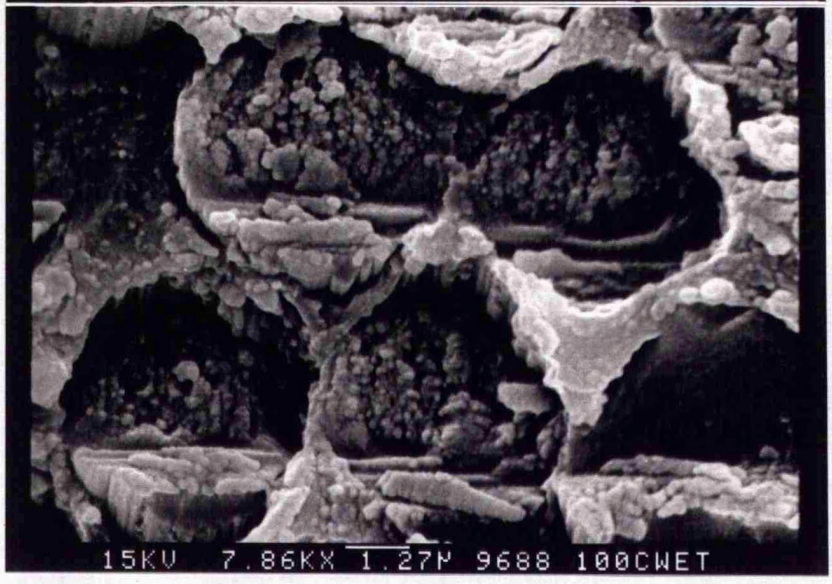

Figure 25 Fracture surface under uniaxial compressive loading at 100°C (with 95% RH) a)Stepped fracture surface b) and c) are higher magnification of (a).

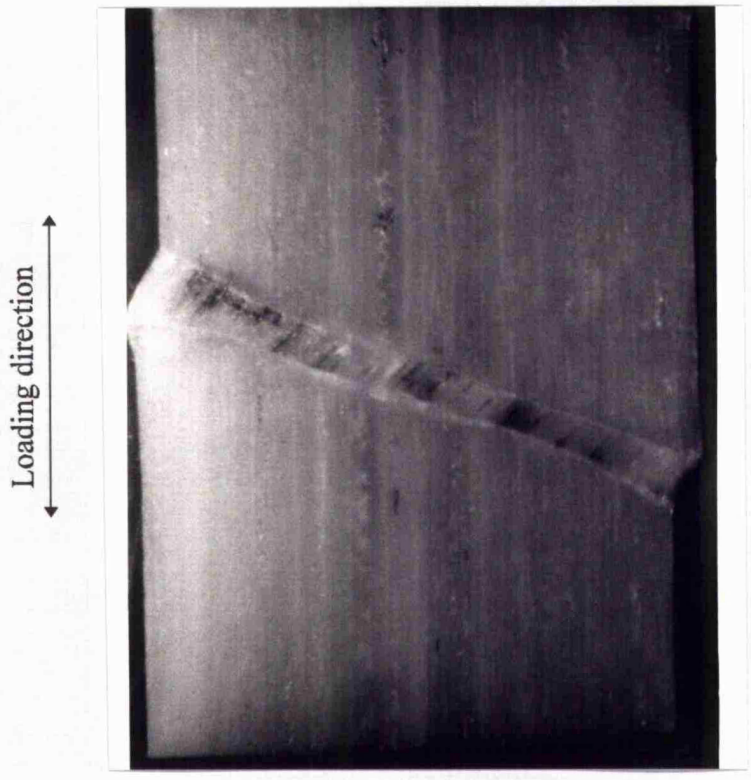

Figure 26 Overall failure mode of a glass/pp laminate. In-plane fibre microbuckling grows across the specimen width (buckle length ≈ 0.6 mm).

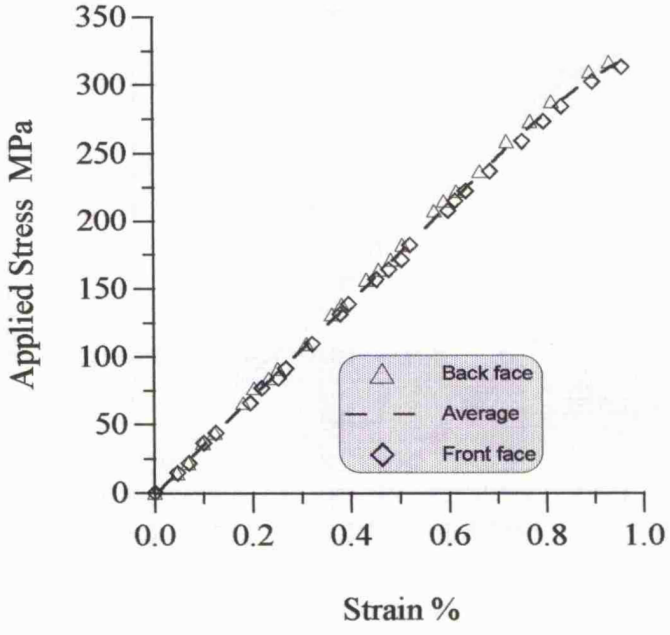

Figure 27 Compressive stress-strain response of a glass/pp laminate (RT-dry) .

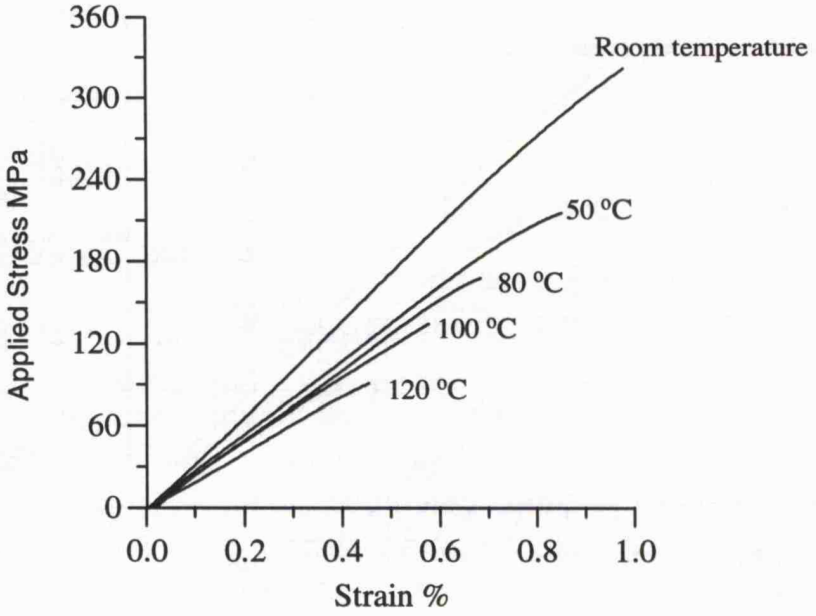

Figure 28 Stress versus strain at various temperatures for a plytron $[0]_{4s}$ laminate loaded in uniaxial compression.

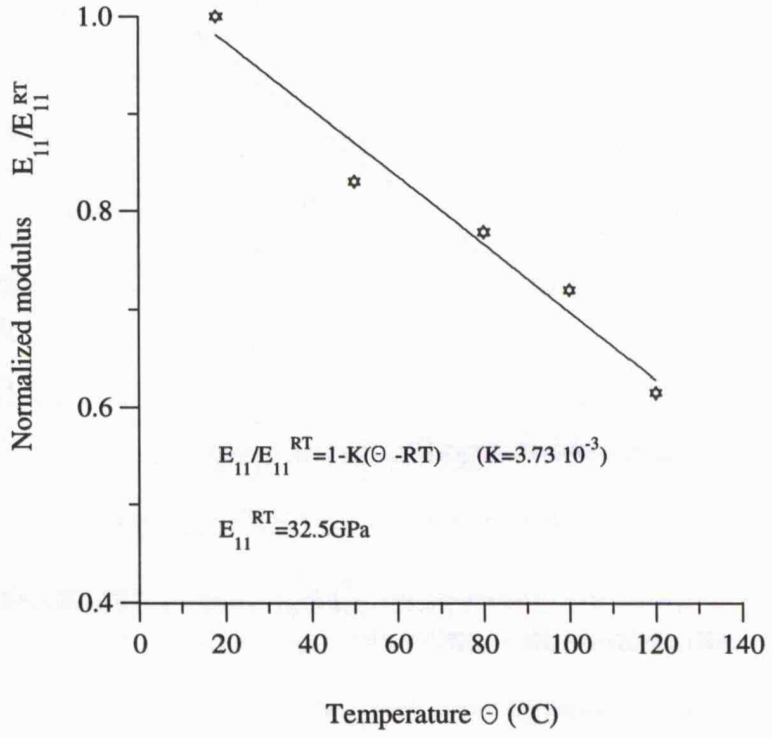

Figure 29 Normalized modulus versus temperature under uniaxial compression

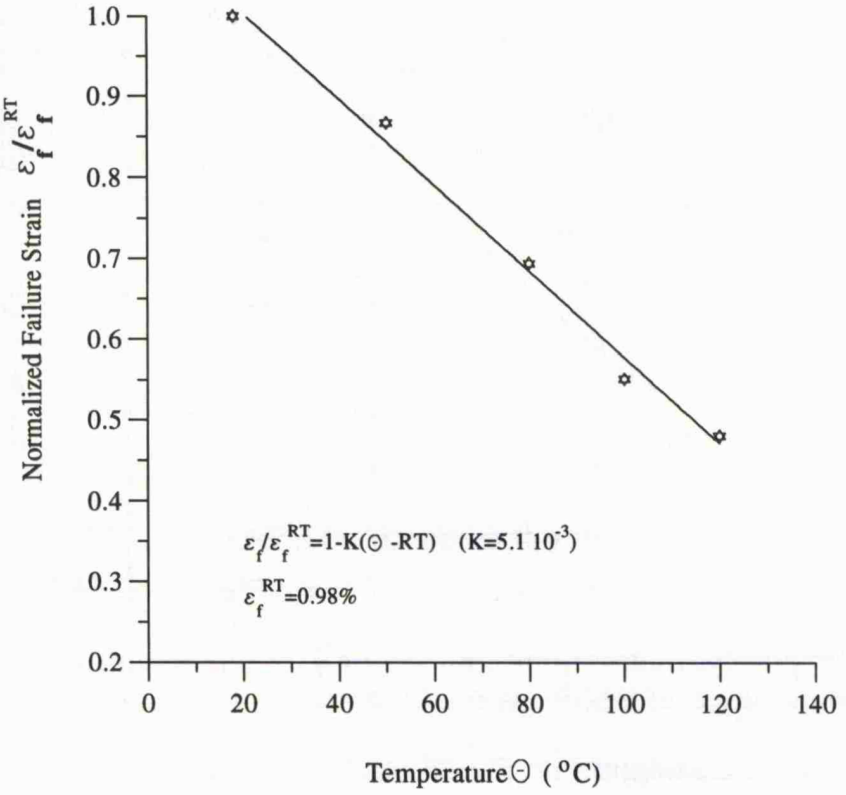

Figure 30 Normalized failure strain versus temperature under uniaxial compression

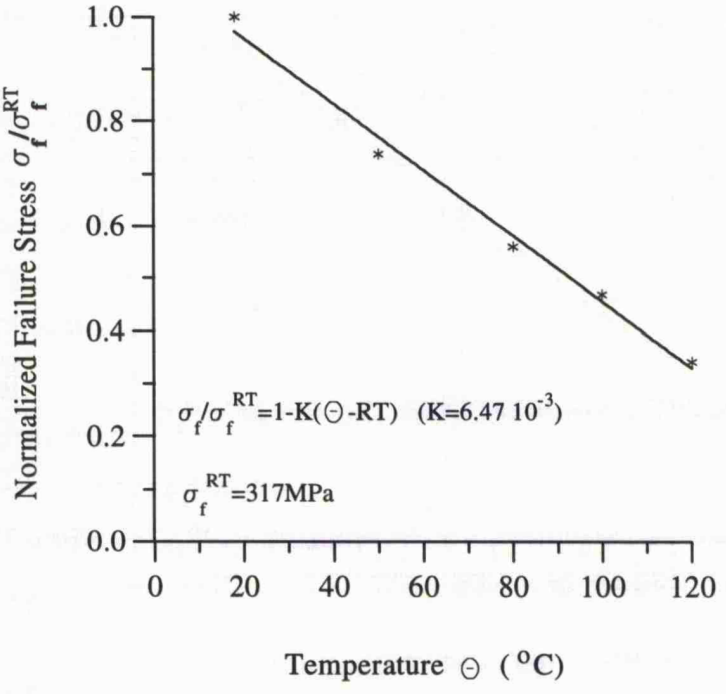

Figure 31 Normalized failure strength versus temperature under uniaxial compression

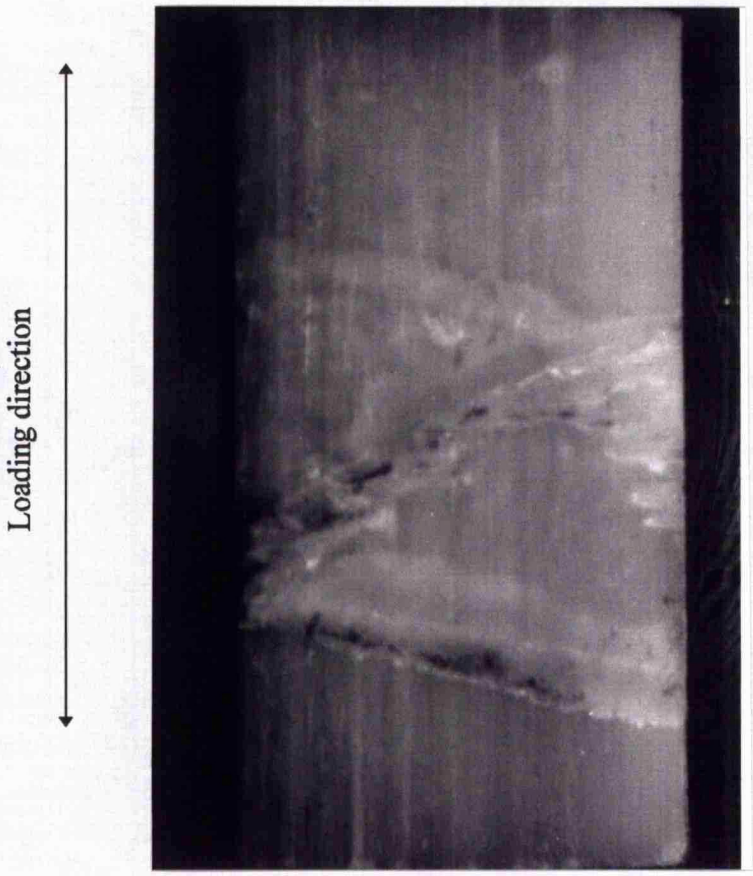

Figure 32 Fibre microbuckling observed in a glass-polypropylene unidirectional laminate loaded in compression. Secondary microbuckling is evident.

SEM photograph showing in-plane fibre m/b in 0 laminate loaded in uniaxial compression

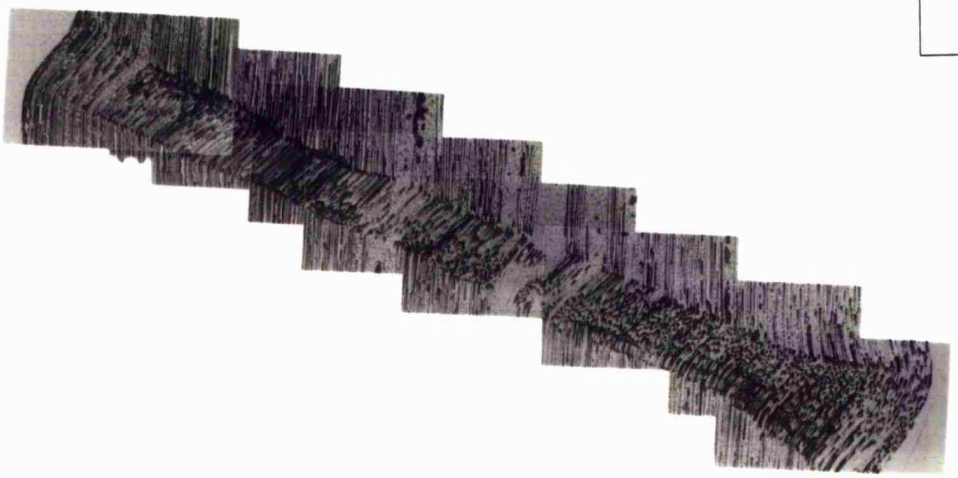

Optical microphotograph illustrating in plane fibre microbuckling

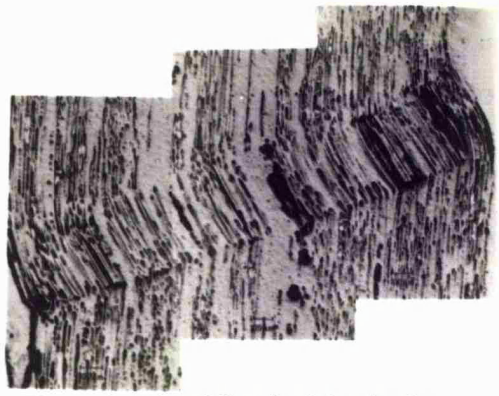

Through thickness fibre microbuckling in 0 laminate

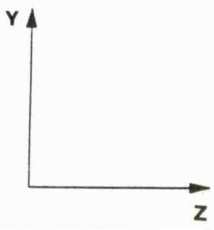

Figure 33 Compressive failure of plytron at room temperature (z=through thickness)

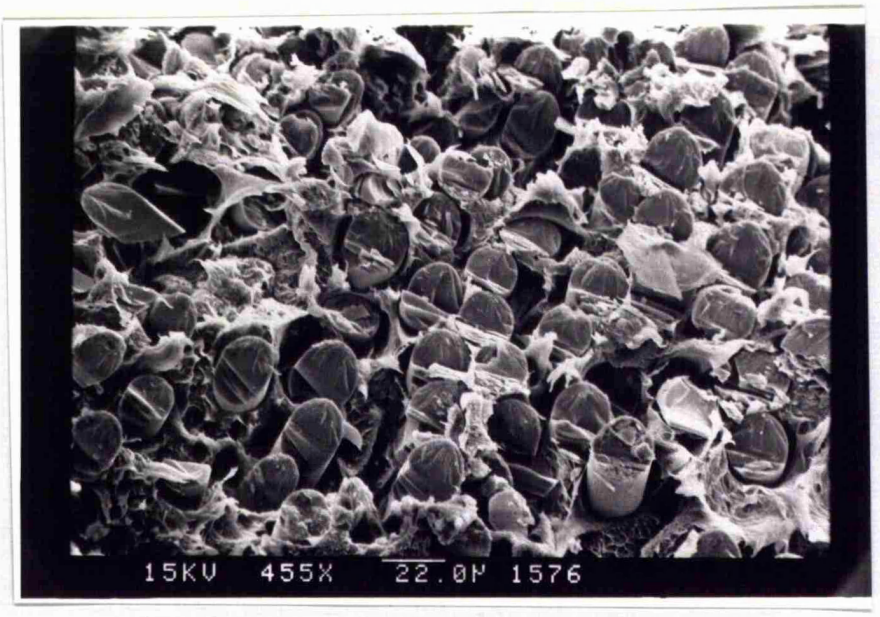

a) Low magnification view

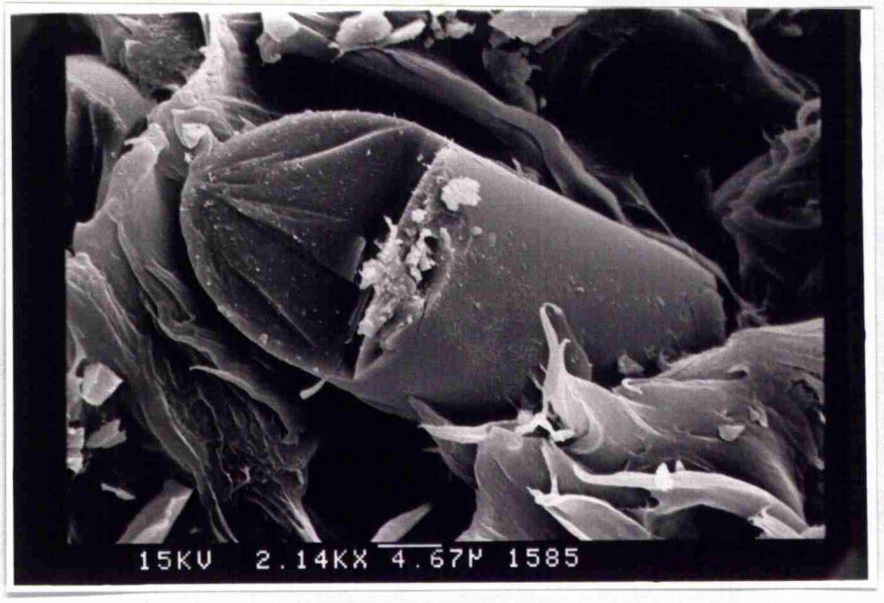

b) High magnification view

Figure 34 Scanning Electron Microphotographs of the fracture surface of a glass/fibre polypropylene lamina after fibre m/b failure (RT-dry)

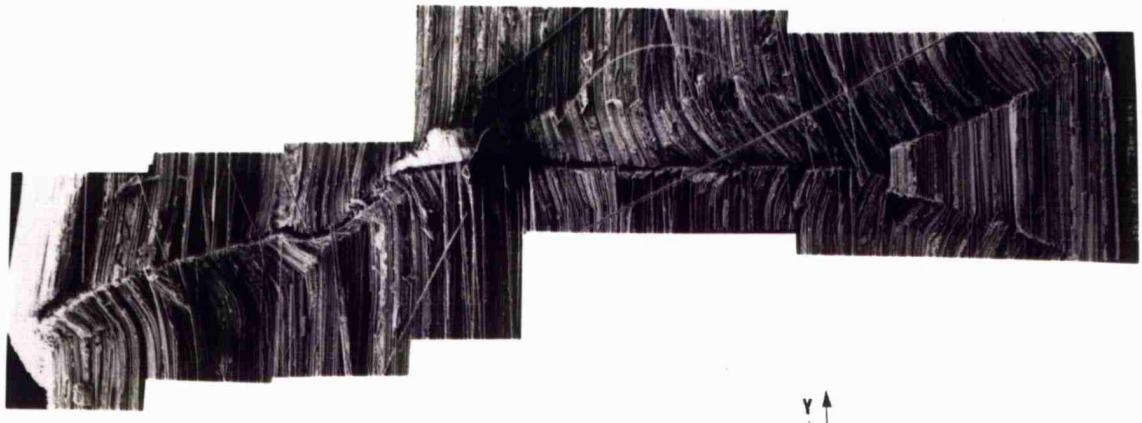

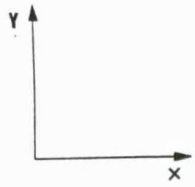

SEM photograph showing out of plane and in-plane fibre m/b
in 0 laminate loaded in uniaxial compression at high temperature

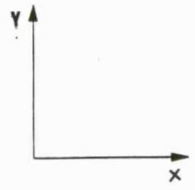

Optical microphotograph illustrating out of plane fibre microbuckling

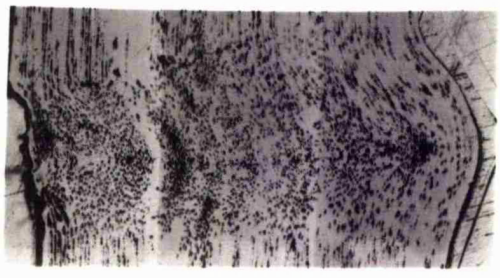

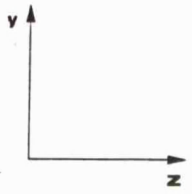

Through thickness fibre microbuckling in 0 laminate

Figure 35 Compressive failure of plytron at 50°C

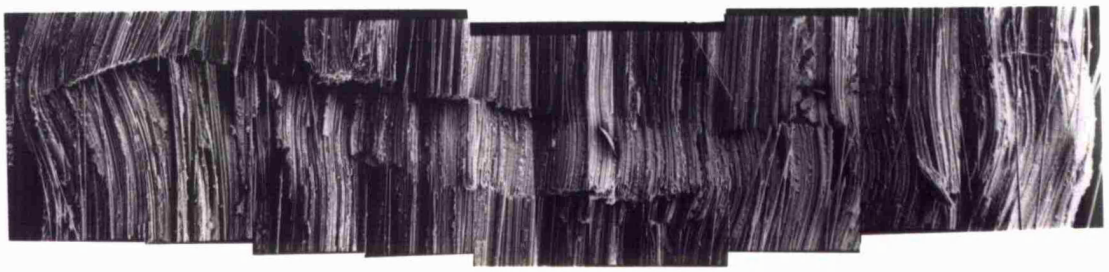

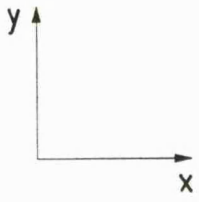

SEM photograph showing out of plane fibre m/b in 0 laminate loaded in uniaxial compression at high temperature

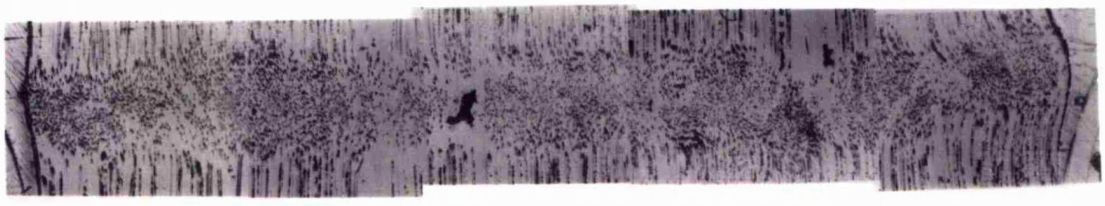

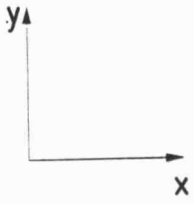

Optical microphotograph illustrating out of plane fibre microbuckling

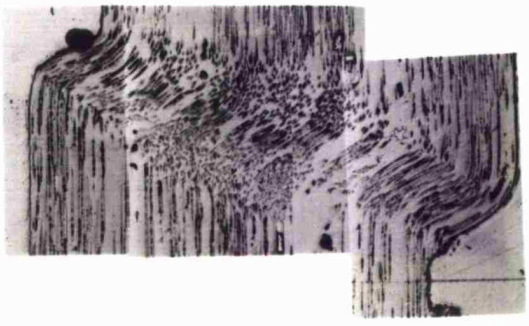

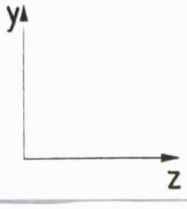

Through thickness fibre microbuckling in 0 laminate

Figure 36 Compressive failure of plytron at 120°C

CHAPTER SIX

PREDICTION OF THE COMPRESSIVE STRENGTH OF UNIDIRECTIONAL LAMINATES

6.1 Introduction

Uniaxially reinforced composites are generally weaker in compression than in tension. Thus in stress states such as bending or thermal stressing, failure usually occurs in compression. In addition, these composites are more nonlinear in compression. Hence, the compressive behavior is in a sense more important to understand, but at present the converse situation prevails.

Small initial fiber misalignments are virtually unavoidable in many practical composite systems. But such misalignments, must in addition have other effects on the mechanical behaviour of composite materials, and these additional effects are the subject matter of the present chapter. Fibre misalignment can significantly affect the compressive stiffness and strength of the composite.

In this chapter, the compressive strength of the T800/924C and the Glass/polypropylene composite systems are determined using recent theoretical models. The compressive stress-strain response is also obtained graphically from the shear stress-strain curve.

6.2 Strength Prediction

A number of theories for the compressive strength of unidirectional composite laminates have been proposed and these have been reviewed by Shuart [1], Hahn [2], Haeberle *et* al. [3], Rosen [4] and more recently Budiansky and Fleck [5]. It is generally agreed that the observed compressive failure stresses can only be explained

on the assumption that initial fibre misalignments are present. In this chapter we apply three commonly used models developed by Rosen[4], Budiansky[5] and Batdorf and Ko[7] to predict the strength.

a) Rosen Model [4]

The classic study of Rosen [4] predicted failure of unidirectional composites under axial compressive loading via buckling of the fibres. Since buckling is restricted by surrounding matrix, the critical stress for the initiation of fibre buckling is governed by matrix shear modulus, G_m and the fiber volume fraction V_f. The former, in turn, is dependent on the temperature and moisture content. At high fiber volumes, the compressive strength, σ_c is given by[4],.

$$\sigma_c = \frac{G_m}{1-V_f} \approx G_c \qquad (1)$$

where G_c is the composite shear modulus. G_m for an isotropic resin can be obtained from,

$$G_m = \frac{E_m}{2(1+\nu_m)} \qquad (2)$$

where E_m is the matrix elastic modulus and ν_m is the material Poisson's ratio. For the glass/pp and the T800/924C laminates Equation 1 is found to significantly overestimate the compressive strength for all temperature levels. The results, summarized in table 1 and 2, indicate that the compressive strength of both materials is only 20-25% of their shear modulus. Larger and June [8] argued that a numerical coefficient that allowed for the three dimensional nature of reinforcement could be introduced into equation 1, whereas Ewins [9] thought that the discrepancy was caused by the irregular spacing of fibres, matrix plasticity, fiber misalignment and poor fibre-matrix bonding. This support that microbuckling is a plastic rather than an elastic failure mode.

Steif[10] extended Rosen's microbuckling analysis to situations in which matrix plasticity occurs; an elastic/perfectly plastic matrix shear response was assumed. He found that the theoretical fibre breaking strains compared reasonably

well with measured failure strains when the kink band was assumed to have the experimentally observed width.

b) Budiansky analysis[5]

Argon [11] proposed an alternative approach based on a model of microbuckling as a plastic collapse event. In this model kinking occurs in a $\beta=0°$ band within which fibres have suffered an initial misalignment angle $\bar{\phi}$, figure 1. The fibres are assumed to be inextensible and suffer a remote compressive axial stress; the associated deformation within the kink band is given by the additional rotation ϕ of the fibres. In a rigid perfectly plastic material having yield stress τ_y in longitudinal shear, additional rotation ϕ can not develop until the critical compressive strength

$$\sigma_c = \frac{\tau_y}{\bar{\phi}} \tag{3}$$

is applied, and subsequently the compressive stress decreases with increasing $\bar{\phi}$. Budiansky [6] extended this result for an elastic-perfectly plastic composite response, and found

$$\sigma_c = \frac{\tau_y}{\gamma_y + \bar{\phi}} = \frac{G}{1 + \bar{\phi}/\gamma_y} \tag{4}$$

where $\gamma_y = \tau_y/G$ is the in-plane shear yield strain of the composite. This result reduces to the Rosen bifurcation solution, equation 1, when $\bar{\phi}=0$ and is asymptotically equivalent to Argon's equation 3, for large $\bar{\phi}$. Figure 2 shows that the compressive strength of Plytron is proportional to the shear yield strength, τ_y, of the composite, supporting equation 3 and 4; here τ_y is taken as half the value of the shear strength τ_f. The slope of the graph in Figure 2 gives $\bar{\phi}=5°$. Figure 2 also

includes data for glass and Kevlar fibre reinforced Polyester, taken from the work of Piggott and Harris [12], but this time $\bar{\phi}$=3.7°. We have observed fibre imperfections between 3 ° and 6 ° in section studies for the glass/pp laminates. When τ_y is increased to sufficiently high values the fibres collapse prior to microbuckling; the uniaxial strain in the composite equals the intrinsic crushing strain of the fibres, figure 2. Equations 3 and 4 are sensitive to fibre misalignment and predict a kink orientation angle β=0°, which is not in agreement with the experimental observation of β=20°-25°. However, it provides an indication of the relative importance of the physical parameters that govern the compressive strength. The compressive strength of glass/pp system versus temperature is plotted for various fibre misalignments (4°-7°) in figure 3. It can be seen that for $\bar{\phi}$=6° the agreement between theoretical and experimental results is acceptable.

The experimental and theoretical compressive strength properties of the T800/924C laminates are given in table 4. It can be seen from table 4, Budiansky's prediction and experiment are in good agreement. The error between theory and experiment is less than 5%. The compressive strength properties of T800/924C composite system are also presented in figure 4 as a function of temperature and various fibre misalignment values. The theoretical values are calculated from equation 3. Figure 4 shows that the compressive strength depends on fiber misalignment. When the fibre misalignment increases the compressive strength of unidirectional materials reduces dramatically. Budiansky's prediction gives good agreement for $\bar{\phi}$=2.5° for the T800/924C system.

c) Batdorf and Ko model [7]

Batdorf and Ko[7] by idealizing the composite as a collection of slightly misaligned volume elements that fail in the kink mode obtained for the compressive failure stress

$$\sigma_c = \frac{\tau_f - \tau_a}{\bar{\phi} + \gamma_f} \qquad (5)$$

where τ_f is the shear failure stress, τ_a is the applied shear stress, (which in the following zero) $\bar{\phi}$ is the initial fibre misalignment and γ_f is the yield strain of the material. Equation 5 indicates that the compressive strength of the composite is equal to the tangent modulus of the material taken at the failure point. For pure compression(τ_a=0) and the elastic-perfectly plastic case equation 5 reduces to Budiansky's solution, equation 4 . To find the compressive strain the authors [7] assumed that this quantity is the sum of two components, one resulting from the elasticity of the fibres (σ / E_{11}) and the other caused by their changing tilt ($\bar{\phi} + \gamma$), i.e.

$$\varepsilon = \varepsilon_1 + \varepsilon_2 = \frac{\sigma}{E_{11}} + (\gamma\bar{\phi} + \frac{1}{2}\gamma^2) \qquad (6)$$

where E_{11} is the elastic modulus of the laminate in the fibre direction.

Batdorf and Ko [7] suggested that if the shear stress- strain curve ($\tau - \gamma$) is known then using equation 5 and 6 the compressive stress-strain ($\sigma - \varepsilon$) response and the strength of the composite can be obtained graphically. This is done by interpreting (τ_f, γ_f) as a sequence of point along the (τ, γ) curve (see figure 5). The method is illustrated in Figures 5&7 for the plytron and T800/924C system, respectively.

The yield value σ_c is given by the Budiansky's value, equation 4 where we take τ_y=0.5τ_{max} (see below). The tangent on the $\tau - \gamma$ curve at (τ_y, γ_y) intersects the abscissa at -$\bar{\phi}$ which corresponds to the initial fibre misalignment (more detail in Appendix A). Regarding this as a pivot through which all lines with a slope ($\tau / (\bar{\phi} + \gamma)$) pass, values of

$$\sigma(\gamma) = \frac{\tau}{\bar{\phi} + \gamma} \qquad (7)$$

$\sigma(\gamma)$ and γ are obtained (figure 5&7). By substituting these values in equation 6, the axial compressive strain ε is determined. The theoretical compressive stress and strain were calculated by using equation 6 and 7. Shear stress and strain values were taken from figure 5 to calculate theoretical compressive stress and strain, shown in figure 6 and 8..

The $\sigma-\varepsilon$ response for plytron at RT-dry and 50°C-dry are shown in figures 6a and 6b, respectively. It is evident that the results are sensitive to $\bar{\phi}$ (changed by varying τ_y) and the calculated nonlinearity is larger than that observed in experiments; the value of $\bar{\phi}=3.5^\circ$ leads to the best correlation between theory and experiment and this corresponds to $\tau_y=0.5\tau_{max}$. Table 3 presents the strength values predicted by equation 7 assuming $\bar{\phi}=3.5^\circ$; the error between the theoretical and experimental values is about 3% at room temperature. At higher temperatures the error increases to almost 15%, and this may be attributed to the different failure mechanism observed (out-of-plane microbuckling).

The fibre misalignment for the T800/924C system is predicted using the same procesures, as 2.5° from figure 7. The compressive and shear strength are given in a tabulated form in table 4 for each temperature level. Theoretical calculations are based on equation 7 (or equation 4). The experimental and theoretical $\sigma-\varepsilon$ curves are presented in figures 8a-b for two different environmental conditions (20°C-dry and 100°C-dry). Agreement between experiment and theory is acceptable.

6.3 Conclusions

The compressive failure of unidirectional glass/pp and T800/924C carbon fiber reinforced (CFRP) laminates occurs due to fibre microbuckling, regardless of temperature. Failure initiation depends on material imperfections such as fiber misalignment, voids, resin reach regions and fibre tilting.

The experimental compressive response of the two composite systems was compared with theoretical predictions.

Equations 4 and 7 developed in [5,7], respectively, can be used to predict compressive strength of glass/polypropylene (plytron) and CFRP laminates tested at various temperatures. Experiment and theory are in good agreement for all temperature levels examined.

Batdorf and Ko[7] model can also be used to predict the compressive response. It is more accurate for the carbon fibre-epoxy system than the glass-pp composite.

It can be concluded that existing plastic kinking analyses of microbuckling are able to account for some but not all of the experimental observations. They correctly predict that shear strength and fibre imperfection are important parameters affecting the compressive strength σ_c of the composite. However, it is not possible to say exactly how σ_c will vary with fibre content and fibre matrix interface. Also the value of fibre misalignment is in change of τ_y quite arbitrary. It does appear, however, that is possible to chose values which give consistant representation of the experimental data.

Appendix A

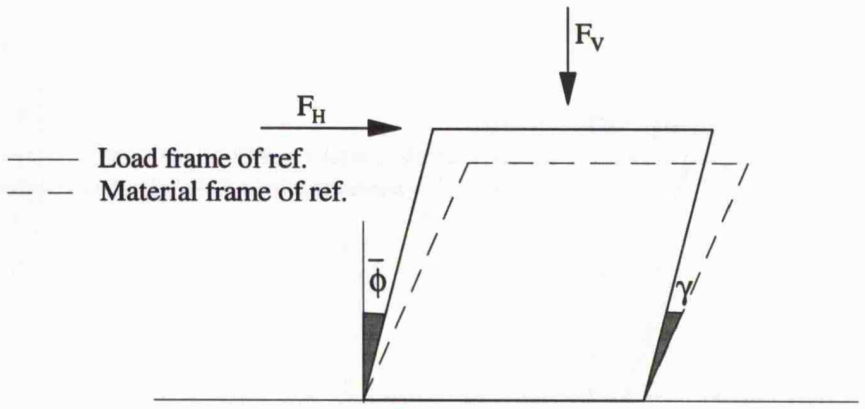

axis transformation

F_v, F_H are the applied forces and result in direct stress (σ_a) and shear stress (τ_a)

$$\sigma = \sigma_a - 2(\bar{\phi} + \gamma)\tau_a \tag{1}$$

$$\tau = \tau_a - (\bar{\phi} + \gamma)\sigma_a \tag{2}$$

Equation 2 can be rearranged as,

$$\sigma_a = \frac{\tau - \tau_a}{\bar{\phi} + \gamma} \tag{3}$$

for pure compression, $\tau_a = 0$ and equation 3 become

$$\sigma_a = \frac{\tau}{\bar{\phi} + \gamma} \tag{4}$$

The maximum stress the element can support occurs when,

$$\frac{\partial \sigma_a}{\partial \gamma} = 0 = \frac{\dfrac{\partial \tau}{\partial \gamma}(\bar{\phi}+\gamma) - \dfrac{\partial}{\partial \gamma}(\bar{\phi}+\gamma)\tau}{(\bar{\phi}+\gamma)^2}$$

$$\frac{\partial}{\partial \gamma}(\bar{\phi}+\gamma)\tau \Rightarrow \tau, \quad \frac{\partial \sigma_a}{\partial \gamma} = \frac{\dfrac{\partial \tau}{\partial \gamma}}{(\bar{\phi}+\gamma)} - \frac{\tau}{(\bar{\phi}+\gamma)^2} = 0$$

$$\frac{\dfrac{\partial \tau}{\partial \gamma}}{(\bar{\phi}+\gamma)} = \frac{\tau}{(\bar{\phi}+\gamma)^2} \Rightarrow \frac{\partial \tau}{\partial \gamma} = \frac{\tau}{(\bar{\phi}+\gamma)} \tag{5}$$

combining equations 4 and 5 get

$$\sigma_a = \frac{\tau_y}{\bar{\phi}+\gamma} = \frac{\partial \tau}{\partial \gamma}(\gamma_y) = G_t(\gamma_y) \tag{6}$$

where G_t is the tangent shear modulus.

Thus, the compressive failure strength of the kink element is the tangent shear modulus of the material taken at the shear yield strain γ_y, where permanent (plastic) deformation occurs. This can now be determined graphically from the $\tau - \gamma$ response, see for example figures 5&7.

REFERENCES

1. Shuart, M.J., Short Wavelength Buckling and Shear Failures for Compression Loaded Laminates, *NASA TM-87640*, 1985.

2. Hahn, H.T, Compression Failure Mechanisms in Composite Structures, *NASA CR-3988*, 1986.

3. Haeberle, J.G. and Mathews, F.L., Compression Test Methods for Composites and Theories Predicting the Compressive Strength of Unidirectional CFRP, *Applied Solid Mechanics*, Vol.3, pp.66-79, 1989.

4. Rosen, B.W., Mechanics of Composite Strengthening, Fibre Composite Materials, *American Society of Metals*, pp.37-75, 1965.

5. Budianky, B. and Fleck, N.A. Compressive Kinking of Fiber composites: a Topical Review, *Applied Mechanics Reviews*, Vol.47, No.6, part 2, p.246, June 1994.

6. Budiansky, B., Micromechanics, *Computer & Structures*, Vol.16, part (1-4), pp.3-12, 1983.

7. Batdorf, S.B. and Ko, W.C. Stress-strain Behaviour and Failure of Uniaxial Composites in Combined Compression and Shear-I. *Internal report, School of Engineering and Applied Science, University of California*, Los Angeles, CA 90024, July 1987.

8. Larger, J.B. and June, R.R., Compressive Strength of Boron/epoxy Composites, *Journal of Composite Materials,* Vol.3, No.1, pp. 48-56, 1969

9. Ewins, P.D., Tensile and Compressive Test Specimens for Unidirectional Carbon Fibre-reinforced Polyester Resins, *RAE Technical Report* 71217, 1971.

10. Steif, P.S., A model for Kinking in Fibre Composites I-II, *Int. J. Solid Structures*, Vol.26, pp. 549-569, 1990.

11. Argon A.S., Fracture of Composites, *Treatise on Materials Science & Technology*, vol.1, Academic Press, New York, pp.79-114, 1972.

12.Piggott, M.R. and Harris, B., Compression Strength of Carbon, Glass and Kevlar-49 Fibre Reinforced Polyester Resins, *J. Materials Science.,* Vol.15 pp. 2523-2538, 1980.

13.Haeberle, J.G. and Mathews, F.L., A Micromechanics Model For Compressive Failure of Unidirectional Fibre-reinforced Plastics. *J. Composite Materials*, Vol.28, No.17, pp.1618-1639, 1994.

14.Saunders, D.E.J. and Soutis, C., The Shear and Compressive Behaviour of Low Temperature Cured CFRP Laminates. *3rd International Conference on Deformation and Fracture of Composites, The institute of Materials.* pp.26-35, Guildford, UK. 27-29 March 1995

Table 1. Strength properties of glass/polypropylene laminates at various test temperatures.

Property	Temperature °C				
	20	50	80	100	120
0^0 Compression					
Strength (MPa)	317	234	178	149	108
Modulus (GPa)	29.5	26.4	23.5	22	20
Strain of failure %	0.98	0.85	0.68	0.54	0.47
0^0 Tension					
Strength (MPa)	550	470	411	350	280
Modulus (GPa)	32.5	27.6	25.3	23.4	20.1
Strain of failure %	1.92	1.8	1.6	1.6	1.4
90^0 Tension					
Strength (MPa)	11	7	5	4	-
Modulus (GPa)	4.1	2.4	1.5	1.4	-
Strain of failure %	0.3	0.5	0.7	0.9	-
$\pm 45^0$ Tension					
Shear strength (MPa)	55	45	38	32	27
Shear modulus (GPa)	2.1	1.3	0.8	0.5	0.3
Shear strain of failure %	19.5	26	32	39	45

Table 2. Strength properties of T800/924C laminates at hot-dry and hot-wet environments

Property	Temperature °C							
	20		50		80		100	
	dry	wet	dry	wet	dry	wet	dry	wet
0^0 Compression								
Strength (MPa)	1395	1060	1230	930	1137	828	973	654
Modulus (GPa)	166.5	-	154	-	148	-	137	-
Strain of failure %	0.925	-	0.842	-	0.742	-	0.728	-
Shear test (Iosipescu)								
Shear strength (MPa)	111	102.4	104.6	96.8	98	90.6	88.8	84.5
Shear modulus (GPa)	6.05	-	5.79	-	5.42	-	4.9	5
Shear strain of failure %	6.4	-	6.77	-	7.43	-	6.39*	-
								-

* Straingauge failure

Table 3 Experimental and theoretical compressive strength of the glass/polypropylene (plytron) u/d laminates ($\bar{\phi} = 35^{o}$) equation 4 [5,7].

Temperature °C	τ_y MPa	γ_y %	σ_c^{th} MPa	σ_c^{exp} MPa	error %
20	28	3	307	317	2.2
50	24	5	216	234	7.6
80	19	6	157	177	10.7
100	16.5	7	126	149	15.4
120	14	9	93	108	13.9

Table 4 Experimental and theoretical compressive strength of the T800/924C u/d laminates ($\bar{\phi} = 25^{o}$)equation 4 [5,7].

Temperature °C	τ_y MPa	γ_y %	σ_c^{th} MPa	σ_c^{exp} MPa	error %
20	85	2	1335	1395	4.3
50	80	2.33	1195	1230	2.8
80	78	2.45	1137	1137	---
100	67	2.56	968	973	0.5

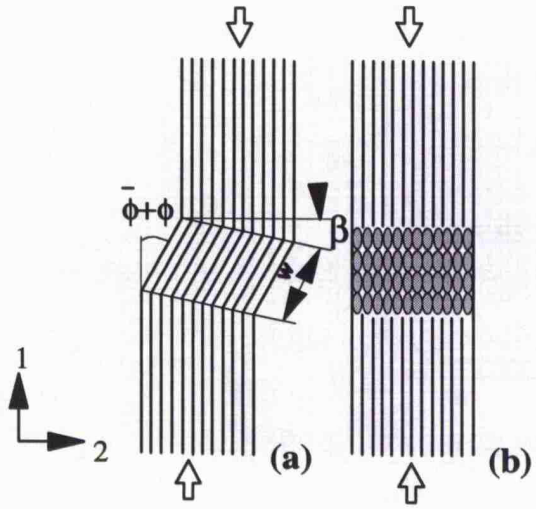

Figure 1 Geometry of fibre microbuckling mode (β=boundary orientation angle; $\bar{\phi}$=initial fibre misalignment, ϕ=inclination angle; w=kink width) (a) and (b) in-plane and out-of-plane microbuckling , respectively.

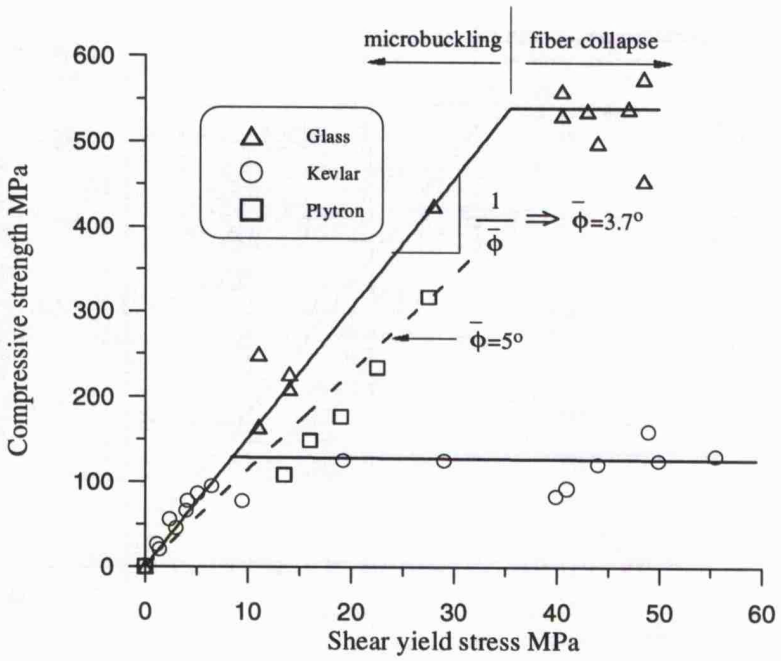

Figure 2 Compressive strength of unidirectional laminates plotted versus the shear yield stress of the composite (glass and Kevlar data taken from [12].

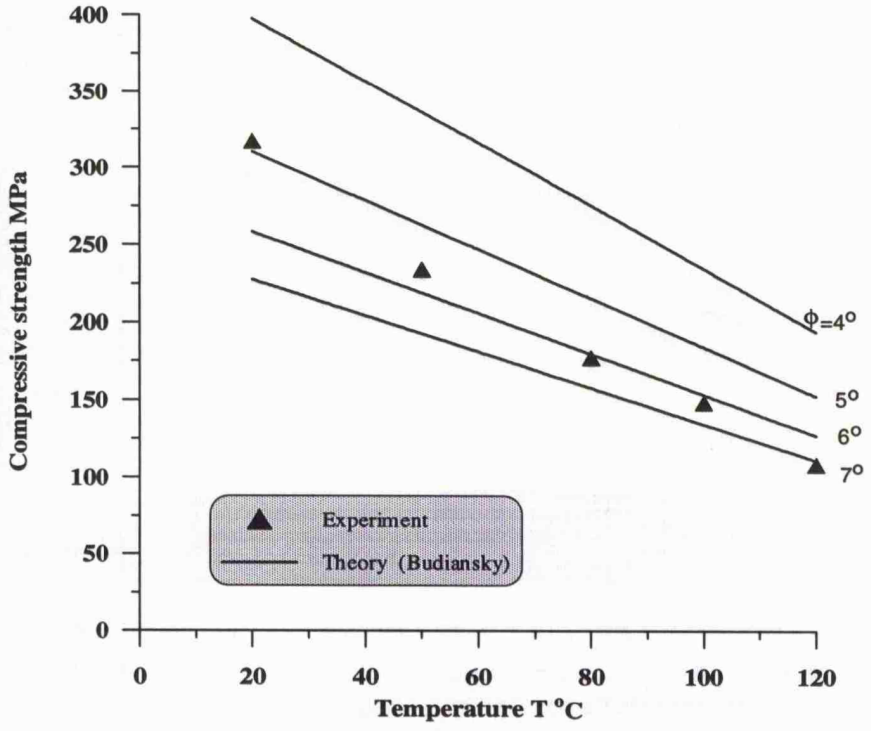

Figure 3 Compressive strength of Plytron laminates as a function of temperature. Theoretical values are obtained from equation (3) [5].

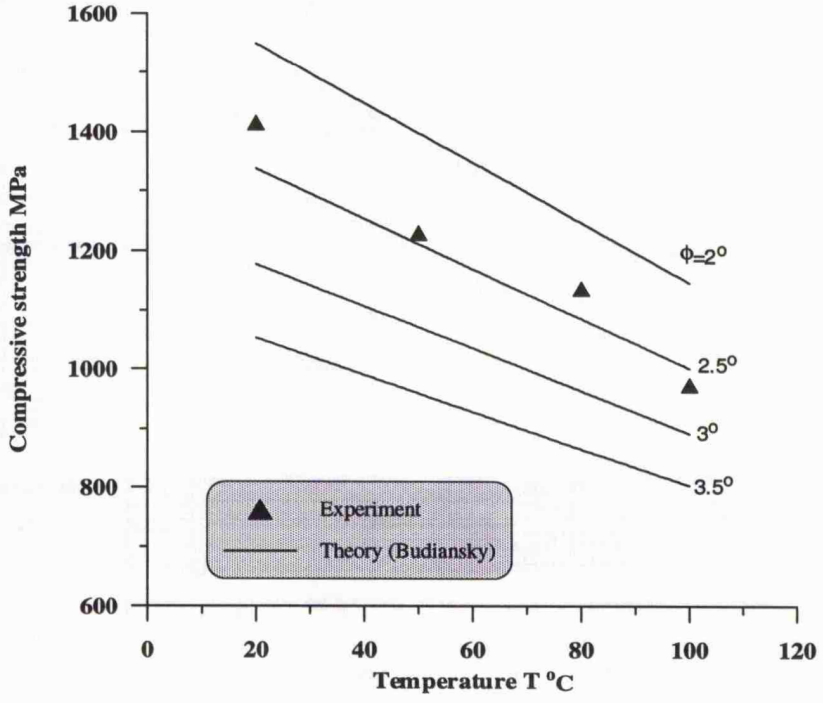

Figure 4 Compressive strength of T800/924C laminates as a function of temperature. Theoretical values are obtained from equation (4) [5].

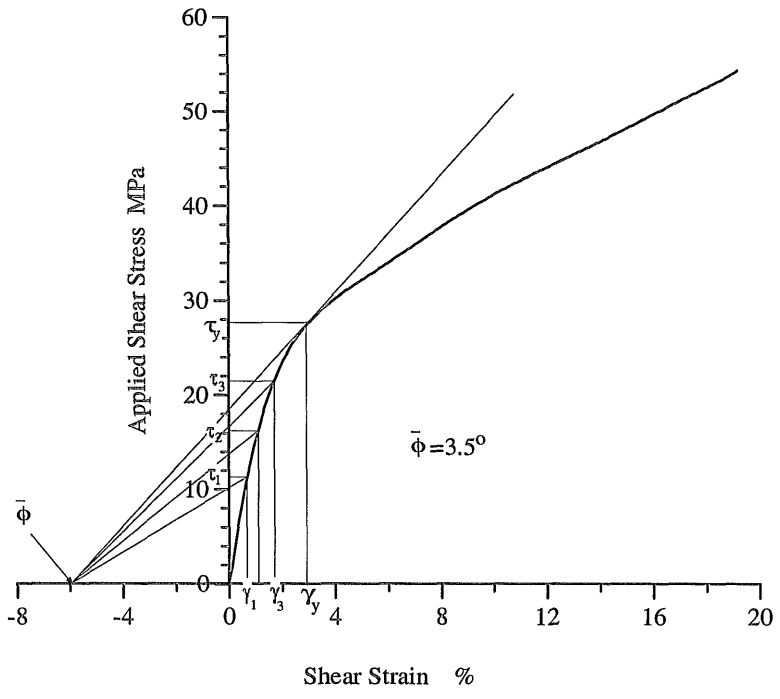

Figure 5 Shear stress-strain curve of a u/d Plytron laminate at 120°C, together with a tangent to the curve as described by Batdorf and Ko [7]

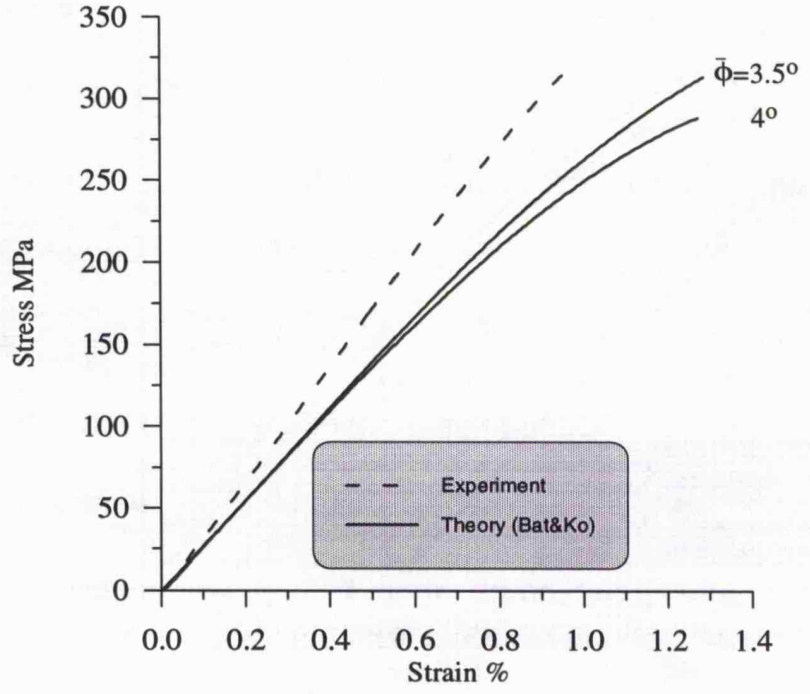

(a) RT-dry

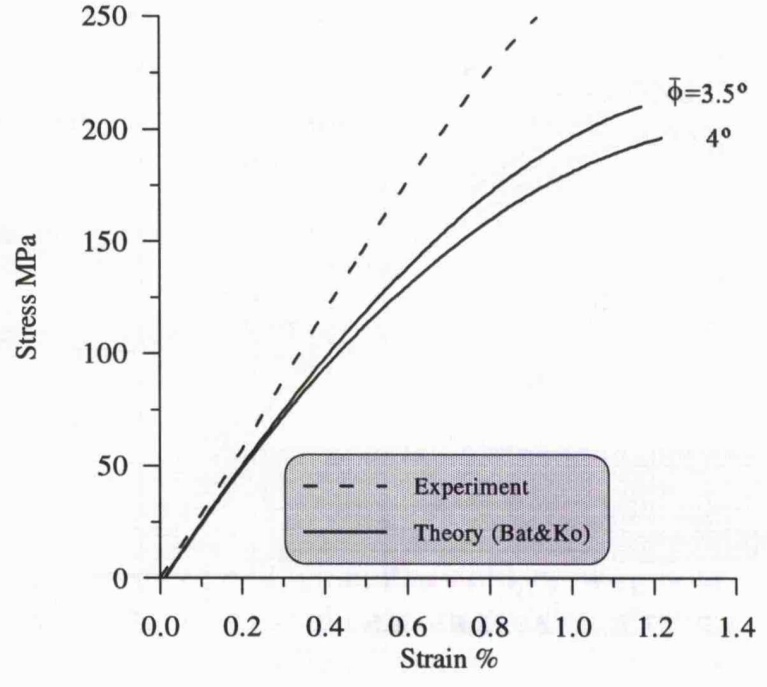

(b) 50°C-dry

Figure 6 Comparison of the compressive stress-strain curves for plytron, obtained from the shear stress-strain data and uniaxial compression test at various temperatures.

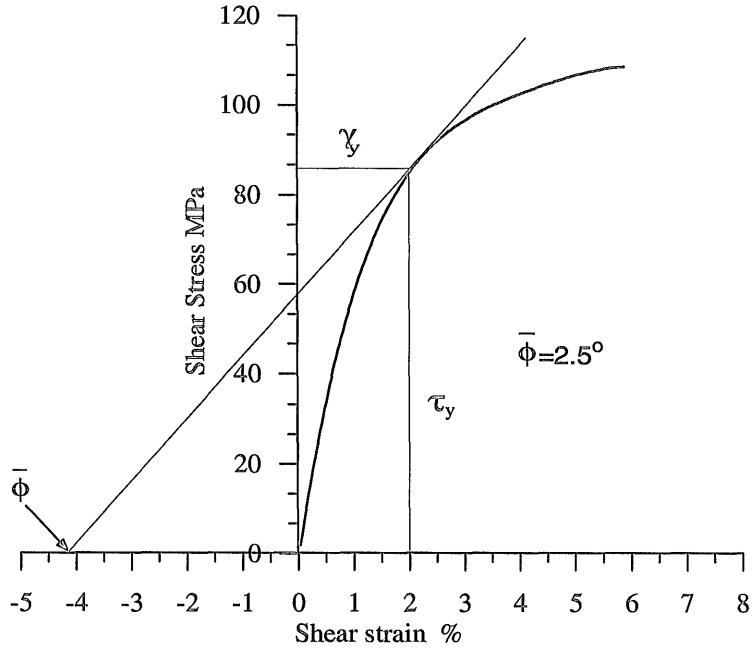

Figure 7 Shear stress-strain curve of a T800/924C u/d laminate at room temperature, together with a tangent to the curve as described by Batdorf and Ko [7]

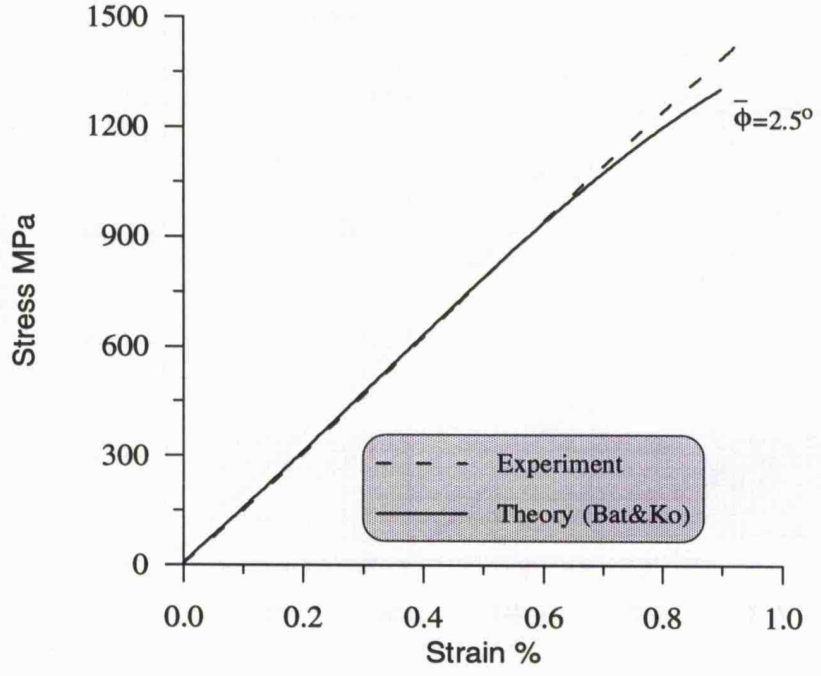

(a) RT-dry

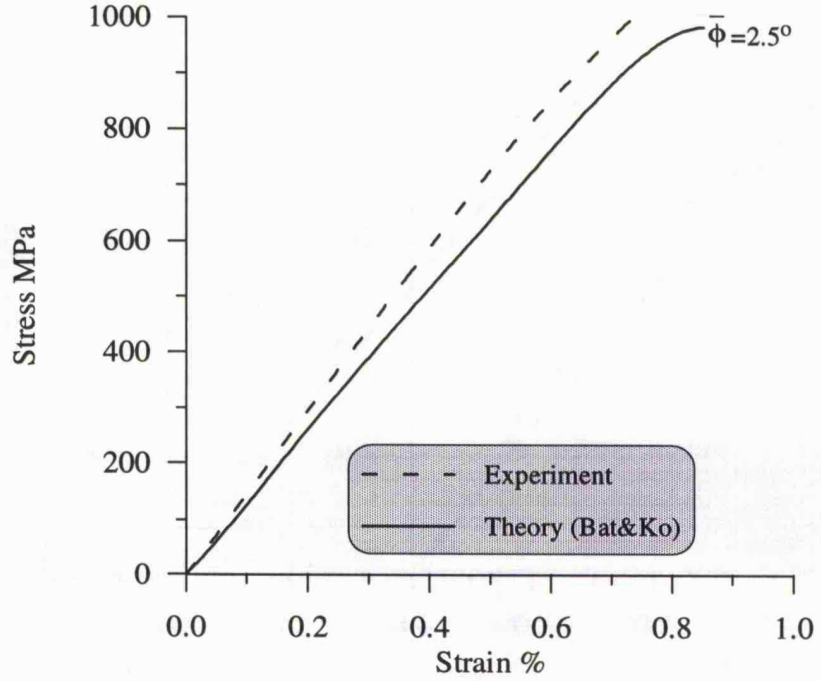

(b) 100°C-dry

Figure 8 A comparison of the compressive stress-strain curves obtained, for the T800/924C obtained from the shear stress-strain data using Batdorf-Ko model and experimental results at various temperatures.

CHAPTER SEVEN

7.1 Conclusions

From this study, on the fracture characteristics of unidirectional carbon fibre-epoxy and glass/polypropylene composite laminates, subjected to compressive loading in hot-dry and hot-wet environments ,the following conclusions can be drawn:

Moisture absorbtion

The T800/924C composite system absorbed 1.42% by weight moisture when exposed to boiled water for 36 days. The diffusion coefficient and the equilibrium moisture content are measured experimentally and used in a computer program to estimate through thickness moisture distribution. It is found that although Fickian diffusion does not exactly model the actual moisture absorption in the T800/924C composite system, it is sufficiently accurate in the cases examined. Moisture absorbtion reduces the glass transition temperature by about 50°C.

Compression testing

Spark-eroded grip inserts can be used for compression testing. No damage to the surface plies is observed in specimens with uniform thickness and specimen preparation cost are substantially reduced. The strength/stiffness properties and failure modes are comparable to those obtained from specimens with carefully bonded aluminum tabs. Hence tabs are not required in compression testing provided that acceptable failure modes and location of failure are obtained.

Failure mode of unidirectional laminates

The compressive failure of glass/pp and T800/924C laminates occurs due to fibre microbuckling, regardless of temperature. In the case of plytron specimens

tested at approximately 50°C the failure mode changes from in-plane to out-of -plane microbuckling, which initiates at lower applied strains. It is observed that the failure mechanism of T800/924C laminate in hot-wet conditions always occurs as a result of out-of-plane fibre microbuckling. This is attributed to the reduction in matrix strength properties and weakening of the ply interface arising from elevated temperature and environmental conditions. Thus, in compression the matrix and interface play a key role in providing side support to the fibres and consequently resistance to fibre microbuckling. Failure initiation also depends on material imperfections, such as voids, resin rich regions and fibre misalignment. It can be concluded that, because the strength of fibres has been substantially increased, while polymeric matrices have changed very little in strength due to demands for high toughness of composite, the fibres fail by microbuckling before their compressive strength is reached.

Failure and compressive strength prediction

The compressive strength of T800/924C and glass/pp laminate are approximately 20-25% of the shear modulus.

At operating temperature of 120 °C the strength has been reduced by more than 60% and failure strain dropped by 50% for the glass/polypropylene laminate.

The compressive strength of the T800/924C composite laminates has been reduced more than 20% due to the reduction of shear strength at 100°C-dry. The compressive strength is further reduced (by 50%) when the laminate contain 1.42% moisture by weight and is tested at 100°C and 95% RH.

The experimental compressive strength properties are compared with theoretical predictions. Budiansky's and Bat&Ko model can be used to predict the compressive strength and $\sigma - \varepsilon$ curve of unidirectional composite laminates. Theory and experiment are in good agreement for both materials examined.

Existing plastic kinking analyses of microbuckling are able to account for some but not all of the experimental observations. They correctly predict that shear strength and fibre imperfection are important parameters affecting the compressive strength of the composite. However, it is not possible to say exactly how

compressive strength will vary with fibre content and the value of fibre misalignment is quite arbitrary. In summary, although there has been research on the subject for more than thirty years prediction of the compressive strength from the properties of the constituents is not yet available.

7.2 Suggestions for Future Work

The tests reported in the this .theses represent an idealized situation which do not correspond closely to the type of circumstances which can occur in practice. Although the results give a clear indication of the order of magnitude of loss of strength of composite due to hot-wet conditions, these are particular condition where that is the possibility of more severe behaviour. For a complete understanding of the problem there is a need experimental work which explores the following circumstances.

One of the more extreme environmental conditions experienced by an epoxy composite matrix occurs during a supersonic dash of a fighter aircraft. The aircraft dives from high altitudes (where outer surface temperature is -20°C to 50°C) into a supersonic, low-altitude run during which aerodynamic heating raises the surface temperature to 100 °C -150 °C, in a matter of minutes[1] On reduction of speed the outer surface temperature drops extremely rapidly at rates up to about 500°C/min, thus exposing the epoxy composite to a thermal spike. Simulation of such thermal spikes demonstrate that they can increase the amount of moisture absorbed by the epoxy composite. In this case the gradient of the moisture content is measured. It is important to understand the effects of such gradient on the failure strength of the composites.

Moisturized specimens need to be tested after drying at various temperature levels. Some studies have shown that the materials may not regain its strength after drying[2].

Further work is required to study the effect of stacking sequence on the moisture diffusion, experimentally and theoretically.

The specimens should be tested at temperatures below zero degrees to find out how the compressive and fracture behaviour of the materials (Winter environments).

Notched and unnotched unidirectional and multidirectional laminates should be tested under various hot-wet environmental conditions.

Further studies on the effect of composite quality (i.e., fibre/matrix interface and the distribution of fibre misalignment) on the compressive strength are required. The interaction of moisture, with these factors needs also to be considered.

REFERENCES

1. VERETTE, R.M., American Institute of Aeronautics and Astronautics Aircraft Systems and Technology Meeting, *AIAA Paper* N0. 75-101, Los Angeles, August 1975.

2. Tang, J.M. and Springer, G.S.. Effect of moisture and temperature on the compressive and short beam shear properties of fiberite T300/976 fabric. *J. Reinforced Plastic and Composites,* Vol. 7, p.120, 1988.

APPENDIX

PUBLISHED PAPERS

ICCM-9 Composite Properties and Application,
Madrid, 12-16 July, 1993, pp.581-589.

HIGH TEMPERATURE EFFECTS ON THE COMPRESSIVE STRENGTH OF GLASS FIBRE-REINFORCED COMPOSITES

C. Soutis and D. Turkmen
University of Leicester, Department of Engineering,
University road Leicester, LE1 7RH, UK.

ABSTRACT

The influence of elevated temperatures on the static compressive behaviour of unidirectional glass/polypropylene (ICI Plytron) laminates is examined. Tests are conducted between 21°C and 120°C to provide variation in the constitutive behaviour of the polymer matrix and thus additional variation in the support provided to the glass fibres. It is found that laminate looses strength as the operating temperature increases and failure occurs due to fibre microbuckling. At about 50°C the failure mode switches from in-plane to out-of-plane microbuckling. As the temperature increases the shear strength/stiffness of the resin is considerably reduced; this decreases the amount of side support for the fibres and reduces the strain level at which fibre microbuckling initiates. Growth of this damage requires little additional load, suggesting that compression strength is controlled by initiation, rather than propagation of microbuckling. Fracture characteristics are identified using optical and scanning electron microscopy. Theoretical models are employed to predict damage.

Keywords: Compression, ICI Plytron, Composite laminates, Fibre microbuckling, High temperature, Fracture analysis.

1. INTRODUCTION

Continuous fibre-reinforced plastics are being used in an ever increasing number of structural applications. However, more efficient use of these materials is limited by their apparent low compressive strength especially under got-wet conditions. Most composite laminates based on carbon and glass fibres, and polymeric resins are weaker in compression than in tension due to fibre microbuckling [1-3]. This is an instability failure mode which nucleates locally (e.g. free-edge, voids, resin rich regions) and propagates under little additional load through the laminate, causing a narrow zone within the 0° plies to loose structural integrity, Figure 1.

From theoretical developments on the compressive strength of unidirectional laminates [4-9] it is suggested that failure induced by fibre microbuckling is

dependent on the shear strength/modulus of the matrix (resin) material. To assess the validity of these models the present study investigates the effect of resin ductility (varied as a function of the test temperature) on the compressive strength of unidirectional glass/polypropylene (glass/pp) laminates. Failure mechanisms are examined and strength measurements are compared with theoretical predictions.

2. EXPERIMENTAL PROCEDURE

2.1 Manufacture of glass/pp laminates

The material selected for this study consists of continuous glass fibre in a thermoplastic matrix of polypropylene (65. vol.% resin content). It comes under the ICI (Imperial Chemical Industries) trade name 'Plytron' and is produced in 240 mm wide prepreg for laminate assembly. An elevated temperature compression moulding technique was employed to manufacture $[0_4]_s$ and $[(\pm 45)_2]_s$ glass/pp laminates. Sheets of the prepreg material were cut to 260 mm by 240 mm using a guillotine and laid together by hand. Eight plies were used in the composite plates which resulted in a cured laminate thickness of approximately 3.8 mm. Teflon coated porous bleed fabric and absorbent cloth were used to sandwich the laminate during compression moulding which resulted in the removal of excess polymer matrix. The manufacturer's standard compression moulding cycle was followed which produced laminates of acceptable quality. There was no visual evidence of any voids or porosity and the surface of the composite plates were flat and smooth. Sectioning and optical microscopy studies revealed that the void content was less than 2% and some fibre misalignment in the $[0_4]_s$ laminate was evident. Initial fibre imperfections in compression testing reduce the laminate strength [3] and therefore extra care must be taken during the moulding process.

2.2 Specimen design and mechanical tests

Unidirectional fibre-reinforced composites are highly anisotropic materials and premature failure due to Poisson deformation (brooming) may occur when axial compression is applied. This failure occurs on the load bearing surfaces and is characterised by extensive longitudinal splitting and lateral movement of material at the specimen ends. In the present investigation the modified Celanese method [10]

was used to evaluate the compressive properties of the unidirectional glass/pp laminates. This test method employs tabbed specimen ends that are shear loaded, thereby eliminating the primary source of brooming. The specimens tested had a gauge length of 13 mm which is a compromise between the requirement to eliminate Euler bending and the need to avoid end effects, while providing adequate space for strain gauges. The specimen width and thickness were 10 mm and 3.8 mm, respectively.

The compressive tests were performed on a screw-driven machine of capacity 10kN at a crosshead displacement of 0.017 mms^{-1}. To measure compressive strength of the laminates as a function of temperature the Celanese rig was adapted to hot air heating. Two extra inspection ports were drilled on the Celanese alignment sleeve and a hot air blower was attached. Symmetric airflow was achieved and the specimen was heated evenly. The temperature of the specimen was monitored by a thermocouple. It took approximately 5 minutes to reach 120°C and the specimens were allowed to 'soak at temperature (21°C), 50°C, 80°C, 100°C and 120°C. Shear strength properties were obtained by testing $[(\pm 45)_2]_s$ laminates in tension at elevated temperature. Mechanical tests were conducted following the procedures outlined in CRAG test methods [10]. Longitudinal and transverse strains for tension and compression were measured by 1 mm long foil strain gauges that retained accuracy over the range of temperatures used in this study.

3. TEST RESULTS AND DISCUSSION

The experimental results consist of stress-strain plots, fracture stresses and strain photographs showing the overall failure mode of selected failed specimens and optical and scanning electron micrographs of fracture surfaces. The tensile properties of the glass/pp system are not discussed in detail but presented in Table 1 for comparison purposes; at least four specimens were tested at each temperature level.

3.1 Stress-strain data

Compressive failure in all specimens is catastrophic and quite localised, Figure 2. A kink band structure (fibre microbuckling) occurs without warning and immediately leads to laminate breakage. Fracture is within the specimen gauge length implying that

the test is successful. A plot of the applied axial stress as a function of average axial strain measured by back-to-back strain gauges is

Table 1. Tensile strength properties of glass/polypropylene laminates at various test temperatures.

Property	Temperature °C				
	20	50	80	100	120
0^0 Tension					
Strength (MPa)	550	470	411	350	280
Modulus (GPa)	32.5	27.6	25.3	23.4	20.1
Strain of failure %	1.92	1.8	1.6	1.6	1.4
90^0 Tension					
Strength (MPa)	11	7	5	4	
Modulus (GPa)	4.1	2.4	1.5	1.4	-
Strain of failure %	0.3	0.5	0.7	0.9	-
					-
$\pm 45^0$ Tension					
Shear strength (MPa)	55	45	38	32	27
Shear modulus (GPa)	2.1	1.3	0.8	0.5	0.3
Shear strain of failure %	19.5	26	32	39	45

shown in Figure 3, for two typical specimens tested at room temperature. The mean compressive strength is 317 MPa, which is less than 60% of the tensile strength. The average failure strain and the Young's modulus (measured at 25% applied strain) are 0.98% and 29.5GPa, respectively. The effect of temperature on compressive properties of the unidirectional laminate can be seen in Table 2.

Table 2. Compressive strength properties of unidirectional glass/pp laminates as afunction of temperature

Property	Temperature °C				
	20	50	80	100	120
0^0 Compression					
Strength (MPa)	317	234	178	149	108
Modulus (GPa)	29.5	26.4	23.5	22	20
Strain of failure %	0.98	0.85	0.68	0.54	0.47

The values quoted in Table 2 are based on the average of four specimens tested at each temperature level. The results demonstrate that temperature has a marked influence on the compressive strength. At operating temperature of 120°C the strength has been reduced by more than 60% and the failure strain has dropped by approximately 50%. This is because the modulus of matrix is reduced substantially with increasing temperature, Table1. In uniaxial compression reduced in matrix modulus means reduced side support for the fibres which promotes premature failure of the composite by fibre microbuckling. The results in tables 1 and 2 suggest that the compressive strength is more temperature dependent than the tensile strength. In general, the tensile strength of a composite depends more on its fibre reinforcement, but compressive strength relies more upon its matrix material.

3.2 Compressive fracture modes

Damage to the room temperature unidirectional specimens involves fibre movement in the plane of the laminate (in-plane fibre microbuckling) along a 20^0-25^0 line from the transverse axis, Figure 4. In Figure 4 the optical micrograph shows that the fibres break at two points, which create a band inclined at $\beta \approx 25^\circ$ to the horizontal axis (or 65° to the fibre axis). It was observed in all specimens that angle β remains constant. The microbuckle once started from the free edge or a pre-existing material imperfection, such as voids resin rich regions and fibre misalignment, keeps its orientation and propagation. Berg and Salama [11] argued that kink band must be inclined in order to permit the buckled fibres to undergo both compressive and shear deformation. The reason is that microbuckling along planes, which permit shear displacement as buckling proceeds requires smaller compressive stress than does buckling on a plane that does not permit shear displacement. (i.e. planes perpendicular to the fibre axis.) The broken fibre segments in Figure 4 are approximately 25-30 fibre diameters long and have rotated by almost 30° from the loading axis ($\phi = 30^{o)}$. Once failure has occurred, the kink inclination angle ϕ can increase rapidly if the load is not immediately removed. This values are similar to those reported by Hahn [12] for S-glass epoxy composite. For a carbon fibre epoxy system examined in [3], β was found equal to 5°-15°, $\phi = 30^\circ$ and w=8-10 fibre diameters. Whether the angle of kink band inclination and the kink band width are of significance is still unclear. A

scanning electron micrograph of the fracture surface of a selected specimen is shown in Figure 5. It exhibits well defined steps and it is evident from Figure 5b that each fibre fails in bending.

In the case of specimens tested at temperatures higher than 50°C damage was confined to out-of-plane deformation in an almost 90° kink band across the specimen width. The kink band width measured 35-40 fibre diameters. Failed specimens show features quite distinct from those observed in specimens in which fibre buckling occurred in-plane, Figure 6. The strain level at which out-of-plane microbuckling initiates is reduced with increasing temperature and at 120°C is less than 50% of strain required to initiate in-plane microbuckling. Thus the out-of-plane microbuckling has been precipitated by a weaker ply interface in the hot specimen due to a reduction of fibre/matrix bond. Clearly, any weakening of the matrix or fibre/matrix interface arising from elevated temperature increases the probability of out-of-plane buckling of the fibres.

4 STRENGTH PREDICTIONS

A number of theories for the compressive strength of unidirectional composite laminates have been proposed and these have been reviewed by Stuart [13], Hahn [12], Haberle *et* al. [14] and Soutis [3]. In the present section we apply Rosen's [4] and more recently developed Budiansky's [8] model to predict the strength of the glass/pp system. The classic study of Rosen [4] is based on buckling theory for bars on an elastic foundation and suggests that the compressive strength σ_c is only dependent on the (initial) matrix shear modulus G_m and the fibre volume fraction V_f.

$$\sigma_c = \frac{G_m}{1 - V_f} \approx G_c \qquad (1)$$

where G_c is the composite shear modulus. For the glass/pp laminates Equation 1 is found to significantly over estimate the compressive strength for all temperature levels. More detailed investigations, for instance incorporating a three-dimensional continuum rather than treating matrix and fibre as two dimensional plates [5] produced similar results. This suggests that microbuckling is a plastic rather than an

elastic event. Results presented in Table 1 and 2 indicate that the compressive strength of Plytron is only 20-25% of the shear modulus.

Argon [6] and Budiansky [8] identified the shear yield strength of the composite τ_y and the initial misalignment angle $\bar{\phi}$ of the fibres as the main factors governing the compressive strength. For a rigid perfectly plastic matrix materials, Budianky found that the compressive strength σ_c is given by

$$\sigma_c = \frac{\tau_y}{\bar{\phi}} \qquad (2)$$

where τ_y is a matrix dominated property. In Figure 7 the compressive strength of the glass/pp laminates predicted by equation 2 is plotted versus test temperature T; the τ_y is taken as half the value of the shear strength τ_f, Table 1, and $\bar{\phi}$ is taking values between 4° and 7°. We have observed such fibre imperfections is section studies for the glass/pp laminates. It can be seen that for $\bar{\phi} \approx 6°$ the agreement between theoretical and experimental results is acceptable.

Budiansky's analysis predicts correctly that shear strength and fibre imperfection are important parameters affecting the compressive strength σ_c of the composite. However, it is not possible to say exactly how σ_c will vary with fibre content, which makes verification of equation 2 may be unreliable.

Recently, Steif [9] has modelled the effect of fibre-matrix debonding upon the elastic microbuckling of composites. The model is an adaptation of the Rosen [4] analysis in situations where slip occurs at the fibre-matrix interface; slip begins when the interfacial shear stress attains a critical value. Interfacial shear failure is similar in may respects to shear yielding of the matrix. Steif found that the theoretical fibre breaking strains compared reasonably well with measured failure strains when the kink band was assumed to have the experimentally observed width. His model fails to predict the kink band boundary orientation angle, β.

In summary, although there has been research on the subject for more than twenty years, a unique theoretical model which can predict the compressive strength from the properties of the constituents is still not available.

5 CONCLUDING REMARKS

The compressive failure of unidirectional glass/pp laminates occurs due to fibre microbuckling, regardless of temperature. In the case of specimens tested at approximately 50°C the failure mode changes from in-plane to out-of-plane microbuckling, which initiates at lower applied strains. Failure initiation depends also on material imperfections, such as voids, resin rich regions and fibre misalignment. The progressive decrease in strength with increasing temperature T is associated with the reduction in matrix shear strength properties with increasing T. Thus, in compression the matrix and interface play a key role in providing side support to the fibres and consequently resistance to fibre microbuckling. In currently used composites the strength of glass fibres has been substantially increased while polymeric matrices have changed very little in strength due to demands for high toughness of composite. As a result, the fibres fail by microbuckling beforetheir compressive strength is reached.

Existing elastic and plastic kinking analyses of microbuckling are able to account for some but not all of the experimental observations. Fibre bending and fibre matrix interface must be modelled expilicity in order to predict successfully the geometry of the microbuckle band and the compressive strength of the composite.

6. ACKNOWLEDGMENTS

The authors are grateful for founding from the Royal Society and wish to thank ICI Advanced Materials for supplying the glass/pp composite system. They also would like to express their appreciation to Mr. C.J. Morrison from Leicester University for assisting with the experimental work.

7. REFERENCES

1. Hahn, H.T. and Sohi, M.M., *Buckling of a Fibre Bundle Embedded in Epoxy*, Composites Science& Technology, vol.27, pp25-41, 1986

2. Harper, J.F. and Huemann, T.O. *Failure Mechanisms in Uniaxial Compression in Fibre Composites,* 4th International Conference on Fibre Reinforced Composites, Proceedings of the Institution of the Mechanical Engineers, pp.231-235, 1990.

3. Soutis, C. *Measurement of the Static Compressive Strength of Carbon Fibre/Epoxy Laminates*, Composites Science & Technology, vol. 42, 1991, pp.373-392.

4. Rosen, B.W., *Mechanics of Composite Strengthening, Fibre Composite Materials*, American Society of metals, 1965, pp.37-75.

5. Chung, W. and Testa, R.B., *The elastic Stability of Fibres in a Composite Plate*, J. Composite Materials, vol.3, 1969, pp.58-80.

6. Argon A.S., *Fracture of Composites*, Treatise on Materials Science & Technology, vol.1, Academic Press, New York 1972, pp.79-114.

7. Evans, A.G. and Adler, W.F., *Kinking as a Mode of Structural Degradation in Carbon Fibre Composites*, Acta Metallurgica, vol.22, 1977, pp.725-738.

8. Budiansky, B., *Micromechanics*, Computer & Structures, vol.16(1-4), 1983, pp.3-12.

9. Steif, P.S., *A model for kinking in Fibre Composites I-II*, Int. J. Solid Structures, vol.26, 1990, pp.549-569.

10. Curtis, P.A., CRAG *Test Methods for the Measurement of Engineering Properties of Fibre-Reinforced plastics*, RAE Technical Report 85099, 1985.

11. Berg, C.A. and Salama, M., *Fatigue of Graphite Fibre-Reinforced Epoxy in Compression*, Fibre Science & Technology, vol.6, 1973, pp.725-738.

12. Hahn, H.T, *Compression Failure mechanisms in Composite Structures*, NASA CR-3988, 1986.

13. Shuart, M.J., Short *Wavelength Buckling and Shear Failures for Compression Loaded Laminates*, NASA TM-87640, 1985.

14. Haeberle, J.G. and Mathews, F.L., *Compression Test Methods for Composites and Theories Predicting the Compressive Strength of Unidirectional* CFRP, Applied Solid Mechanics, vol.3, 1989, pp.66-79.

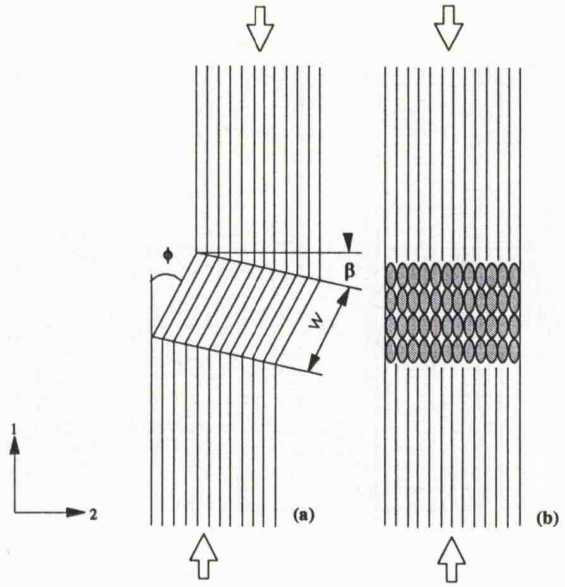

Figure 1 Geometry of fibre microbuckling mode [7] (β = boundary orientation angle; ϕ =inclination angle w=mibrobuckling width) a) in plane b) aut-of-plane microbuckling

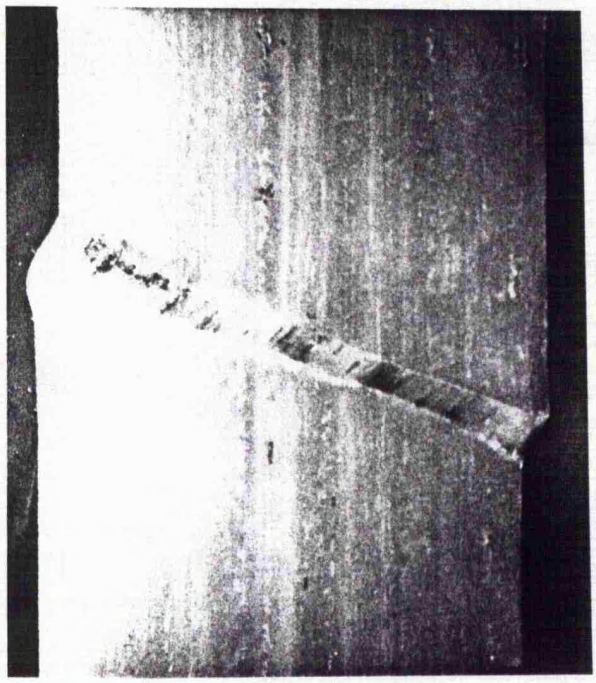

Figure 2. Overall failure mode of glass/pp laminate (buckle length ≈ 0.6 mm).

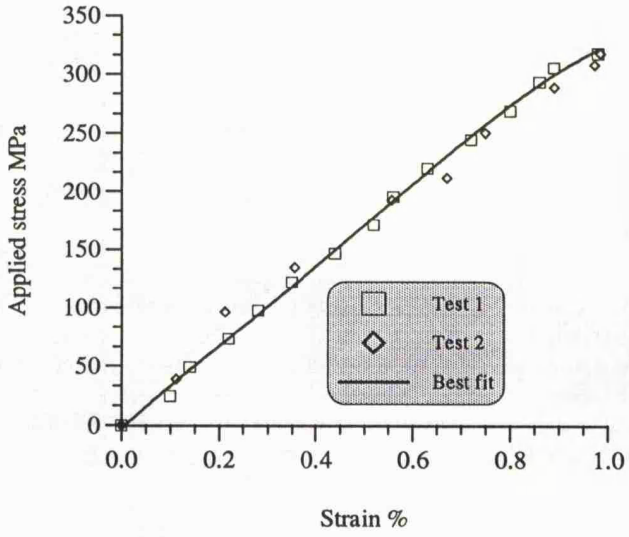

Figure 3 Compressive stress-strain responce of glass/pp laminate

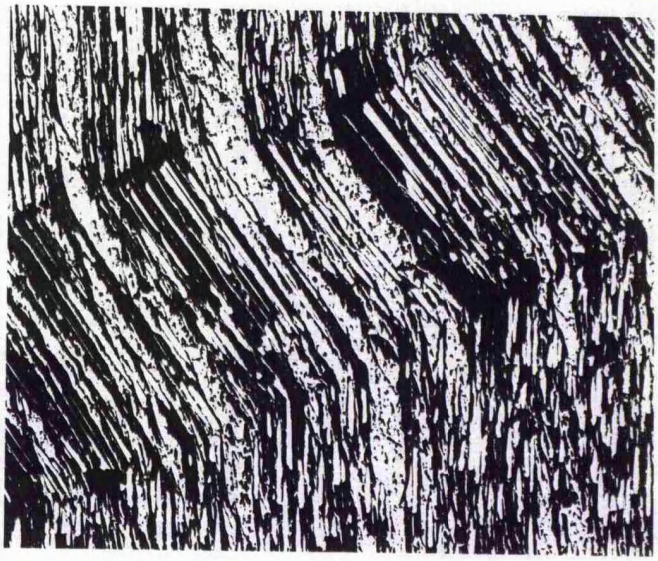

Figure 4 Optical microphotograph showing in-plane fibre microbuckling in a glass/pp laminate (β=25° to the horizantal axis, w ≈ 0.6mm)

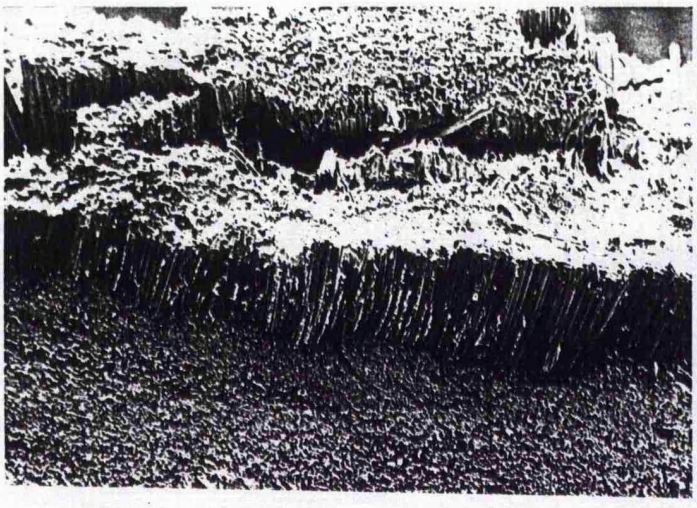

Figure 5.a Fracture surface of glass/pp laminate after buckling. It shows rows of buckled fibres (26x)

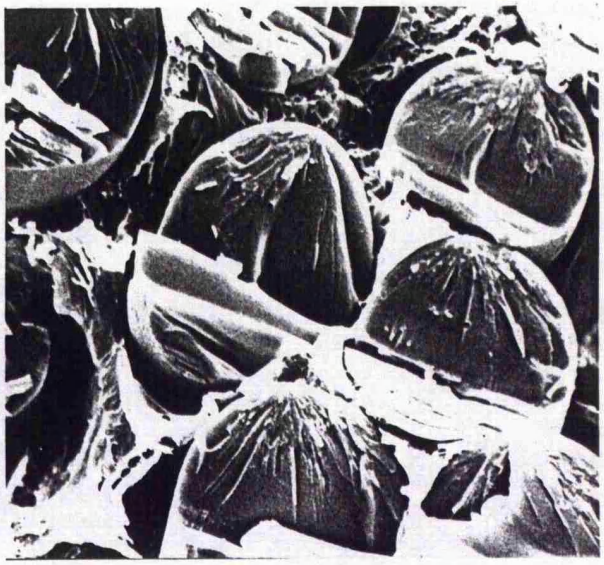

Figure 5b. Higher magnification of (5a) showing that each fibre fails in bending (1700x)

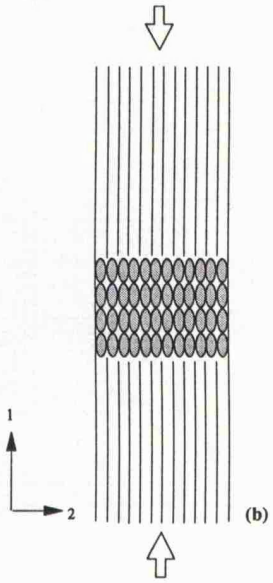

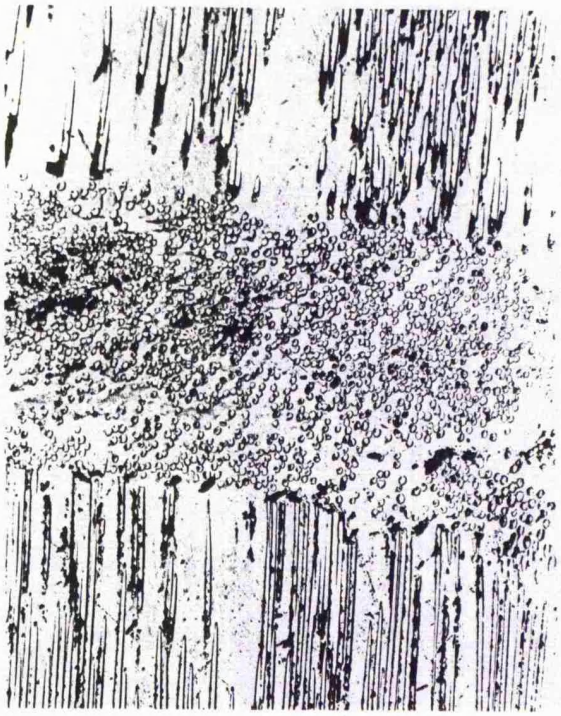

Figure 6. Optical microphotograph showing out-of-plane fibre microbuckling in a glass/pp laminate (w=1mm).

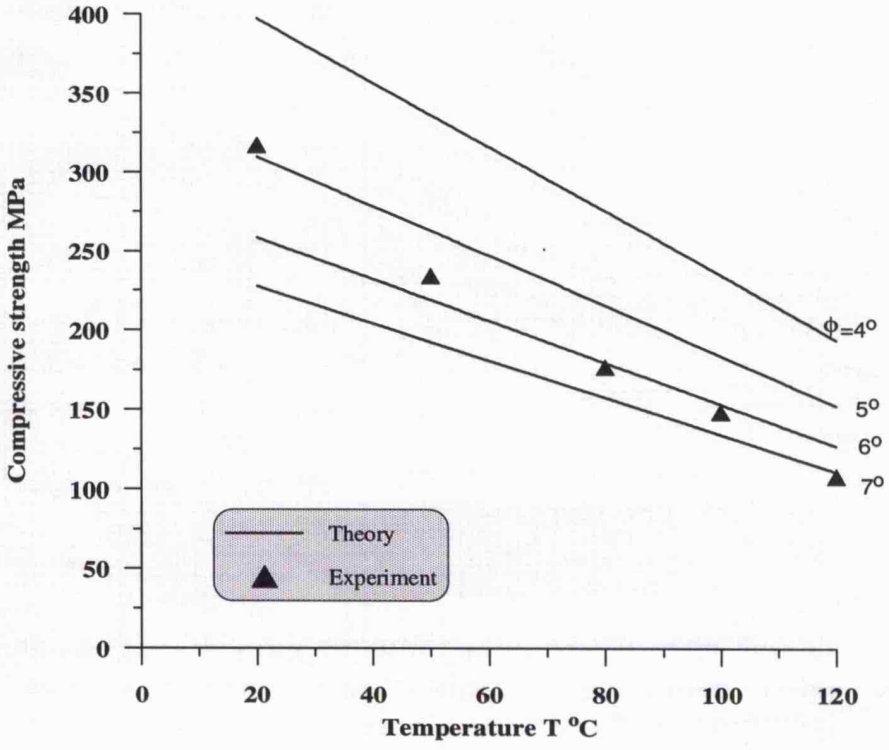

Figure 7. Compressive strength of glass/pp laminates as a function of temperature. Theoretical values are obtained from Budiansky's model [8].

ECCM-CTS2, September 13-15, 1994
Hamburg, Germany, pp. 169-177

COMPRESSIVE FAILURE OF UNIDIRECTIONAL COMPOSITES AT ELEVATED TEMPERATURE USING UNTABBED SPECIMENS

C. Soutis, D. Turkmen and C.J. Morrison
University of Leicester, Department of Engineering
University Road, Leicester LE1 7RH, UK

ABSTRACT

This paper describes an experimental study of the compressive failure of T800/924C carbon fibre-epoxy unidirectional laminates at elevated temperatures. Tests are conducted in a screw-driven machine between 20°C and 100°C, using untabbed straight-sided specimens in a modified Celanese test rig; the faces of the grip inserts are spark-eroded to produce a surface finish of approximately 20Ra. No damage to the surface plies is observed and the specimen preparation costs are substantially reduced. Strength and failure modes are comparable to those obtained from specimens with carefully bonded aluminium tabs.

1 INTRODUCTION

Compressive data are more difficult to generate than tensile data for carbon fibre reinforced plastics (CFRP), because compression testing is sensitive to factors such as Euler buckling, specimen misalignment in the test fixture, fibre misalignment in the specimen and bending/stretching coupling in the laminate [1,2].

As test methods originally designed for metals cannot in most cases be applied to composites, new test methods had to be developed. These methods include the Celanese [3], the Illinois Institute of Technology Research Institute (IITRI) [4] and the sandwich beam compression test loading method [5]. The Celanese method, first standardised by the ASTM in 1975 remained as the only composite material compression testing standard until 1987 when the IITRI and sandwich test methods were added to the ASTM standard D3410.

The Celanese and IITRI methods rely on shear to transfer the load from the testing machine through fixture grips into the specimen via tabs. Tab region failures

are quite common due to stress peaks near tab ends. These are more severe for fatigue loading and hot/wet conditions. Debonding due to interlaminar shear stresses and fibre breaks due to high axial stresses are often noticed [6]. Although stress concentrations can be reduced by using compliant ($\pm 45^{\circ}$ glass/epoxy) tabs with low taper angles (7°-10°), special care is needed for bonding tapered tabs and achieving valid failure modes.

In the present study, untabbed straight-sided specimens are tested using the RAE modified Celanese test rig [7]. The grip inserts of the apparatus have been specially textured so that no damage occurs in the composite. Test results are compared to those obtained in [2] from specimens with aluminium tabs.

2 EXPERIMENTAL PROCEDURE

2.1 Materials

All work reported here was performed on unidirectional Toray 800 carbon fibre/924C epoxy (Ciba-Geigy) laminates made from prepreg material. The composite contained approximately 65% by volume fibres and was moulded to a nominal thickness of 2mm. The $[0_8]_s$ laminates were cured in an autoclave at the Royal Aerospace Establishment, Farnborough, at a temperature of 170°C for 1h and subsequently post-cured for 4hrs at 190°C. the quality of the moulded laminates was checked by ultrasonic C-scanning and the void content was found less than 2%. Test material was sealed in a plastic bag and kept in an ambient laboratory-air environment prior to use.

2.2 Specimen Geometry

Test specimens, 10mm wide, were cut from the $[0_8]_s$ panels using a diamond-tipped saw. They have a constant rectangular cross-section and the thickness variation is less than 2%. The overall specimen length is 110mm and the gauge length is 13mm; the gauge length must be short enough to be free from Euler buckling, yet long enough to both allow stress decay to uniaxial compression and minimise Poison restraint effects due to the grips. The specimens were instrumented with 1mm long strain gauges on either side of the gauge section to measure strain and any bending.

2.3 Apparatus and Mechanical Tests

Compression tests were performed following the procedures outlined in CRAG test methods [7], using the modified Celanese test jig, Fig.1, at a constant compression rate of 1mm/min on a screw-driven machine of load capacity 50kN.

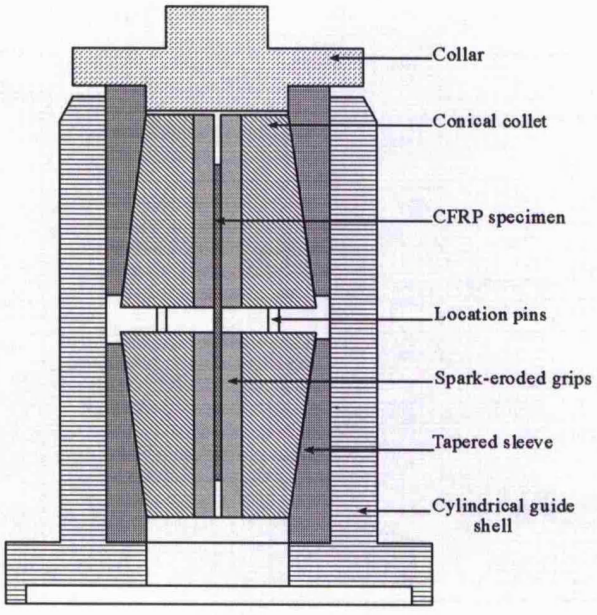

Fig.1. Celanese compression-test fixture [7].

The conventional serrated grip faces of the Celanese jig, Fig.2, were replaced by spark eroded inserts to eliminate adhesively bonded tabs on the specimen ends; tab misalignments, unequal tapers and variation or irregularity in the thickness of tabs or adhesive layers are problems which may cause premature failure in the composite and are all avoided in the present investigation.

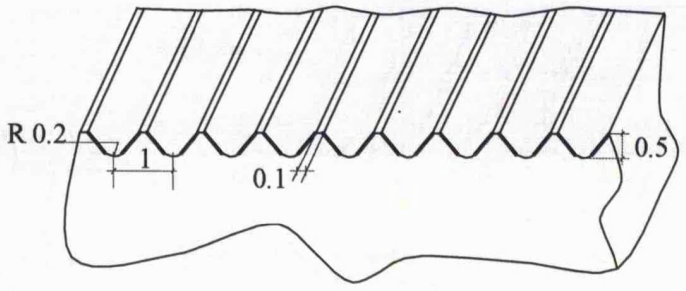

Fig.2 Conventional serrated grip faces (dimensions in mm).

The new grip inserts were cut from quench hardened 817M40 CrNi Mo steel and their faces were spark-eroded to produce a surface roughness of approximately

20 Ra, Fig.3. Fig.3 shows a surface typical of those produced by the electro discharge machine (or spark machining) process [8]. The surface has a random structure, caused by the electrical discharges randomly impinging on the surface through the di-electric fluid during the machining process. The magnitude of the Ra parameter is controlled by the energy in the spark; as the current is increased, so the roughness increases. In order to measure the compressive strength of the unidirectional laminates

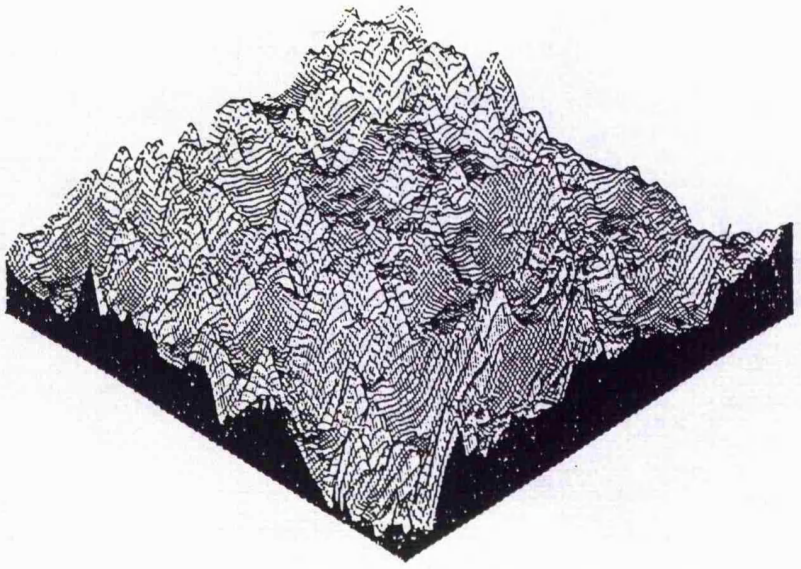

Fig.3 Axonometric projection of surface roughness of spark-eroded grips [8].

as a function of temperature the Celanese rig was further modified and adapted to hot air heating. Two extra inspection port were drilled on the Celanese alignment sleeve and a hot air blower was attached. Symmetric airflow was achieved and the specimen was heated evenly. The temperature of the specimen was monitored regularly by a thermocouple. It took less than 5min to reach 100°C and the environmental conditioning chamber was capable of maintaining the temperature to within ±3°. The specimens were allowed to 'soak' at temperature for about 10min before being tested.

Using this apparatus at least five tests were carried out per test condition (20°C, 50°C, 80°C and 100°C, dry).

3. TEST RESULTS AND DISCUSSION

3.1 Gripping Effects

The surface roughness of the specimen in the gripping area was measured before and after testing and was found equal to 2 Ra and 3 Ra, respectively. No fibre

breakage was detected on the surface plies when the specimens were examined under the scanning electron microscope, Figs.4a,b.

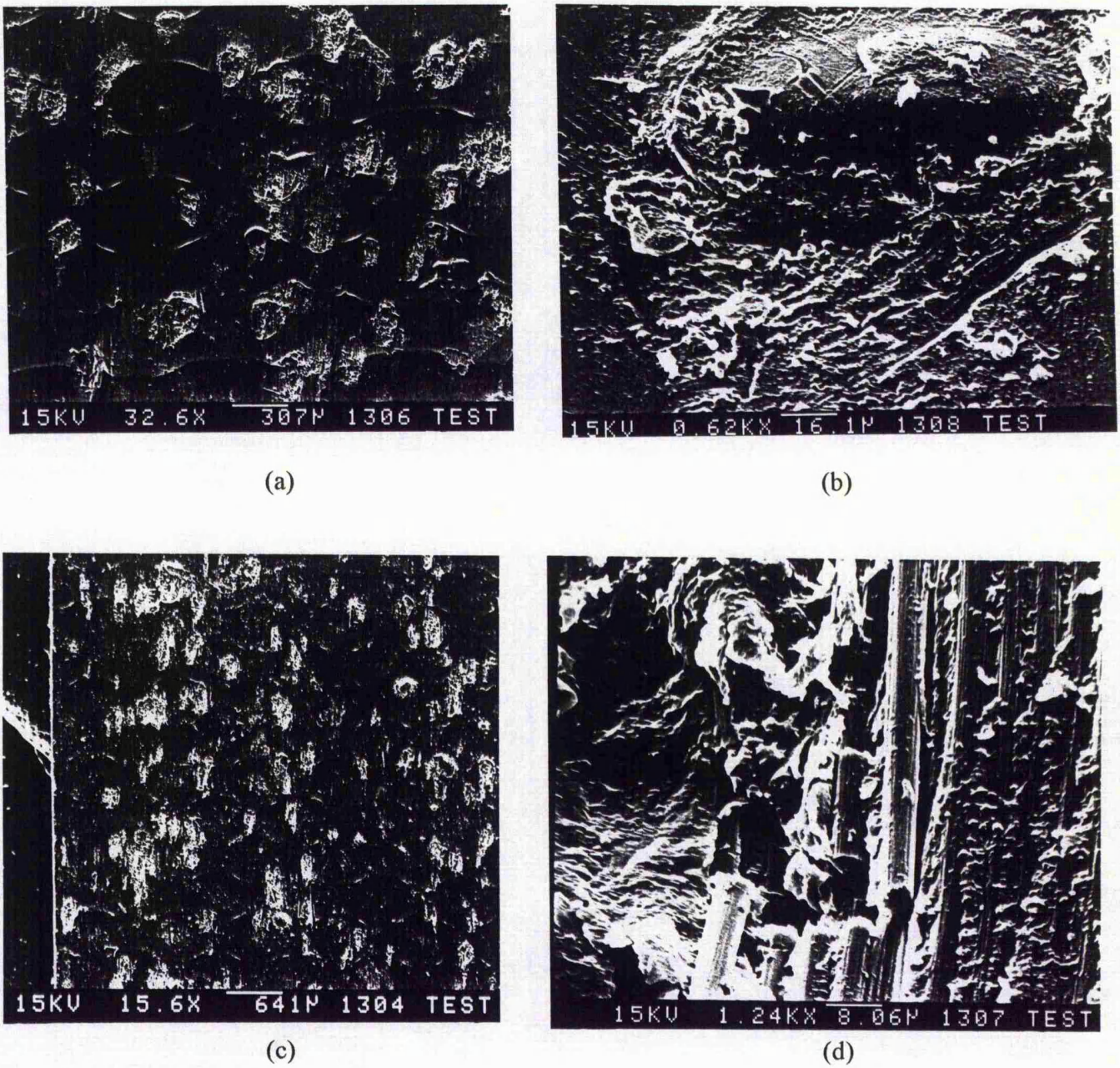

(a) (b)

(c) (d)

Fig.4. Specimen gripping area under the scanning electron microscope (SEM)
a) No slippage. b) Higher magnification of (a), showing no fibre damage.
c) Slippage occurs during loading. d) Higher magnification of (c), showing broken fibres on the surface plies.

However, in specimen with non-uniform thickness(more than 2% variation), the spark-eroded grip inserts do not hold the specimen adequately and slippage occurs during loading; Figs.4c,d show slippage in such a specimen. It can be seen that slippage causes substantial fibre damage, which may result in premature failure of the composite laminate.

3.2 Stress-Strain Data

The room temperature response of a selected specimen is shown in Fig.5. The longitudinal strain on the two faces of the coupon is initially the same but as the applied load is increased the strains diverge indicating bending. The bending cannot be totally avoided in compression testing. It may be the result of an initial imperfection in the specimen. The mean line plotted through the strain points exhibits an initial straight portion with an elastic (secant) modulus of 160 GPa, followed by a continuously curved portion with a tangential modulus at failure approximately 10% less than that of the linear part. This non-linear stress-strain response is attributable to

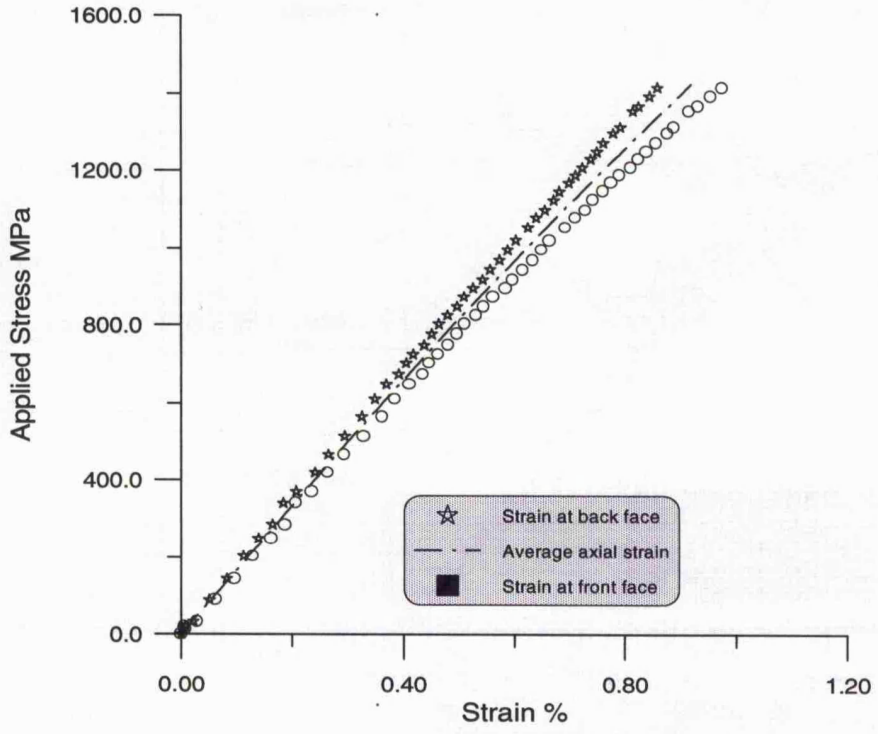

Fig.5 Compressive stress-strain response of unidirectional T800/924C laminate at room temperature (Tested using spark-eroded grip)

elastic fibre microinstability which is initiated, as soon as compression loading commences, by any initial fibre waviness or misalignment. The failure strength is 1429 MPa and the mean failure strain 0.93%; the maximum compressive strain on one

face of the specimen at failure (i.e., the sum of the direct and bending strains) is approximately 1%. If this value of 1% is used in conjuction with the projected mean stress-strain response of Fig.5, it is evident that it represents a stress of 1500 MPa. Similar results were obtained in previous work [2] from straight-sided specimens with carefully bonded aluminium tabs, Table 1. This suggests that the spark-eroded grip inserts used in the present study introduce successfully the compressive load into the specimen, without causing any damage on the faces of the composite and hence premature failure is avoided.

Table 1 Compressive strength properties of T800/924C unidirectional laminates

Test temperatures °C	Average Failure Strength MPa	Average failure strain %	Poisson's Ratio ν_{12}	Young's mod. $(E_{11})^*$ GPa
20	1415	0.950	0.353	160
20+	1485	0.980	0.35	158
50	1230	0.842	0.359	155
80	1137	0.787	0.361	149
100	973	0.728	0.37	136

*Secant modulus measured at 0.25% axial strain. + Specimens tested with aluminium tabs [2]

The effect of temperature under dry conditions on the compressive strength/stiffness of the T800/924C unidirectional laminate is also presented in Table 1. It can be seen that high temperature has a marked influence on the composite's compressive behaviour. At operating temperature of 100°C the strength has been reduced by more than 30% and the failure strain has dropped by approximately 24%. This is because the stiffness of the epoxy resin is reduced substantially with increasing temperature. In uniaxial compression reduction in matrix modulus means reduced support for the fibres, which promotes premature failure of the composite by out-of-plane fibre microbuckling [9]. Note that the results quoted in Table 1 are based on the average of five specimens tested at each temperature level; the coefficient of variation is less than 3%.

3.3 Failure Modes

Filure of the room temperature specimens is sudden and occurs mainly within the specimen gauge length. Some grip failures still occur due to stress concentrations induced by the clamping forces. To avoid this completely specimens with waisted gauge section should be used [2]. In-plane fibre microbuckling is considered as the critical damage mechanism, which causes the catastrophic fracture. Longitudinal splits and fibre/matrix debonding do not occur gradually but take place suddenly and concurrently with the final failure. The specimens generally fail along a 15° line from the transverse axis, which is similar to the fracture line observed in [2].

In the case of specimens tested at temperatures higher than 50°C damage occurs in the middle of the specimen and grows almost perpendicular to the loading axis. Subsequent examination by scanning electron microscopy revealed that the fibres underwent out-of-plane microbuckling. The strain at which this failure mode initiates is reduced with increasing temperature and at 100°C is only 75% of the strain required to initiate in-plane microbuckling. Thus, any weakening of the matrix or fibre/matrix interface arising from elevated temperatures increases the probability of out-of-plane buckling of the fibres which results in degraded compressive strength.

4. CONCLUSIONS

Untabbed straight-sided specimens are used in a modified Celanese test rig. The faces of the grip inserts are spark-eroded to produce a surface finish of approximately 20 Ra. No damage to the surface plies is observed in specimens with uniform thickness and specimen preparation costs are substantially reduced. The strength/stiffness properties and failure modes are comparable to those obtained from specimens with carefully bonded aluminium tabs [2]. Hence tabs are not required in compression testing provided that acceptable failure modes and location of failure are obtained.

In the case of specimens tested at temperatures higher than 50°C fracture occurs at much lower applied loads due to out-of-plane fibre microbuckling. This is attributed to the reduction in matrix strength properties with increasing temperature. Thus, in compression the matrix plays a key role in providing side support to the fibres and consequently resistance to fibre buckling.

elastic fibre microinstability which is initiated, as soon as compression loading commences, by any initial fibre waviness or misalignment.

The authors are grateful for funding from The Royal Society and wish to thank the Defence Research Agency (Royal Aerospace Establishment, Farnborough) for providing the composite laminates.

6 REFERENCES

1. John H. Sinclair and Christos C. Chamis 'Compressive behaviour of unidirectional fibrous composites' ASTM STP 808 1983 pp 155-174.
2. Soutis, C., 'Measurement of static compressive strength of fibre/epoxy laminates', Composite Science and Technology, 1991 (42) 373-392.
3. 'Standard test method for compressive properties of unidirectional or crossply fibre resin composites', ASTM Standard D 3410-87, American Society for Testing and Materials, Philadelphia, PA, 1992.
4. Hofer, Jr., K.E. and Rao, P.N., 'A new static compression fixture for advanced composite Materials', Journal of Testing and Evaluation, July 1977, Vol.5, (4) pp 278-283.
5. Shuart, M.J. 'An evaluation of sandwich beam compression test method for composites', Test method and design allowables for fibrous composites, ASTM STP 734. C.C Chamis, Ed., American Society for Testing and Materials, 1981, pp 152-165.
6. Chaterjee, S., Adams, D. and Oplinger, D.W., 'Test methods for composites a status report', Compression test methods. Volume II. *DOT/FAA/CT-93/17,* II, June 1993.
7. Curtis, P.A., 'CRAG test methods for the measurement of the engineering properties of fibre-reinforced plastics', RAE Technical Report 85099, 1985.
8. Stount K.J., Davis E.J., and Sullivan P.J., Atlas machined surfaces, Chapman and Hall, 1990.
9. Soutis C. and Turkmen D. 'High temperature effects on the compressive strength of glass fibre-reinforced composites' , Proceedings of the Ninth International Conference on Composite Materials (ICCM/9), Madrid, 12-16 July 1993, pp 581-588.

ICCM10, August 14.-18, 1995, CANADA

HYGROTHERMAL EFFECTS ON THE COMPRESSIVE STRENGTH OF T800/924C CFRP LAMINATES

C. Soutis and D. Turkmen
Department of Aeronautics
Imperial College of science Technology & Medicine
Prince Consort Road, London SW7 2BY, UK.

ABSTRACT

The objective of the present work is to evaluate the response of the T800/924C carbon fibre-epoxy composite system (currently available for aerospace structural applications) in hot-wet environments. The weight gains, maximum moisture contents and diffusion coefficients of unidirectional and various multidirectional laminates immersed in boiling water (accelerated ageing) are reported. Data also is presented on the effects of moisture and temperature on the compressive strength/failure mode of unidirectional laminates and multidirectional plates with an open hole. It is observed that the failure in the hot wet specimens always occurs as a result of out-of-plane microbuckling of the 0^{o} plies. This is attributed to the reduction in matrix strength properties and weakening of the ply interface arising from elevated temperatures and environmental conditioning.

INTRODUCTION

Fibre reinforced plastics are increasingly being used in the manufacture of aircraft structural components and in order to certify these components for service use it is important to examine their mechanical behaviour under a range of environmental conditions. It is known that hot and humid environments can degrade some aspects of the material performance in particular the compressive strength [1,2]. Water absorption by the epoxy resin leads to a reduction in the glass transition temperature and to a softening of the resin with a loss of stiffness and strength which causes fibre microbuckling and premature laminate failure [3]. The degradation increases as the conditions become more severe. The quantity of water absorbed by a laminate is

therefore of considerable importance, in particular to designer when setting design limits for structures operating in moist environments.

The aim of the present work is to evaluate the water absorption of the T800/924C carbon fibre-epoxy system and determine its effect on the compressive strength of unidirectional and multidirectional laminates with an open hole. A computer program [4] is used for the calculation of the quantity of water absorbed by the composite laminates and the profile of the moisture distribution through the laminate thickness during exposure to boiled water (accelerated ageing). The numerical results are confirmed by experimental measurements.

EXPERIMENTAL PROCEDURE

MATERIALS AND TEST SPECIMENS

Laminates measuring 1000 mm x 300 mm were manufactured from T800/924C carbon fibre- epoxy prepreg supplied by 'Ciba-Geigy' Plastics Company; the composite contained approximately 65% by volume fibres. The laminates were consolidated and cured in an autoclave at the Royal Aerospace Establishment (DRA-Farnborough), at a temperature of 170°C for 1 hr and subsequently post cured for 4 hrs at 190°C. Three different lay-ups were produced: a 16 ply unidirectional (ud) and two 24-ply multidirectional (md) laminates having a stacking sequence of $[(\pm 45/0_2)_3]_s$ and $[(90_2/0_2)_3]_s$. Immediately after manufacture, the laminates were cut into specimens measuring 110 mm x 10 mm for the unidirectional and 240 mm x 50 mm for the multidirectional, and stored in a desiccator to minimise moisture absorption prior to testing or environmental conditioning. A 5 mm diameter hole was drilled at the center of each multidirectional specimen using a tungsten carbide bit; by drilling from both sides of the specimen using a 2 mm pilot hole, the break through occurred at about mid-thickness which generally prevented any splitting or delamination of the outer plies [1].

ENVIRONMENTAL EXPOSURE

In order to predict mathematically the content and distribution of moisture in a laminate it is necessary to know the equilibrium level M_∞ (i.e. the maximum amount of moisture that can be absorbed by a laminate at a given humidity) and the diffusion coefficient D. To measure these data normally requires exposure times of over six months, even for relatively thin laminates of say 1 mm thick [4]. In this work the conditioned specimens were immersed in boiling water so the equilibrium level was reached in a period of few weeks. During the conditioning the specimens were periodically removed from the environment and weighed using an electronic balance accurate to ± 0.0001 g. Their weight gain, expressed as a percentage of their dry weight, was plotted against square root time as illustrated in Figs. 1a and 1b; the slope of the linear part is used subsequently in the calculation of the diffusion coefficient. After the maximum moisture content reached the specimens were removed and weighed once more before being machined in readiness for through thickness slitting. Each specimen was sliced carefully all the way through to give six slices. By weighing, drying and reweighing each slice its percentage uptake of water was found and plotted against trough thickness position to give the moisture distribution, Figs.2a and 2b.

As stated all specimens were initially stored in a desiccator to minimize moisture ingress. Those to be tested in the dry condition were loaded to failure within about 10 minutes of being removed from the desiccator and although it is acknowledged that moisture absorption might have occurred, it is assumed that the moisture content in these specimens is negligible[1].

APPARATUS AND MECHANICAL TESTS

Unidirectional Specimens

Compression tests on the unidirectional specimens were performed following the procedures outlined in CRAG test methods [5], using a modified Celanese jig [6,7] at a constant compression rate of 0.017 mm s^{-1} on a screw-driven machine of

load of capacity 50 kN. The conventional serrated grip faces of the Celanese were replaced by spark eroded inserts to

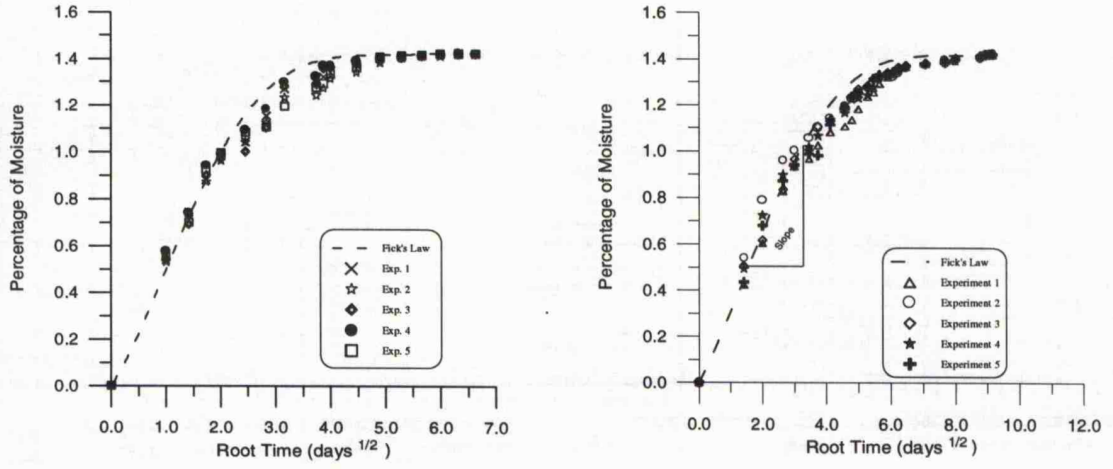

(a) (b)

Fig. 1. Comparison of experimental and Fickian moisture uptake against root time. a)T800/924C unidirectional laminate and b) T800/924C $[(\pm 45/0_2)_3]_s$ laminate

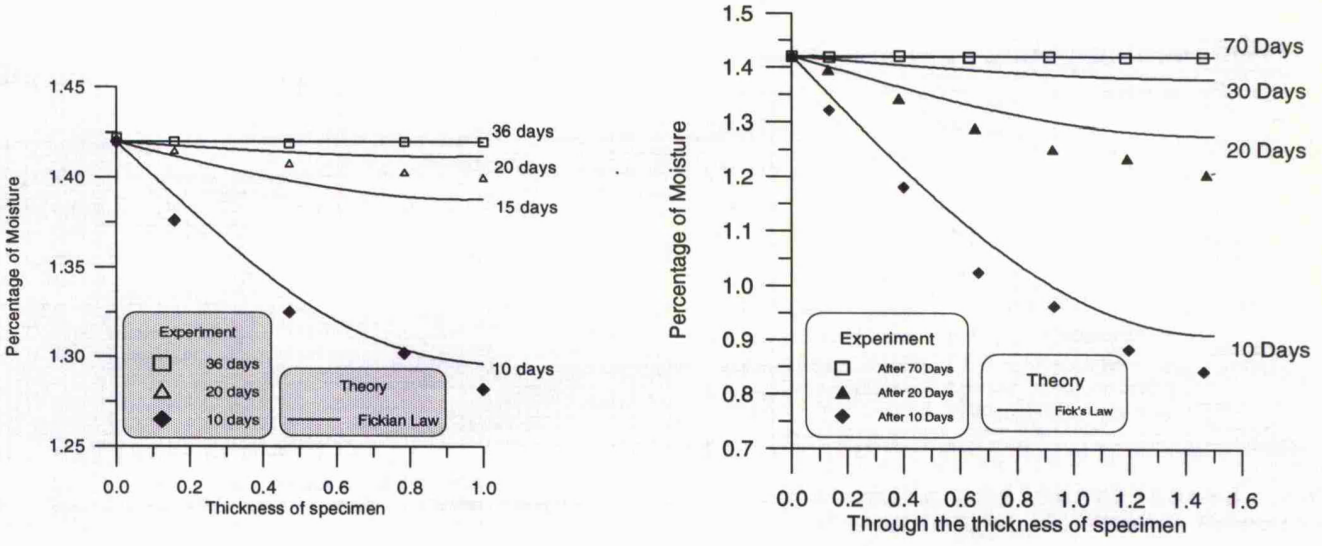

(a) (b)

Fig.2. Comparison of experimental and Fickian through-thickness moisture distribution a) $[0_8]_s$ and b) $[(\pm 45/0_2)_3]_s$ (both laminates immersed in boiling water).

eliminate adhesively bonded tabs on the specimen ends [7]; by having no tabs the entire surface of the specimen was exposed for water absorption.

In order to measure the compressive strength as a function of temperature and humidity, two extra inspection port were drilled on the Celanese alignment sleeve, so a hot air blower and a steam pipe could be attached. Symmetric airflow was achieved and the specimen was heated evenly. The temperature and humidity of the environment were monitored regularly by a thermocouple and a Testotherm hygrometer. It took less then five in to reach 100°C and the environmental conditioning chamber was capable of maintaining the temperature to within $\pm 3^{o}$. The specimens were allowed to 'soak' for about 10 min before being tested. At least five tests were carried out per test condition, hot-dry (20 °C-100 °C) and hot-wet (20 °C-100 °C, 95% RH). Strain gauges were used on both faces of all specimens to be tested in hot-dry conditions to measure axial and monitor the degree of bending.

Multidirectional Specimens

The multidirectional notched specimens were tested under the same hot-dry and hot-wet conditions as the unidirectional specimens using a home made environmental chamber in a servo-hydraulic test machine at a loading rate of 1 kN. s^{-1}. The specimens were untabbed straight-sided and were loaded by shear action by means of wedge grips with a spark-eroded surface finishing. They were of gauge section 120 mm x 50 mm, and were tested by using an anti-buckling device to prevent macrobuckling (Euler bending) during the test. The unti-buckling device increases the flexural stiffness of the composite plate but carries no load. Considerations of importance throughout the compressive test procedure were alignment of the specimen in the grips and proper attachment of the anti-buckling device to the specimen. Full details on the experimental technique have been documented previously by Soutis [8].

TEST RESULTS AND DISCUSSION

The experimental results consists of moisture absorption measurements, compressive strength/stiffness data for unidirectional and multidirectional notched

laminates. The shear properties of the T800/924C system (measured by using the Iosepescu specimen) are also presented in order to understand how shear strength/stiffness effects the compressive behaviour.

MOISTURE ABSORPTION

In a carbon fibre reinforced epoxy resin, moisture is absorbed by resin; the fibers do not absorb the moisture. Most of the evidence in the literature suggests that water is absorbed by a bulk diffusion mechanism in the resin and for flat plates rate of moisture absorption $\partial M / \partial t$ through the thickness direction (z) can be described by Fick's second law:

$$\frac{\partial M}{\partial t} = D\frac{\partial^2 M}{\partial z^2} \qquad (1)$$

where D is known as the diffusion coefficient. It should be remembered that the two main characteristics of Fickian law behaviour are: i)the absorption curve should be linear initially and ii) the moisture content should reach a saturation level (M_∞) at large values of time. The analytical solution of Eqn (1) yields the amount of moisture uptake which varies with time as [9]

$$M(t) = M_o + (M_\infty - M_o)\frac{4}{h}\sqrt{\frac{Dt}{\pi}} \qquad (2)$$

where M_o is initial amount of moisture in the solid, M_∞ is the final amount of equilibrium and 'h' is the laminate thickness. From Eqn.(2) it is clear why the initial part of the plot of M(t) versus the square root of time should be a straight line. The diffusivity can be now determined using the value of M for two different of time:

$$D = \pi\left(\frac{h}{4(M_\infty - M_o)}\right)^2\left(\frac{M(t_2) - M(t_1)}{\sqrt{t_2} - \sqrt{t_1}}\right)^2 \qquad (3)$$

Eqn (3) is often is considered with M_o=0. The diffusivity can now be determined by using Eqn (3) and the slope of Figs. 1a and 1b for the unidirectional and $[(\pm 45/0_2)_3]_s$ multidirectional laminate, respectively.

The slope $M/\sqrt{t}$ is obtained from using the complete specimen(finite plate) and therefore includes moisture diffused through all six surfaces. This gives a greater slope than would have been obtained for an infinite plane sheet as moisture had diffused through six sides instead of two. To give better estimate of the true one dimensional coefficient D_∞ a correction factor given by Shen and Springer [10] is used:

$$D_\infty = D\left(1+\frac{h}{W}+\frac{h}{\ell}\right)^{-2} \qquad (4)$$

where w and ℓ are the specimen width and length, respectively. The numerical results for D and

D_∞ are presented in Table 1.

Table 1. Coefficient of moisture diffusion for T800/924C laminates

Diffusivity mm^2/s	$[0_8]_s$	$[(\pm 45/0_2)_3]_s$
D	$1.25x10^{-6}$	$1.07x10^{-6}$
D_∞	$8.42x10^{-7}$	$9.3x10^{-7}$

The diffusivity of the multidirectional laminate is about 30% higher than of the unidirectional laminate, probably due to more entrances available for the water to diffuse through the plate and due to larger interfacial absorption of the 45° plies [11]. The diffusion coefficient and the equilibrium moisture content (M_∞ =1.42%) are used with the computer program developed in [4] to estimate the through thickness moisture distribution, Figs.2a and 2b. It is clear that although Fickian diffusion does not exactly model the actual diffusion, it is sufficiently accurate for the cases examined.

COMPRESSIVE STRENGTH OF UNIDIRECTIONAL LAMINATES

Strength Data and Failure Modes

The effect of temperature and environmental conditioning on the compressive strength/stiffness of the T800/924C unidirectional laminate is presented in Table 2; shear strength properties are also given. It can be seen that moisture and high temperature has a marked influence on the composite's compressive behaviour. At operating temperature of 100°C dry the strength has been reduced by more 30% and the failure strain has dropped from 0.96% to 0.73% (approximately 24% reduction). This is because stiffness of the epoxy resin is reduced substantially with increasing temperature; the shear modulus has been reduced by almost 20%, Table 2. In uniaxial compression reduction in matrix modulus means reduced support for the fibres, which promotes premature failure of the composite by out-of-plane fibre microbuckling. The compressive strength is further reduced (by 54%) when the laminate contains 1.4% by weight moisture and tested at 100°C and 95%RH. It can be seen from the results shown in Table 2, that the compressive strength (σ_c) is only 20% of the elastic shear modulus; remember that Rosen's analysis of fibre buckling predicts that σ_c is equal to the shear modulus. This suggests that a plastic-buckling analysis is required in order to estimate strength more accurately. The results quoted in Table 2 are based on the average of five specimens tested at each environmental condition; the coefficient of variation is less than 5%.

Table Compressive strength results for T800/924C laminates with a 5 mm hole

Test Conditions °C	Compressive Strength MPa	Young's* Modulus GPa	Shear Strength MPa	Shear Modulus GPa
20-dry	1415	160	110	6.0
20-wet	1060	-	-	-
50-dry	1230	155	105	5.8
50-wet	930	-	-	-
80-dry	1137	149	98	5.4
80-wet	828	-	-	-
100-dry	973	136	90	4.9
100-wet	654	-	-	-

*Secant modulus measured at 0.25% axial strain

Failure of the room temperature specimens was sudden and occurred mainly within the specimen gauge length. In-plane fibre microbuckling is considered as the critical damage mechanism, which causes the catastrophic fracture, Fig.3a. Longitudinal splits and fibre/matrix debonding do not occur gradually but take place suddenly and concurrently with the final failure. The specimens generally fail along a 15^{o} ($=\beta$) line from the transverse axis, which is similar to the fracture line observed in [6]

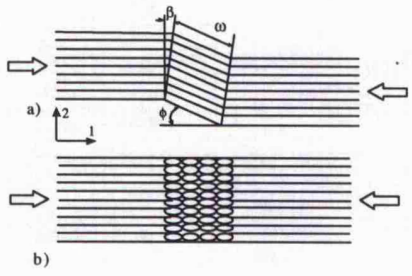

Fig.3. A schematic representation of the microbuckling mode: a) in-plane, b) out-of-plane.

In the case of specimens tested at hot-wet conditions damage occurs in the middle of the specimen and grows almost perpendicular of the loading axis, Fig.3b. Subsequent examination by scanning electron microscopy revealed that the fibres underwent out-of-plane microbuckling.

The strain at which this failure mode initiates is reduced with increasing temperature and at 100°C is only 75% of the strain required to initiate in-plane microbuckling. Thus, any weakening of the matrix or fibre/matrix interface arising from elevated temperatures and environmental conditioning increases the probability of out-of-plane buckling of the fibres which results in degraded compressive strength.

COMPRESSIVE STRENGTH OF MULTIDIRECTIONAL LAMINATES

Strength of Data and Failure Modes

Compressive strength results of two multidirectional laminates with a 5 mm hole tested at various environmental conditions are summarised in Table 3. Strength

values are based on the cross-sectional area of the test piece. It is clear that the compressive strength of the $[(\pm 45/0_2)_3]_s$ laminate is reduced by almost 38% when the specimen contains 1.42% moisture and is tested at 100°C-wet conditions (the room temperature unnotched strength is 810 MPa). The scatter in strength is less than 10% and all specimens failed from the hole in a direction

Table 2 Compressive strength results for T800/924C laminates with a 5 mm hole

Test Conditions °C	Notched Strength MPa $[(\pm 45/0_2)_3]_s$	Notched Strength MPa $[(90_2/0_2)_3]_s$
20-dry	451.75	351.65
20-wet	402.00	-
50-dry	421.50	324.67
50-wet	357.50	-
80-dry	371.50	291.37
80-wet	325.00	-
100-wet	282.00	-

almost perpendicular to the loading axis. Penetrant-enhanced X-ray radiography and scanning electron microscopy reveal that failure is always by microbuckling of the 0° plies, and is accompanied by delamination between the off -axis and 0° layers, and by plastic deformation in the off-axis plies; similar observations were made in [8].

CONCLUSION REMARKS

Untabbad straight-sided unidirectional and multidirectional specimens are tested following the procedure outlined in CRAG test methods [5]. The faces of the grip inserts of the test apparatus are spark-eroded to produce a surface finish of approximately 20 Ra. No damage to the surface plies is observed in specimens with uniform thickness and acceptable failure modes and location of failure are obtained. The diffusion coefficient and the equilibrium moisture and location of failure are obtained. The diffusion coefficient and the equilibrium moist content are measured and used with a computer program developed in [4] to estimate through thickness moisture distribution. It is found that although Fickian diffusion does not exactly model the actual moisture absorption, it is sufficiently accurate for the cases examined.

The strength properties of the specimens tested in hot-wet conditions are substantially reduced and the final failure always occurs due to out-of-plane fibre microbuckling. This is attributed to the reduction in matrix strength properties and weakening of the ply interface with increasing temperature and environmental conditioning. Thus, in compression the matrix and interface play a key role in providing side support to the fibres and consequently resistance to fibre buckling.

ACKNOWLEDGMENTS

The authors are grateful for funding from the Engineering and Physical Sciences Research Council (CR/K57466) and wish to thank the Defence Research Agency (Royal Aerospace Establishment, Farnborough) for assisting with the manufacture of the composite laminates.

REFERENCES

1. Potter and . P.Purslow The environmental degradation of notched CFRP in compression *Composites,* 14(3), 206-225 (1983).
2. Barker and V. Balasundaram, Compression testing of carbon fibre-reinforced plastics exposed to humid environments, *Composites*, 18(3), 217-226 (1987).
3. Browning, C.E. Husman and J.M. Whitney, Moisture effects in epoxy matrix composites, *AFML-TR-77-41* (1977)
4. Copley, A Computer Program to Model moisture Diffusion and its Application to Accelerated Ageing of Composites, *RAE Tech. Rep.* 82010, Jan.1982.
5. Curtis, CRAG test methods for the measurement of the engineering properties of fibre reinforced plastics, , *RAE TR* 851099 (1984).
6. Soutis, C. and Turkmen, D., High temperature effects on the compressive strength of glass fibre-reinforced composites, *Proceedings of the Ninth International Conference on Composite Materials (ICCM/9),* Madrid, 12-16 July, 581-588 (1993).
7. Soutis, C., Turkmen, D. and Morrison, C.J., Compressive failure of unidirectional composites at elevated temperature using untabbed specimens, *ECCM CTS2*, 169-177(1994).

8. Soutis, C. and Fleck, N.A., Static compression failure in carbon fibre T800/924C composite plate with an open hole, *J.Comp. Mater.*, 24, 538-556(19990).
9. Wilde, De. and P. Frokovic, P., The modelling of moisture absorption in epoxies: effects at boundaries, *Composites*, 25(2), 119-127 (1994).
10. Shen, C. and Springer, S.G., Moisture absorption and desabsorption of composite materials, *J. Comp. Mater.*, 10 2-20 (1976).
11. Naeem, M., The resistance of glass reinforced thermosetting polymers to thermohumid conditions, *Ph.D. Thesis*, Loughborough University of Technology 1985).

Advanced Cposite Letters, 4(4), 1995, pp.115-120

Moisture Diffusion in T800/924C Carbon fibre-epoxy laminates

C. Soutis and D. Turkmen
Department of Aeronautics
Imperial College of science Technology & Medicine
Prince Consort Road, London SW7 2BY, UK.

The objective of the present work is to evaluate the response of the T800/924C epoxy composite system (currently available for aerospace structural applications) in hot-wet environments. The weight gains, maximum moisture contents and diffusion coefficients of unidirectional and an orthotropic multidirectional laminates immersed in boiling water (accelerated ageing) are reported.

Introduction

Fibre reinforced plastics are increasingly being used in the manufacture of aircraft structural components and in order to certify these components for service use it is important to examine their mechanical behaviour under a range of environmental conditions. It is known that hot and humid environments can degrade some aspects of the material performance in particular the compressive strength [1,2]. Water absorption by the epoxy resin leads to a reduction in the glass transition temperature and to a softening of the resin with a loss of stiffness and strength which causes fibre microbuckling and premature laminate failure [3]. The degradation increases as the conditions become more severe. The quantity of water absorbed by a laminate is therefore of considerable importance, in particular to designer when setting design limits for structures operating in moist environments.

The aim of the present work is to evaluate the water absorption of the relatively new T800/924C carbon fibre-epoxy system. A FORTRAN finite difference program [4] is used for the calculation of the quantity of water absorbed by the composite laminates and the profile of the moisture distribution through the laminate thickness during exposure to boiled water (accelerated ageing). The numerical results are confirmed by experimental measurements.

Materials and test specimens

Laminates measuring 1000 mm x 300 mm were manufactured from T800/924C carbon fibre-epoxy prepreg supplied by Ciba composites; the composite contained approximately 65% by volume fibres. The laminates were consolidated and cured in an autoclave at the Royal Aerospace Establishment (DRA-Farnborough), at a temperature of 170°C for 1 hr and subsequently post cured for 4 hrs at 190°C. Three different lay-ups were produced: a 16 ply unidirectional and a 24-ply multidirectional laminate having a stacking sequence of $[(\pm 45/0_2)_3]_s$. Immediately after manufacture, the laminates were cut into specimens measuring 110 mm x 10 mm for the unidirectional and 240 mm x 50 mm for the multidirectional, and stored in a desiccator to minimise moisture absorption prior to testing or environmental conditioning to minimise moisture ingress[1].

Environmental exposure

In order to predict mathematically the content and distribution of moisture in a laminate it is necessary to know the equilibrium level M_∞ (i.e. the maximum amount of moisture that can be absorbed by a laminate at a given humidity) and the diffusion coefficient D. To measure these data normally requires exposure times of over six months, even for relatively thin laminates of say 1 mm thick [4]. In this work the conditioned specimens were immersed in boiling water so the equilibrium level was reached in a period of few weeks. During the conditioning the specimens were periodically removed from the environment and weighed using an electronic balance accurate to ± 0.0001g. Their weight gain, expressed as a percentage of their dry weight, was plotted against square root time as illustrated in Figs. 1a and 1b; the slope of the linear part is used subsequently in the calculation of the diffusion coefficient. After the maximum moisture content reached the specimens were removed and weighed once more before being machined in readiness for through thickness slitting. Each specimen was sliced carefully all the way through to give six slices. By weighing, drying and reweighing each slice its percentage uptake of water was found and plotted against trough thickness position to give the moisture distribution, Figs.2a and 2b.

Test results and discussion

In a carbon fibre reinforced epoxy resin, moisture is absorbed by the resin; the fibers do not absorb the moisture. Most of the evidence in the literature suggests that water is absorbed by a bulk diffusion mechanism in the resin and for flat plates the rate of moisture absorption $\partial M / \partial t$ through the thickness direction (z) can be described by Fick's second law:

$$\frac{\partial M}{\partial t} = D\frac{\partial^2 M}{\partial z^2} \qquad (1)$$

where D is known as the diffusion coefficient. It should be remembered that the two main characteristics of Fickian law behaviour are: i)the absorption curve should be linear initially and ii) the moisture content should reach a saturation level (M_∞) at large values of time. The analytical solution of Eqn. (1), that can be obtained by the method of separation of variables [5], yields the amount of moisture uptake which varies with time as

$$M(t) = M_0 + (M_\infty - M_0)\frac{4}{h}\sqrt{\frac{Dt}{\pi}} \qquad (2)$$

where M_0 is initial amount of moisture in the solid, M_∞ is the final amount of equilibrium and 'h' is the laminate thickness. From Eqn.(2) it is clear why the initial part of the plot of M(t) versus the square root of time should be a straight line. The diffusivity can be now determined using the value of M for two different of time:

$$D = \pi \left(\frac{h}{4(M_\infty - M_o)} \right)^2 \left(\frac{M(t_2) - M(t_1)}{\sqrt{t_2} - \sqrt{t_1}} \right)^2 \qquad (3)$$

Eqn (3) is often is considered with M_o=0. The diffusivity can now be determined by using Eqn (3) and the slope of Figs. 1a and 1b for the unidirectional and $[(\pm 45/0_2)_3]_s$ multidirectional laminate, respectively.

The slope $M/\sqrt{t}$ is obtained from using the complete specimen(finite plate) and therefore includes moisture diffused through all six surfaces. This gives a greater slope than would have been obtained for an infinite plane sheet as moisture had diffused through six sides instead of two. To give better estimate of the true one dimensional coefficient D_∞ a correction factor given by Shen and Springer [6] is used:

$$D_\infty = D\left(1 + \frac{h}{W} + \frac{h}{\ell}\right)^{-2} \qquad (4)$$

where w and ℓ are the specimen width and length, respectively. The numerical results for D and D_∞ are presented in Table 1.

Table 1. Coefficient of moisture diffusion for T800/924C laminates

Diffusivity mm^2/s	$[0_8]_s$	$[(\pm 45/0_2)_3]_s$
D	1.2×10^{-6}	1.07×10^{-6}
D_∞	8.42×10^{-7}	9.3×10^{-7}

The diffusivity of the multidirectional laminate is about 10% higher than that of the unidirectional laminate, probably due to more entrances available for the water to diffuse through the plate and due to larger interfacial absorption of the 45° surface plies [7]. The diffusion coefficient and the equilibrium moisture content (M_∞=1.42%) are used with the computer finite difference program developed in [4] to estimate the through thickness moisture distribution, Figs.2a and 2b. The program models one-dimensional moisture diffusion in materials which exhibits Fickian diffusion characteristics; it is interactive and it accepts either a diffusion coefficient and surface moisture level or the environmental conditions, i.e., temperature and humidity. From Figs 2a&2b, it is clear that although Fick's law does not exactly model the actual diffusion, it is sufficiently accurate for the cases examined.

Concluding remarks

The diffusion coefficient and the equilibrium moist content are measured and used with a computer program developed in [4] to estimate through thickness moisture distribution. It is found that although Fickian diffusion does not exactly model the actual moisture absorption, in the T800/924C composite system, it is sufficiently accurate for the cases examined. Further work is required to study the effect of stacking sequence on the moisture diffusion.

Acknowledgements

The authors are grateful for funding from the Engineering and Physical Sciences Research Council (CR/K57466) and wish to thank the Defense Research Agency (Royal Aerospace Establishment, Farnborough) for assisting with the manufacture of the composite laminates.

REFERENCES

1. Potter and . P.Purslow The environmental degradation of notched CFRP in compression *Composites,* 14(3), 206-225 (1983).
2. Barker and V. Balasundaram, Compression testing of carbon fibre-reinforced plastics exposed to humid environments, *Composites*, 18(3), 217-226 (1987).
3. Browning, C.E. Husman and J.M. Whitney, Moisture effects in epoxy matrix composites, *AFML-TR-77-41* (1977)
4. Copley, S.M., A Computer Program to Model moisture Diffusion and its Application to Accelerated Ageing of Composites, *RAE Tech. Rep.* 82010, Jan.1982.
5. De wilde, W.P. and Frokovic, P. The Modelling of Moisture Absorption in Epoxies: Effects at Boundaries, *Composites,* 25(2), 119-127 (1994).
6. Shen, C. and Springer, S.G., Moisture absorption and desabsorption of composite materials, *J. Comp. Mater.,* 10 2-20 (1976).
7. Naeem, M., The resistance of glass reinforced thermosetting polymers to thermohumid conditions, *Ph.D. Thesis*, Loughborough University of Technology 1985).

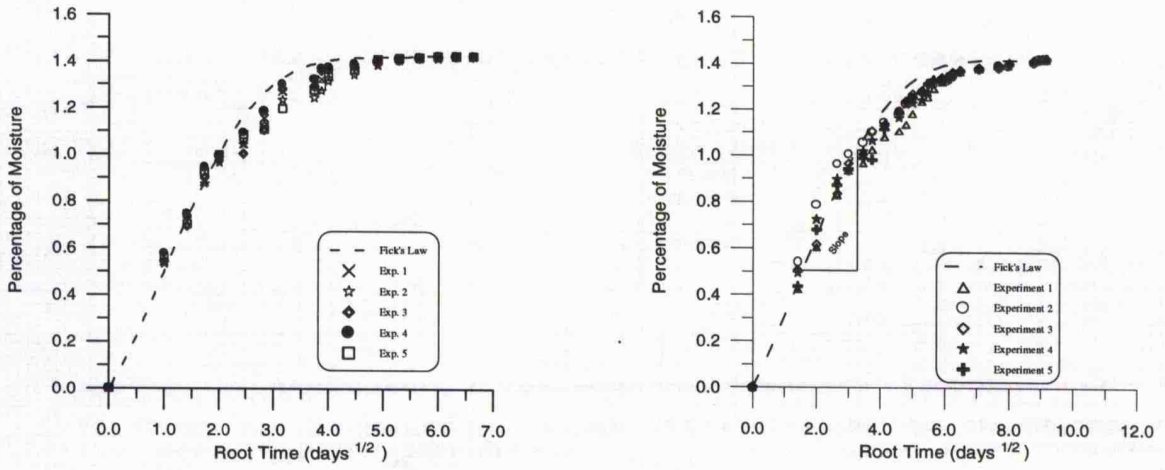

(a) (b)

Fig. 1. Comparison of experimental and Fickian moisture uptake against root time. a)T800/924C unidirectional laminate and b) T800/924C $[(\pm 45/0_2)_3]_s$ laminate

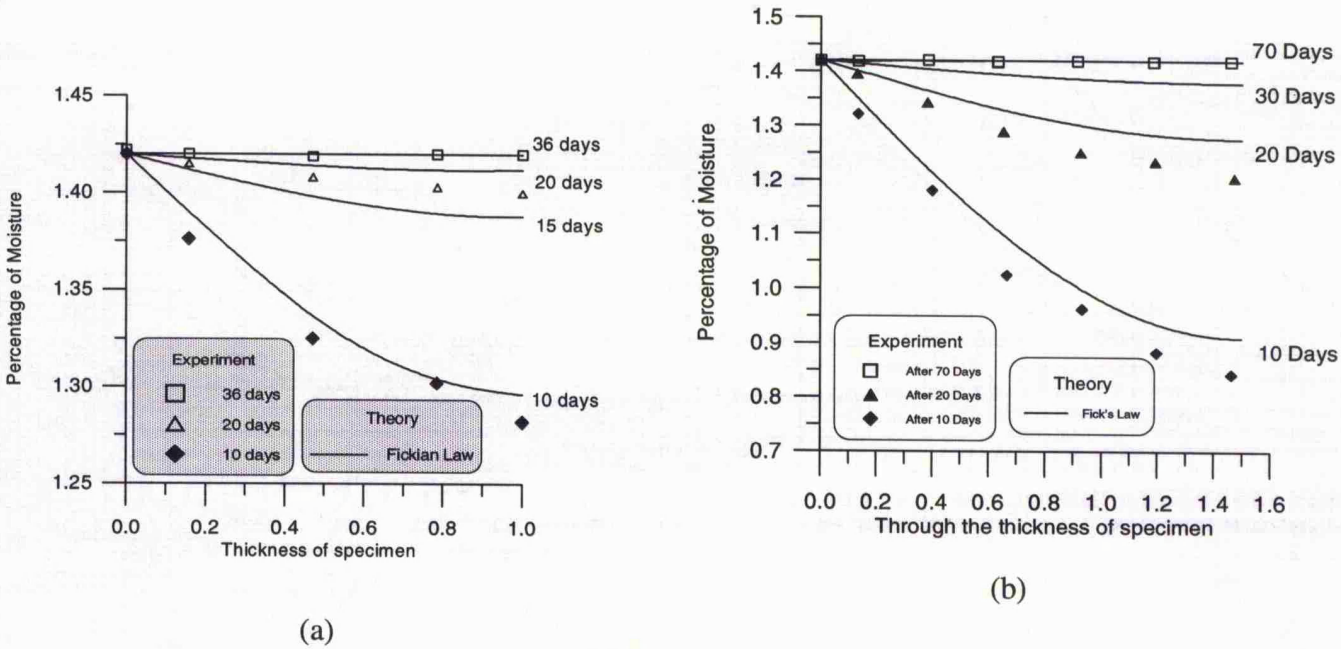

(a) (b)

Fig.2. Comparison of experimental and Fickian through-thickness moisture distribution a) $[0_8]_s$ and b) $[(\pm 45/0_2)_3]_s$ (both laminates immersed in boiling water).

Submitted 27 September 1995
Will appear in Applied Composite Materials

INFLUENCE OF SHEAR PROPERTIES OF THE COMPRESSIVE BEHAVIOUR OF GFRP LAMINATES

C. Soutis and D. Turkmen
Department of Aeronautics
Imperial College of Science, Technology and Medicine
Prince Consort Road
London SW7 2BY,UK

ABSTRACT

The influence of shear strength properties on the compressive behaviour of unidirectional glass fibre-polyropylene laminates is examined. Test are conducted between 20°C and 120°C to provide variation in the constitutive behaviour of the polymer matrix and thus additional variation in the support provided to the glass fibres. It is found that the laminate looses strength as the operating temperature increases and failure occurs due to fibre microbuckling. At temperatures higher than 50°C the failure mode switches from in-plane to out-of-plane microbuckling. As the test temperature increases the shear strength and stiffness of the resin are considerably reduced; this decreases the amount of side support for the fibres and reduces the strain level at which fibre buckling initiates. Growth of this controlled by initiation, rather than propagation of microbuckling. Fracture characteristics are identified using optical and scanning electron microscopy. Recent theoretical models are employed to predict the compressive stress-strain response and strength.

1. INTRODUCTION

Continuous fibre-reinforced plastics are being used in an ever increasing number of structural applications. However, more efficient use of these materials is limited by their apparent low compressive strength. Modern composite laminates based on carbon or glass fibres, and polymeric resin are approximately 30%-40% weaker in compression than in tension due to fibre microbuckling [1-4]. This is an instability failure mode which nucleates locally (e.g. free-edge, void, resin rich regions) and

propagates under little additional load through the laminate, causing a narrow zone within the 0° plies to loose structural integrity, Figure 1.

From theoretical developments on the compressive strength of unidirectional laminates [5-10] it is suggested that failure induced by fibre microbuckling is dependent on the shear properties of the matrix (resin) material. To assess the validity of these models the present study investigates the effect of resin ductility (varied as a function of the test temperature) on the compressive strength of unidirectional glass/polypropylene (glass/pp) laminates. Failure mechanisms are examined and strength measurements are compared with theoretical predictions.

2. EXPERIMENTAL PROCEDURE

2.1. Manufacture of glass/pp laminates

The material selected for this study consists of continuous glass fibres in a thermoplastic matrix of polypropylene (65 vol.% resin content). It comes under the ICI (Imperial Chemical Industries) trade name 'Plytron' and is produced in 240 mm wide prepreg for laminate assembly. An elevated temperature compression moulding technique was employed to manufacture $[0_4]_s$ and $[(\pm 45)_2]_s$ glass/pp laminates. Sheets of the prepreg material were cut to 260 mm by 240 mm using a guillotine and laid together by hand. Eight plies were used in the composite plates which resulted in a cured laminate thickness of approximately 3.8 mm. Teflon coated porous bleed fabric and absorbent cloth were used to sandwich the laminate during compression moulding which resulted in the removal of excess polymer matrix. The manufacturer's standard compression moulding cycle was followed which produced laminates of acceptable quality. There was no visual evidence of any voids or porosity and the surface of the composite plates were flat and smooth. Sectioning and optical microscopy studies revealed that the void content was less than 2% and some fibre misalignment in the $[0_4]_s$ laminate was evident. Initial fibre imperfections in compression testing reduce the laminate strength [3,4] and therefore extra care must be taken during the moulding process.

2.2 Specimen design and mechanical tests

Unidirectional fibre-reinforced composites are highly anisotropic materials and premature failure due to Poisson deformation (brooming) may occur when axial compression is applied. This failure occurs on the load bearing surfaces and is characterized by extensive longitudinal splitting and lateral movement of material at the specimen ends. In the present investigation the modified Celanese method [11] was used to evaluate the compressive properties of the unidirectional glass/pp laminates. The conventional serrated grip faces of the Celanese jig were replaced by spark eroded inserts to eliminate adhesively bonded tabs on specimen ends [4,12]. The specimens tested had a gauge length of 13 mm which is a compromise between the requirement to eliminate Euler bending and the need to avoid end effects, while providing adequate space for strain gauges. The specimen width and thickness were 10 mm and 3.8 mm, respectively.

The compressive tests were performed on a screw-driven machine of capacity 10kN at a crosshead displacement of 0.017 mms^{-1}. To measure compressive strength of the laminates as a function of temperature the Celanese rig was adapted to hot air heating. Two extra inspection ports were drilled on the Celanese alignment sleeve and a hot air blower was attached. Symmetric airflow was achieved and the specimen was heated evenly. The temperature of the specimen was monitored by a thermocouple. It took approximately 5 minutes to reach 120°C and the specimens were allowed to 'soak' at temperature for 10-15 minutes to before being tested. Using this apparatus tests were carried out at room temperature, 50°C, 80°C, 100°C and 120°C. Shear strength properties were obtained by testing $[(\pm 45)_2]_s$ laminates in tension at the same temperature levels. Mechanical tests were conducted following the procedures outlined in CRAG test methods [11]. Longitudinal and transverse strains for tension and compression were measured by 1 mm long foil strain gauges that retained accuracy over the range of temperatures used in this study.

3. TEST RESULTS AND DISCUSSION

The experimental results consist of stress-strain plots, fracture stresses and strains, photographs showing the overall failure mode of selected failed specimens and

optical and scanning electron micrographs of fracture surfaces. The tensile properties of the glass/pp system are not discussed in detail but presented in Table 1 for comparison purposes; at least four specimens were tested at each temperature level.

3.1 Stress-strain data

Compressive failure in all specimens is catastrophic and quite localized, Figure 2. A kink band structure (fibre microbuckling) occurs without warning and immediately leads to laminate breakage. Fracture is within the specimen gauge length implying that the test is successful. A plot of the applied axial stress as a function of average axial strain measured by back-to-back strain gauges is shown in Figure 3, for two typical specimens tested at room temperature. The mean compressive strength is 317 MPa, which is less than 60% of the tensile strength. The average failure strain and the Young's modulus (measured at 25% applied strain) are 0.98% and 29.5GPa, respectively. The effect of temperature on compressive properties of the unidirectional laminate can be seen in Table 2. The results demonstrate that temperature has a marked influence on the compressive strength. At operating temperature of 120°C the strength has been reduced by more than 60% and the failure strain has dropped by approximately 50%. This is because the strength properties of matrix are reduced substantially with increasing temperature, Table1. In uniaxial compression reduced in matrix stiffness/strength means reduced side support for the fibres which promotes premature failure of the composite by fibre microbuckling. The results in tables 1 and 2 suggest that the compressive strength is more temperature dependent than the tensile strength. In general, the tensile strength of a composite depends more on its fibre reinforcement, but compressive strength relies more upon its matrix material.

3.2 Compressive fracture modes

Damage to the room temperature unidirectional specimens involves fibre movement in the plane of the laminate (in-plane fibre microbuckling) along a 20^0-25^0 line from the transverse axis, Figure 4. In Figure 4 the optical micrograph shows that the fibres break at two points, which create a band inclined at $\beta \approx 25^o$ to the horizontal axis. It was observed in all specimens that angle β remains constant. The

microbuckle once started from the free edge or a pre-existing material imperfection, such as voids resin rich regions and fibre misalignment, keeps its orientation and propagation. Berg and Salama [13] argued that kink band must be inclined in order to permit the buckled fibres to undergo both compressive and shear deformation. The reason is that microbuckling along planes, which permit shear displacement as buckling proceeds requires smaller compressive stress than does buckling on a plane that does not permit shear displacement. (i.e. planes perpendicular to the fibre axis.) The broken fibre segments in Figure 4 are approximately 25-30 fibre diameters long ($d_f \approx 20\,\mu m$) and have rotated by almost 30° from the loading axis (ϕ=30°). Once failure has occurred, the kink inclination angle ϕ can increase rapidly if the load is not immediately removed. This values are similar to those reported by Hahn [14] for S-glass epoxy composite. For a carbon fibre epoxy system, β varies between 5° and 20°, ϕ=30° and w=8-10 fibre diameters. Whether the angle of kink band inclination and the kink band width are of significance is still unclear. Scanning electron micrographs of the fracture surface of a selected specimen are shown in Figure 5a&5b. It exhibits well defined steps and it is evident from Figure 5b that each fibre fails in bending.

In the case of specimens tested at temperatures higher than 50°C damage was confined to out-of-plane deformation in an almost 90° kink band across the specimen width. The kink band width measured 35-40 fibre diameters. Failed specimens show features quite distinct from those observed in specimens in which fibre buckling occurred in-plane, Figure 6. The strain level at which out-of-plane microbuckling initiates is reduced with increasing temperature and at 120°C is less than 50% of strain required to initiate in-plane microbuckling. Thus the out-of-plane microbuckling has been precipitated by a weaker ply interface in the hot specimen due to a reduction of fibre/matrix bond. Clearly, any weakening of the matrix or fibre/matrix interface arising from elevated temperature increases the probability of out-of-plane buckling of the fibres.

4 STRENGTH PREDICTIONS

A number of theories for the compressive strength of unidirectional composite laminates have been proposed and these have been reviewed by Stuart [15], Hahn [14], Haberle *et al.* [16], Soutis [3] and more recently Budiansky and Fleck [17]. It is generally agreed that the observed compressive failure stresses can only be explained on the assumption that initial fibre misalignments are present. In this chapter we apply three commonly used models developed by Rosen[5], Budiansky[9] and Batdorf and Ko[18] to predict the strength of glass/pp system.

4.1 Rosen Model [5]

The classic study of Rosen [5] based on buckling theory for slender columns on an elastic foundation and suggests that the compressive strength σ_c is only dependent on the (initial) matrix shear modulus G_m and the fiber volume fraction V_f

$$\sigma_c = \frac{G_m}{1 - V_f} \approx G_c \qquad (1)$$

where G_c is the composite shear modulus. For the glass/pp laminates Eqn. (1) is found to significantly overpredict the compressive strength for all temperature levels. The results are presented in Table 1 and 2 indicate that the compressive strength of plytron is only 20-25% of shear modulus. Larger and June [19] argued that a numerical coefficient that allowed for the three dimensional nature of reinforcement could be introduced into eqn. (1), whereas Ewins [20] thought that the discrepancy was caused by the irregular spacing of fibres, matrix plasticity, fiber misalignment and poor fibre-matrix boding. Steif[10] extended Rosen's microbuckling analysis to situations in which matrix plasticity occurs; an elastic/perfectly plastic matrix shear response was assumed. The author [10] found that the theoretical fibre breaking strains compared reasonably well with measured failure strains when the kink band was assumed to have the experimentally observed width. This support that microbuckling is a plastic rather than an elastic failure mode.

4.2 Budiansky analysis[9]

Argon [7] proposed an alternative approach based on a model of microbuckling as a plastic collapse event. In this model kinking occurs in a $\beta=0^{\circ}$ band within which fibres have suffered an initial misalignment angle $\bar{\phi}$, Figure 1. The fibres are assumed to be inextensible and suffer a remote compressive axial stress; the associated deformation within the kink band is given by the additional rotation ϕ (or γ) of the fibres. In a rigid perfectly plastic material having yield stress τ_y in longitudinal shear, additional rotation ϕ can not develop until the critical compressive

$$\sigma_c = \frac{\tau_y}{\bar{\phi}} \qquad (2)$$

is applied, and subsequently the compressive stress decreases with increasing ϕ. Budiansky [9] extended this result for an elastic-perfectly plastic composite response, and found

$$\sigma_c = \frac{\tau_y}{\gamma_y + \bar{\phi}} = \frac{G}{1 + \bar{\phi}/\gamma_y} \qquad (3)$$

where $\gamma_y = \tau_y/G$ is the in-plane shear yield strain of the composite. This result reduces to the Rosen bifurcation solution equation 1 when $\bar{\phi}=0$ and is asymptotically equivalent to Argon's equation 2 for large $\bar{\phi}$. Figure 7 shows that the compressive strength of plytron is proportional to the shear yield strength, τ_y, of the composite, supporting equation 2 and 3; here τ_y is taken as half the value of the shear strength τ_f. The slope of the graph in Figure 7 gives $\bar{\phi}=5^{\circ}$. Fig. 7 also includes data for glass and Kevlar fibre reinforced Polyester, taken from the work of Piggott and Harris [21], but this time $\bar{\phi}=3.7^{\circ}$. We have observed fibre

imperfections between 3 ° and 6 ° in section studies for the glass/pp laminates. When τ_y is increased to sufficiently high values the fibre collapse prior to microbuckling; the uniaxial strain in the composite equals the intrinsic crushing strain of the fibres, Fig. 7. Equation 3 is sensitive to fibre misalignment and predicts a kink orientation angle $\beta=0°$, which is not in agreement with the experimental observation of $\beta=20°$-$25°$. However, it provides an indication of the relative importance of the physical parameters that govern the compressive strength. Budiansky and Fleck [22] using equation 3 have shown that variation $\delta\tau_y$, δG and $\delta\bar{\phi}$ in the shear yield stress, elastic shear modulus, and initial misalignment are related to a change $\delta\sigma_c$ in the critical stress by

$$\frac{\delta\sigma_c}{\sigma_c}=\left(\frac{\sigma_c}{G}\right)\frac{\delta G}{G}+\left(1-\frac{\sigma_c}{G}\right)\frac{\delta\tau_y}{\tau_y}-\left(1-\frac{\sigma_c}{G}\right)\frac{\delta\bar{\phi}}{\bar{\phi}} \qquad (4)$$

Thus, for instance, if $\sigma_c / G=1/4$, a fractional increase of yield stress is three times as effective in raising the kinking stress as is a similar relative change in the shear modulus, and the same is true for a fractional decrease in the initial fibre imperfection[22]. In more recent studies Fleck and co-workers [23-25] have considered the effect of non-zero kink angle ($\beta\neq 0$), combined remote axial compression and in-plane shear loading, random initial fibre waviness, and plastic strain hardening on the predicted critical stress for microbuckling. These model requires a knowledge of the shear strength properties, the initial fibre imperfection or the spectral density of fibre misalignment and kink band orientation angle, β, which is a post-failure geometric parameter; β is a function of fibre imperfection (short-wave or long-wave), the elastic modulus of the laminate in the transverse direction, the shear modulus and the kinking failure stress, σ_c [9].

4.3 Batdorf and Ko model [18]

Batdorf and Ko[18] by idealizing the composite as a collection of slightly misaligned volume elements that fail in the kink mode obtained for the compressive failure stress

$$\sigma_c = \frac{\tau_f - \tau_a}{\bar{\phi} + \gamma_f} \qquad (5)$$

where τ_f is shear failure stress, τ_a is applied shear stress, $\bar{\phi}$ is initial fibre misalignment and γ_f is yield strain of material. Eqn. 5 indicates that the compressive strength of the composite is the tangent modulus of the material taken at the failure point. For pure compression and the elastic-perfectly plastic case eqn. 5 reduces to Budiansky's solution, eqn. 3 . To find the compressive strain the authors [18] assumed that this quantity is the sum of two components, one resulting from the elasticity of the fibres (σ / E_{11}) and the other caused by their changing tilt ($\bar{\phi} + \gamma$), i.e.

$$\varepsilon = \frac{\sigma}{E_{11}} + (\gamma\bar{\phi} + \frac{1}{2}\gamma^2) \qquad (6)$$

where E_{11} is elastic modulus of the laminate in the fibre direction.

Batdorf and Ko [18] suggested that if the shear stress-strain response ($\tau - \gamma$) is known then using eqns. 5 and 6 the compressive stress-strain ($\sigma - \varepsilon$) curve and the strength of the composite can be obtained graphically. The method is illustrated in Fig. 8 for the Plytron system. In these figures the shear stress-strain curve determined from ±45 tensile test is presented; the compressive strength equals the tangent shear modulus G_t of the composite at the yield shear strain γ_y

$$\sigma_c = \frac{\partial\tau}{\partial\gamma}(\gamma_y) = G_t(\gamma_y) \qquad (7)$$

The tangent on the $\tau - \gamma$ curve intersects the abscissa at $-\bar{\phi}$ which corresponds to the initial fibre misalignment. Regarding this as a pivot through which all sloping lines pass, values of $\sigma(\gamma)$ and γ are obtained, and by substituting in eqn. (6), the values of the axial compressive strain ε are determined. Fig. 9 compares the calculated $\sigma - \varepsilon$ response at room temperature with the experimental one. It is evident that the results are sensitive to $\bar{\phi}$ and the calculated nonlinearity is larger

than that observed in experiments; have value of $\bar{\phi}=3.5^{o}$ leads to a better correlation between theory and experiment. Table 4 presents the strength values predicted by eqn. (7) assuming $\bar{\phi}=3.5^{o;}$ the error between the theoretical and experimental values is about 3% at testing temperatures up to 50°C. At higher temperatures the error increases to almost 14%, and this may be attributed to the different failure mechanism observed (out-of-plane microbuckling). This graphical method has also been applied with some success to carbon fibre-epoxy system [26,27].

5 CONCLUDING REMARKS

The experimental evidence presented in this paper show that the compressive failure of unidirectional glass/pp laminates occurs due to fibre microbuckling (plastic buckling), regardless of temperature. In the case specimens tested at above 50°C the failure mode changes from in-plane to out-of-plane microbuckling, which initiates at lower applied strains. Failure initiation depends also on material imperfections, such as voids, resin rich regions and fibre misalignment. The progressive decrease in strength with increasing temperature T is associated with the reduction in matrix shear strength with increasing T. Thus, in compression the matrix plays a key role in providing side support to the fibres and consequently resistance of fibre microbuckling. in currently used composites the strength of glass fibres has been substantially increased while polymeric matrices have changed very little in strength due to demands for high toughness of composite. As a result, the fibres fail by microbuckling before their compressive strength is reached.

Existing elastic and plastic kinking analyses of microbuckling are able to account for some but not all of the experimental observations. They correctly predicted that shear strength and fiber imperfection are important parameters affecting the compressive strength σ_c of the composite. However, it is not possible to exactly how σ_c will vary with fibre content and the value of fibre misalignment is quite arbitrary. In summary, although there has been research on the subject for more than twenty years, a unique theoretical model which can predict the compressive

strength from the properties of the constituents is still not available. Further studies on the effect of composite quality (i.e., fibre/matrix interface and the distribution of fibre misalignment) on the compressive strength are required. The influence of moisture needs also to be considered.

6. ACKNOWLEDGMENTS

The authors are grateful for founding from the Engineering and Physical Sciences Research Council (EPSRC, GR/K57466) and wish to thank ICI Advanced Materials for supplying the glass/pp composite system.

Table 1. Tensile strength properties of glass/polypropylene laminates at various test temperatures.

Property	Temperature °C				
	20	50	80	100	120
0^0 Tension					
Strength (MPa)	550	470	411	350	280
Modulus (GPa)	32.5	27.6	25.3	23.4	20.1
Strain of failure %	1.92	1.8	1.6	1.6	1.4
90^0 Tension					
Strength (MPa)	11	7	5	4	-
Modulus (GPa)	4.1	2.4	1.5	1.4	-
Strain of failure %	0.3	0.5	0.7	0.9	-
$\pm 45^0$ Tension					
Shear strength (MPa)	55	45	38	32	27
Shear modulus (GPa)	2.1	1.3	0.8	0.5	0.3
Shear strain of failure %	19.5	26	32	39	45

Table 2. Compressive strength properties of unidirectional glass/pp laminates as a function of temperature

Property	Temperature °C				
	20	50	80	100	120
0^0 Compression					
Strength (MPa)	317	234	178	149	108
Modulus (GPa)	29.5	26.4	23.5	22	20
Strain of failure %	0.98	0.85	0.68	0.54	0.47

Table 3 Strength properties and kink band geometry of various fibre reinforced composite systems.

Property	T300/5208 [14]	T800/924 [3]	GRFP [14]	Plytron	KFRP [14]
v_f	0.6	0.6	0.65	0.36	0.65
σ_c^{exp}	1300	1600	670	317	228
τ_y	68	70	39	28	27
β^{exp}	19°	5°-15°	32°	20°-25°	39°
w/mm	0.07	0.06	1.2	1.0	0.45
w/d_f	12	10	48	40	25
w/d_f	(8)	(8)	(7)	(7.3)	(15)

( ) predicted by: $\frac{w}{d_f} = \frac{\pi}{4}\sqrt{\frac{E_f}{\sigma_f}}$ [9]

Table 4 Experimental and theoretical compressive strength of Glass/pp u/d composite laminate ($\bar{\phi} = 35^{o}$)

Temperature °C	τ_y MPa	γ_y %	σ_c^{th} MPa	σ_c^{exp} MPa	error %
20	28	3	307	317	3.15
50	24	5.5	206	234	7.6
80	19	6	157	177	10.7
120	14	9	93	108	13.9

REFERENCES

1. Hahn, H.T. and Sohi, M.M., Buckling of a Fibre Bundle Embedded in Epoxy, *Composites Science& Technology*, vol.27, pp25-41, 1986

2. Harper, J.F. and Huemann, T.O. Failure Mechanisms in Uniaxial Compression in Fibre Composites, *4th International Conference on Fibre Reinforced Composites, Proceedings of the Institution of the Mechanical Engineers*, pp.231-235, 1990.

3. Soutis, C. Measurement of the Static Compressive Strength of Carbon Fibre/Epoxy Laminates, *Composites Science & Technology*, vol. 42, pp.373-392, 1991.

4. Soutis, C. and Turkmen, D., High Temperature Effects on the Compressive Strength of Glass Fibre reinforced Composites. *ICCM-9,* Composites Properties and Applications, Ed. A. Miravete, Vol. VI, pp.581-588, Madrid, Spain, 1993.

5. Rosen, B.W., Mechanics of Composite Strengthening, *Fibre Composite Materials, American Society of Metals*, pp.37-75, 1965.

6. Chung, W. and Testa, R.B., The elastic Stability of Fibres in a Composite Plate, *J. Composite Materials*, vol.3 pp.58-80, 1969.

7. Argon A.S., Fracture of Composites, *Treatise on Materials Science & Technology*, vol.1, Academic Press, New York 1972, pp.79-114.

8. Evans, A.G. and Adler, W.F., Kinking as a Mode of Structural Degradation in Carbon Fibre Composites, *Acta Metallurgica*, vol.22, pp.725-738, 1977.

9. Budiansky, B., Micromechanics, *Computer & Structures*, vol.16(1-4), pp.3-12, 1983.

10. Steif, P.S., A model for Kinking in Fibre Composites I-II, *Int. J. Solid Structures*, Vol.26, pp. 549-569, 1990.

11. Curtis, P.A., CRAG Test Methods for the Measurement of Engineering Properties of Fibre-Reinforced plastics, *RAE Technical Report* 85099, 1985.

12. Soutis, C., Turkmen, D. and Morrison, C.J., Compressive Fracture of Unidirectional Composites at Elevated Temperatures Using Untabbed Specimens. *European Conference on Composites Testing and Standardization*, ECCM-CTS 2

13. Berg, C.A. and Salama, M., Fatigue of Graphite Fibre-Reinforced Epoxy in Compression, *Fibre Science & Technology*, vol.6, pp.725-738, 1973.

14. Hahn, H.T, Compression Failure Mechanisms in Composite Structures, *NASA CR-3988*, 1986.

15. Shuart, M.J., Short Wavelength Buckling and Shear Failures for Compression Loaded Laminates, *NASA TM-87640*, 1985.

16. Haeberle, J.G. and Mathews, F.L., Compression Test Methods for Composites and Theories Predicting the Compressive Strength of Unidirectional CFRP, *Applied Solid Mechanics*, vol.3, pp.66-79, 1989.

17. Budianky, B. and Fleck, N.A. Compressive Kinking of Fiber composites: a Typical Review, *Applied Mechanics Reviews*, 47(6), part 2, June 1994.

18. Batdorf, S.B. and Ko, W.C. Stress-strain Behaviour and Failure of Uniaxial Composites in Combined Compression and Shear (Parts I&II). *Internal report, School of Eng.and Applied Science, Univ. of California*, CA 90024 June 1987.

19. Larger, J.B. and June, R.R., Compressive Strength of Boron/epoxy Composites, *Journal of Composite Materials,* 3(1), pp. 48-56, 1969.

20. Ewins, P.D., Tensile and Compressive Test Specimens for Unidirectional Carbon Fibre-reinforced Polyester Resins, *RAE Technical Report* 71217, 1971.

21. Piggott, M.R. and Harris, B., Compression Strength of Carbon, Glass and Kevlar-49 Fibre Reinforced Polyester Resins, *J. Materials Science.,* 15 pp. 2523-2538, 1980.

22. Budiansky, B. and Fleck, N.A., Compressive Failure of Fibre Composites. *J. Mech. Phys. Solids* 41, pp.183-211, 1993.

23. Fleck, N.A., Deng, L. and Budiansky, B., Prediction of Microbuckle Width in Fibre Composites. *Harward University Report* MECH-203, 1993.

24. Slaughter, W.S., Fleck, N.A., Microbuckling of Fibre Composites: the Roles of Multi-axial Loading and Creep. *J. Engineering Materials and Technology*, 115(3), pp.308-313, 1993.

25. Slaughter, W.S. and Fleck, N.A., Microbuckling of Fibre Composites with Random Initial Fibre Waviness. *To Appear in J. Mech. Phys. Solids,* 1995.

26. Haberle, J.G. and Mathews, F.L., A Micromechanics Model For Compressive Failure of Unidirectional Fibre-reinforced Plastics. *J. Composite Materials*, 28(17) pp.1618-1639, 1994.

27. Saunders, D.E.J. and Soutis, C., The Shear and Compressive Behaviour of Low Temperature Cured CFRP Laminates. *3rd International Conference on Deformation and Fracture of Composites, The institute of Materials.* pp.26-35, Guildford, UK. 27-29 March 1995.

Figures

Figure 1 Geometry of fibre microbuckling mode
(β =boundary orientation angle; ϕ inclination angle; w=kink width)
(a) and (b) in-plane and out-of-plane.

Figure 2 Overall failure mode of a glass/pp unidirectional laminate tested at room temperature
(buckle length $\approx$ 0.6 mm)

Figure 3 Compressive stress-strain response of glass/pp unidirectional laminates

Figure 4 Optical micrograph showing in-plane fibre microbuckling
in a glass/pp laminate ($\beta \approx 25^{\circ}$ to horizontal axis, w $\approx$ 0.6 mm)

Figure 5a Fracture surface of a typical glass/pp laminate after buckling.
It shows rows of buckled fibres (26x)

Figure 5b Higher magnification of Fig. 5a showing that its fails in bending (1700x)

Figure 6 Optical micrograph showing out-of-plane fibre microbuckling
(kink band width w $\approx$ 1 mm).

Figure7 Compressive strength of unidirectional laminates plotted versus the yield stress of the composite (glass and Kevlar data taken from [21]).

Figure 8 Graphical method [18] for finding the compressive strength of a glass/pp laminate tested at room temperature.

Figure 9 Compressive stress-strain response in a glass/pp laminate
theory against experiment.

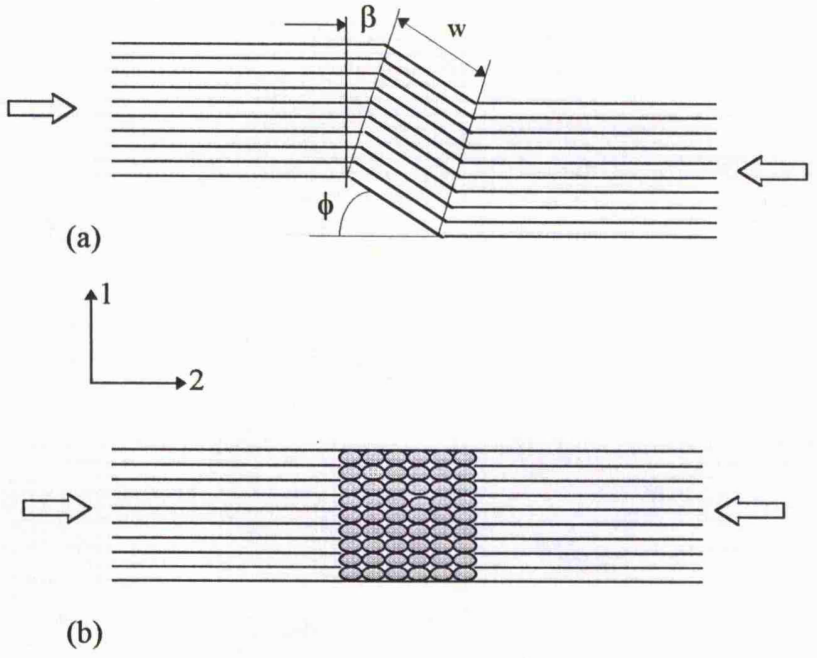

Figure 1 Geometry of fibre microbuckling mode
(β =boundary orientation angle; ϕ inclination angle; w=kink width)
(a) and (b) in-plane and out-of-plane.

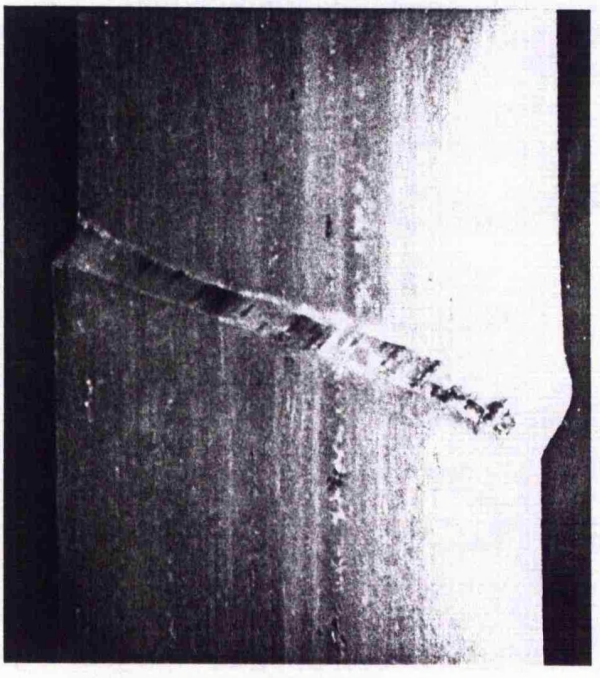

Figure 2 Overall failure mode of a glass/pp unidirectional laminate tested at room temperature
(buckle length $\approx$ 0.6 mm)

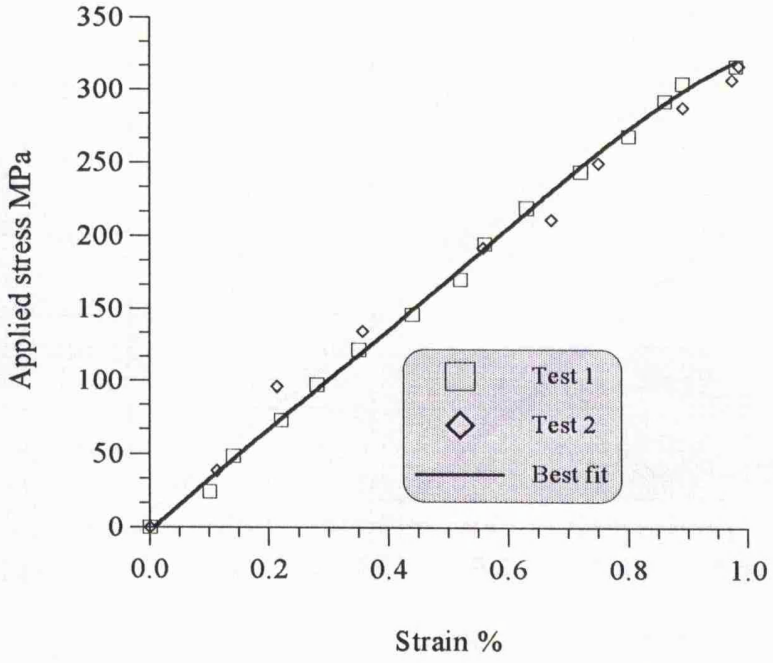

Figure 3 Compressive stress-strain response of glass/pp unidirectional laminates

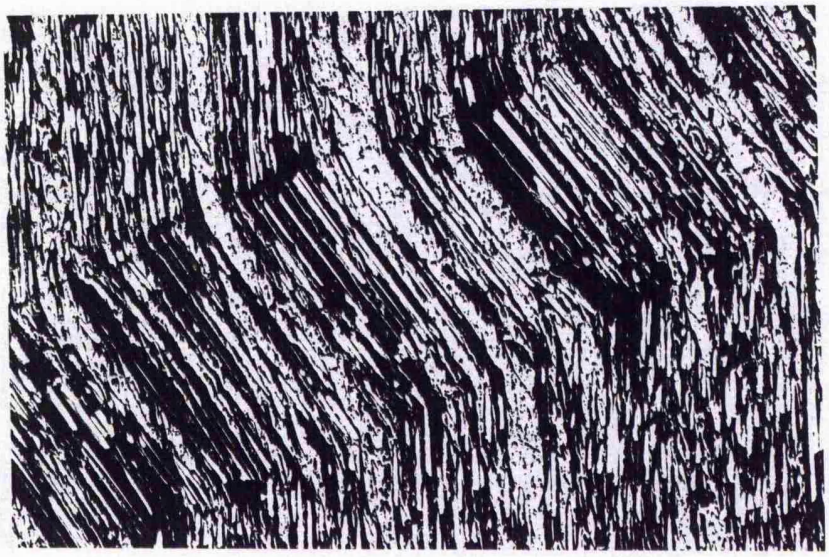

Figure 4 Optical micrograph showing in-plane fibre microbuckling in a glass/pp laminate ($\beta \approx 25^{\circ}$ to horizontal axis, $w \approx 0.6$ mm)

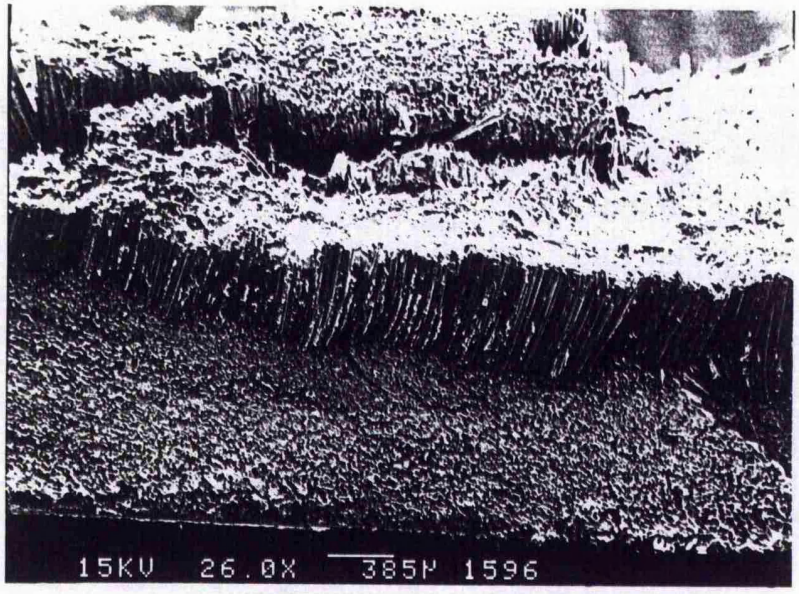

Figure 5a Fracture surface of a typical glass/pp laminate after buckling.
It shows rows of buckled fibres (26x)

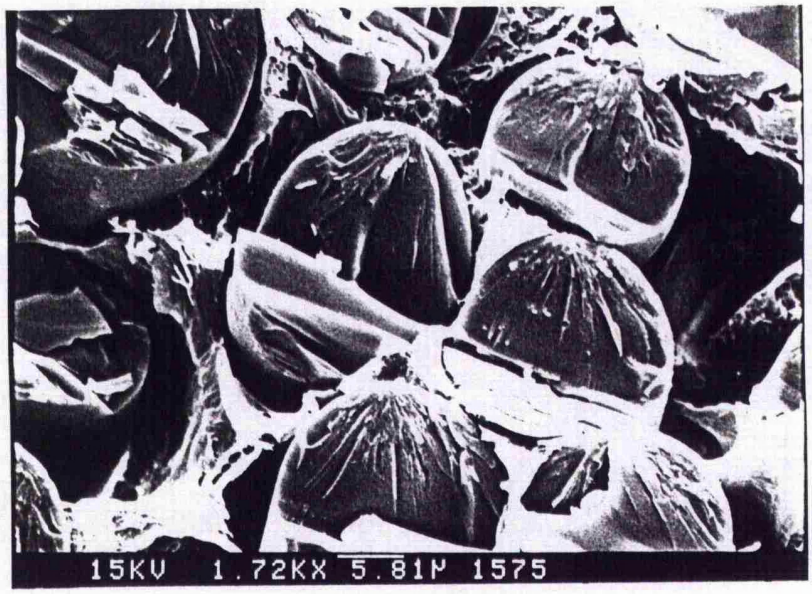

Figure 5b Higher magnification of Fig. 5a showing that its fails in bending (1700x)

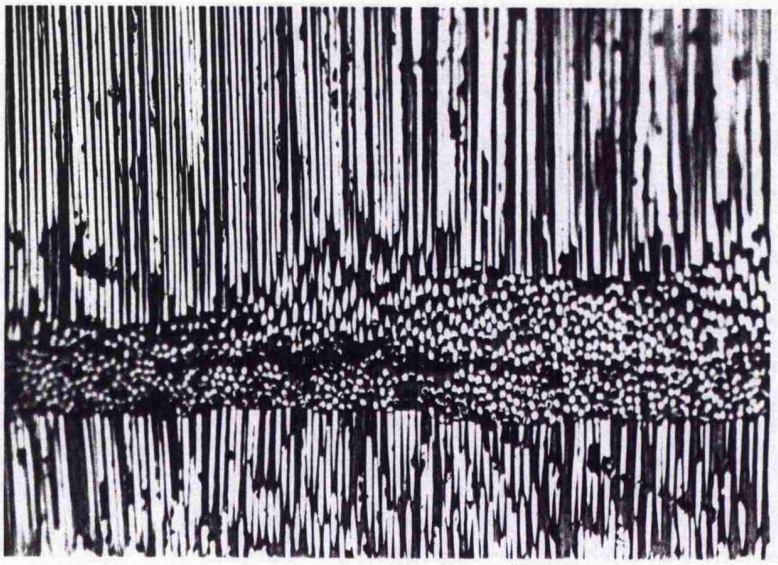

Figure 6 Optical micrograph showing out-of-plane fibre microbuckling (kink band width $w \approx 1$ mm).

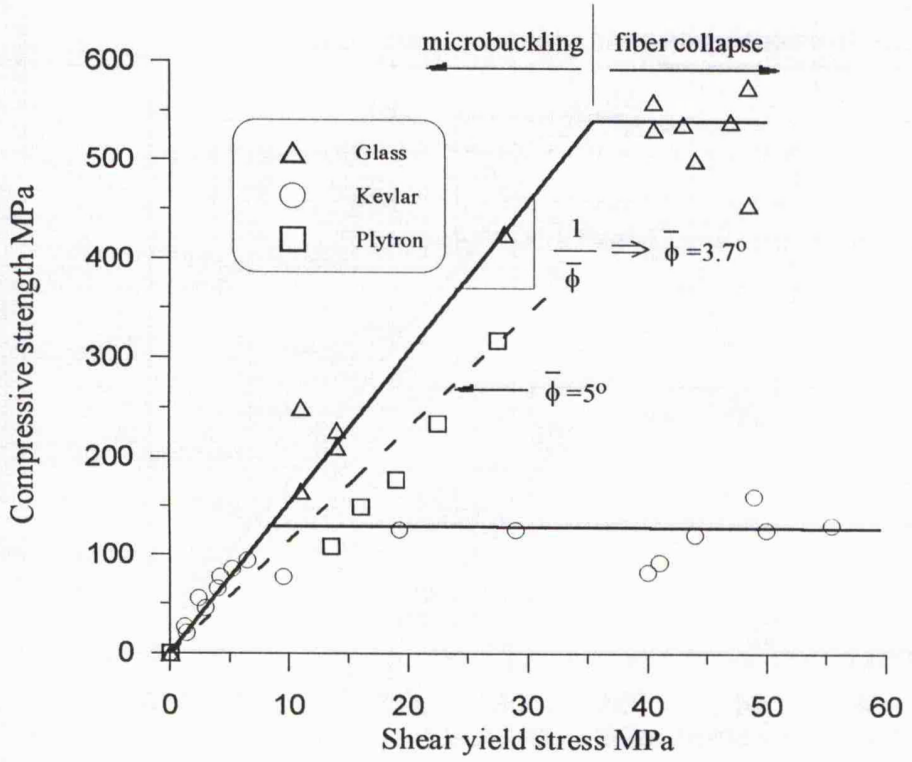

Figure7 Compressive strength of unidirectional laminates plotted versus the yield stress of the composite (glass and Kevlar data taken from [21]).

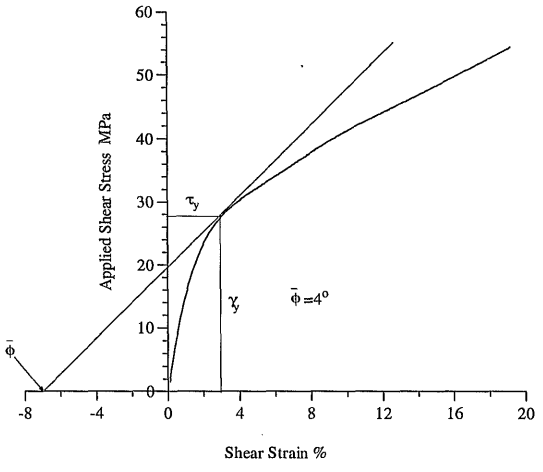

Figure 8 Graphical method [18] for finding the compressive strength of a glass/pp laminate tested at room temperature.

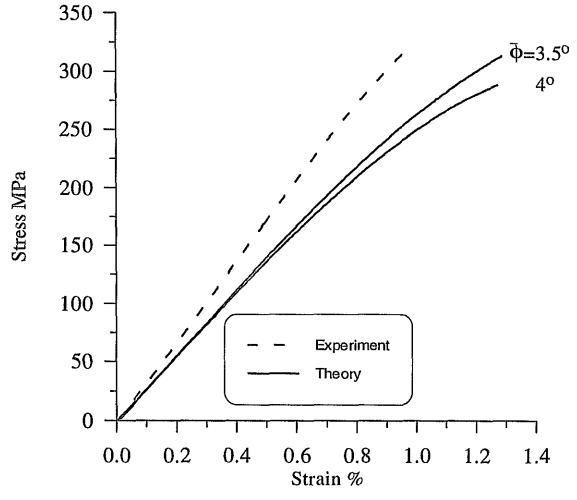

Figure 9 Compressive stress-strain response in a glass/pp laminate theory against experiment.